A Characterization of Mixed Silver Iodide-Silver Chloride Ice Nuclei

by
Paul J. DeMott

Department of Atmospheric Science
Colorado State University
Fort Collins, Colorado

Colorado State University

Department of Atmospheric Science

Paper No. 349

A CHARACTERIZATION OF MIXED SILVER IODIDE-SILVER CHLORIDE ICE NUCLEI

By

Paul J. DeMott

This report was prepared with support provided by
National Science Foundation Grant ATM 79-16504
Principal Investigator, Lewis O. Grant

Department of Atmospheric Science
Colorado State University
Fort Collins, Colorado

August 1982

Atmospheric Science Paper No.349

ABSTRACT

A new approach and methodology to study the ice nucleation properties of aerosols used for weather modification is introduced in this thesis. This approach and methodology is termed mixed aerosol phase change kinetics and is based on an analogy to chemical reaction kinetics. Utlizing this methodology, measurements of the rates of ice crystal formation in a cloudy environment by ice nucleating aerosols, can give inferences to the inter-relationships existing between ice nucleation effectiveness, mechanisms for ice crystal formation, and aerosol physical and chemical characteristics. The chemical kinetic methodology is applied to the study of a specific ice nucleating aerosol in the CSU isothermal cloud chamber. This aerosol, mixed silver iodide - silver chloride (AgI - AgCl), was suspected to be a highly efficient ice nucleus. The mixed AgI - AgCl aerosols were generated by simple solution combustion methods.

The major conclusions in this thesis are the following:

a. The analogy to chemical reaction kinetics appears valid for the study of ice nucleation. An analysis of data based on the kinetic methodology produces clear and detailed information about the nucleation process.

b. Mixed AgI - AgCl aerosols were found to form ice crystals by contact nucleation at cloud liquid water contents of 0.5 gm^{-3} and 1.5 gm^{-3}, and temperatures $-16^{o}C$ and warmer, based on the kinetic analysis and simple confirmatory tests. Nucleation following collision was found to be rapid or does not occur at all, suggesting a competition

between rates of freezing and dissolution at active sites on the nuclei surface after collision.

c. Mixed AgI - AgCl aerosols display effectiveness values which are one order of magnitude larger at $-12^{o}C$ and three orders of magnitude larger at $-6^{o}C$ in comparison to the AgI aerosols generated from the $AgI \cdot NH_4I$ - acetone - water solution combustion system. The improvement must be due to a mechanism which favors the rate of freezing versus dissolution of active sites. Since the AgI aerosols from the $AgI \cdot NH_4I$ - acetone - water system function by the same mechanism in the isothermal cloud chamber, this new nucleant may display enhanced utility when used operationally.

d. At $-20^{o}C$, a hypothesized deposition nucleation mechanism competes with contact nucleation to form ice crystals. A good correlation is found between the percent of particles greater than 500 A^{o} and the percent of ice crystals formed by deposition, suggesting a size cutoff to the appreciable deposition rate at that value.

e. Rates of ice crystal formation by AgI - AgCl aerosols are relatively slow in the isothermal cloud chamber (20-40 minutes for 90% production in a 1.5 gm^{-3} cloud) by either mechanism. In using this nucleant operationally, strong consideration should be given to the contact nucleation behavior at temperatures $-16^{o}C$ and warmer, and to the fact that droplet concentrations in this experiment were much greater than those found in wintertime clouds.

Paul J. DeMott
Atmospheric Science Department
Colorado State University
Fort Collins, Colorado 80523
Summer, 1982

ACKNOWLEDGEMENTS

The author would like to express his deep gratitude to Dr. William G. Finnegan for his guidance and numerous thought provoking discussions during this research. I would also like to thank Professor Lewis O. Grant, Professor William R. Cotton and Professor Branka Ladanyi for their comments and suggestions during the preparation of this thesis. Special thanks is due to the following people for their help and support: Cleon Swain for his maintenance of mechanical operations and assistance in testing procedures; Scott Skogerboe for his assistance in testing procedures; Randy Horn for the design and calibration of instrumentation; Steve Lassman for the reduction of FSSP data; Bob Rilling for computer programming; Bill Kuenning for his assistance and training in techniques of Scanning Electron Microscopy; Randy Borys for arranging and performing the Neutron Activation Analysis; the Rhode Island Nuclear Science Center for the use of their facilities; Lucy McCall for drafting the numerous figures and Ruta Radziunas for dedicated typing.

This research was supported by the National Science Foundation Grant No. ATM-79-16504.

TABLE OF CONTENTS

	PAGE
I. INTRODUCTION	1
1.1 Background	1
1.2 Specific Objectives	3
1.3 General Approach	3
II. LITERATURE REVIEW	6
2.1 Chemistry of AgI Aerosols Used for Weather Modification	6
2.2 Reasons for the Ice Nucleating Ability of AgI Aerosols	7
2.3 Laboratory Determination of the Ice Nuclei Effectiveness of Aerosols	10
2.4 Ice Nucleation Mechanisms	13
2.5 Rates of Ice Crystal Formation	20
III. THEORETICAL CONSIDERATIONS	22
3.1 A Chemical Kinetics Approach as Applied to the Experiment	22
3.2 Kinetics Determined from Aerosol-Droplet Collision Theory	29
IV. INSTRUMENTATION AND EXPERIMENTAL PROCEDURES	36
4.1 Facility Instrumentation and Techniques	36
4.1.1 Isothermal Cloud Chamber	36
4.1.2 Vertical Dilution Tunnel	41
4.1.3 Electrostatic Precipitator	43

4.1.4 Scanning Electron Microscope 43

4.1.5 Neutron Activation Analysis 44

4.2 Ice Nuclei Effectiveness Determination 44

4.3 Analysis of Rates of Ice Crystal Formation 47

4.3.1 Graphical Representation of Rates of Ice Crystal Formation 47

4.3.2 Experimental Kinetics Plots 49

4.4 Data Correction for Dilution Mechanisms 50

4.5 Experimental Procedures 53

V. RESULTS 55

5.1 Aerosol Analysis 55

5.1.1 Composition 55

5.1.2 Particle Sizes 56

5.2 Ice Nuclei Effectiveness 63

5.3 Rates, Kinetics, and Mechanisms for Ice Crystal Formation 69

VI. SUMMARY AND CONCLUSIONS 100

6.1 Summary and Conclusions 100

6.2 Experimental Implications and Significance 105

6.3 Suggestions for Further Research 110

VII. REFERENCES 113

APPENDIX A: Cloud Droplet Size Distributions 118

APPENDIX B: The Electrostatic Precipitator 122

LIST OF TABLES

TABLE		PAGE
1.	Kinetic Slope Correction for Airflow	51
2.	Neutron Activation Analysis Results for Solution Combustion Aerosols	55
3.	Aerosol Size and the Percent of Ice Crystals Formed by Deposition	83
4.	Contact Nucleation Time Constants	93
5.	LWC Ratio (0.5 gm^{-3}/1.5 gm^{-3}) of Kinetic Slope at $-12^{o}C$	94

LIST OF FIGURES

		PAGE
Fig. 1	Analytical separation of two first order chemical processes producing the same product	27
Fig. 2	Isothermal Cloud Chamber schematic	37
Fig. 3	Cloud introduction airflow versus precooler air pressure	39
Fig. 4	Total cloud droplet concentration versus temperature	42
Fig. 5	Tunnel dilution as a function of updraft velocity	46
Fig. 6	Comparison of average rate of ice crystal formation to Component rates at a given temperature and Liquid Water Content	48
Fig. 7	Typical particle distribution within the electrostatic precipitator	57
Fig. 8	a) $2AgI \cdot NH_4I$ particle size distribution b) $2AgI \cdot NH_4I$ with 20 mole % NH_4ClO_4 particle size distribution	59
Fig. 9	a) $2AgI \cdot NH_4I$ with 30 mole % NH_4ClO_4 particle size distribution b) $2AgI \cdot NH_4I$ with 40 mole % NH_4ClO_4 particle size distribution	60
Fig. 10	a) Maximum draft aerosol size distribution b) 6 weight % AgI aerosol size distribution	61
Fig. 11	$2AgI \cdot NH_4I$ with 20 mole % particle size distribution by nucleopore filter	62
Fig. 12	$2AgI \cdot NH_4I$ effectiveness results	64

Fig. 13 $2AgI \cdot NH_4I$ with 10 mole % NH_4ClO_4 effectiveness results 64

Fig. 14 $2AgI \cdot NH_4I$ with 20 mole % NH_4ClO_4 effectiveness results 65

Fig. 15 $2AgI \cdot NH_4I$ with 30 mole % NH_4ClO_4 effectiveness results 65

Fig. 16 $2AgI \cdot NH_4I$ with 40 mole % NH_4ClO_4 effectiveness results 66

Fig. 17 Average effectiveness of natural draft aerosols 66

Fig. 18 Maximum draft aerosol effectiveness results 68

Fig. 19 6% $AgI \cdot NH_4I$ with 20 mole % NH_4ClO_4 effectiveness results 68

Fig. 20 $2AgI \cdot NH_4I$ ice crystal formation rates 70

Fig. 21 $2AgI \cdot NH_4I$ with 10 mole % NH_4ClO_4 ice crystal formation rates 70

Fig. 22 $2AgI \cdot NH_4I$ with 20 mole % NH_4ClO_4 ice crystal formation rates 70

Fig. 23 $2AgI \cdot NH_4I$ with 30 mole % NH_4ClO_4 ice crystal formation rates 70

Fig. 24 $2AgI \cdot NH_4I$ with 40 mole % NH_4ClO_4 ice crystal formation rates 71

Fig. 25 Maximum draft aerosol ice crystal formation rates 71

Fig. 26 6% $AgI \cdot NH_4I$ with 20 mole % NH_4ClO_4 ice crystal formation rates 71

Fig. 27 $2AgI \cdot NH_4I$ raw kinetics 73

Fig. 28 $2AgI \cdot NH_4I$ with 10 mole % NH_4ClO_4 raw kinetics 73

Fig. 29 $2AgI \cdot NH_4I$ with 20 mole % NH_4ClO_4 raw kinetics 74

Fig. 30 $2AgI \cdot NH_4I$ with 30 mole % NH_4ClO_4 raw kinetics 74

Fig. 31 $2AgI \cdot NH_4I$ with 40 mole % NH_4ClO_4 raw kinetics 74

Fig. 32 a) Kinetics versus LWC at $-12^{\circ}C$

b) Kinetics versus LWC at $-20^{\circ}C$ 76

Fig. 33 Airflow corrected kinetics versus LWC at $-12^{o}C$ and $-20^{o}C$ 76

Fig. 33d Generalized plots for a series first order reaction with equivalent rate constants (two stage). 77

Fig. 34 $2AgI \cdot NH_4I$ corrected kinetics 81

Fig. 35 $2AgI \cdot NH_4I$ with 10 mole % NH_4ClO_4 corrected kinetics 81

Fig. 36 $2AgI \cdot NH_4I$ with 20 mole % NH_4ClO_4 corrected kinetics 82

Fig. 37 $2AgI \cdot NH_4I$ with 30 mole % NH_4ClO_4 corrected kinetics 82

Fig. 38 $2AgI \cdot NH_4I$ with 40 mole % NH_4ClO_4 corrected kinetics 82

Fig. 39 Percent deposition versus percent particles $> 500\ A^{o}$ at $-20^{o}C$ 84

Fig. 40 a) Maximum draft aerosol raw kinetics

b) Maximum draft aerosol corrected kinetics 86

Fig. 41 a) 6% $AgI \cdot NH_4I$ with 20 mole % NH_4ClO_4 raw kinetics

b) 6% $AgI \cdot NH_4I$ with 20 mole % NH_4ClO_4 corrected kinetics 88

Fig. 42 Theoretical kinetics of Brownian coagulation, nuclei diffusion to the walls, and airflow dilution 90

Fig. 43 $2AgI \cdot NH_4I$ with 20 mole % NH_4ClO_4 theoretical kinetics (Natural Draft) 92

Fig. 44 $2AgI \cdot NH_4I$ with 20 mole % NH_4ClO_4 theoretical kinetics (Maximum Draft) 92

Fig. 45 Size dependency of the composite nucleation efficiency 97

Fig. 46 a) Ice crystal formation rate in the Elk Mountain cap cloud of January 10, 1975

b) Kinetics of ice crystal production in the Elk Mountain cap cloud 108

Fig. 47 Cloud droplet size (radius) distribution determined from soot coated slides 119

Fig. 48 - Fig. 57 Cloud droplet size distribution at various cloud temperatures for liquid water contents of 0.5 gm^{-3} and 1.5 gm^{-3} (determined using the FSSP). 119-121

Fig. 58 Schematic of the electrostatic precipitator 124

Fig. 59 Precipitator collection efficiency (%) versus particle size, determined theoretically 124

I. INTRODUCTION

1.1 Background

Silver iodide containing aerosols have been used as ice nuclei for weather modification field experimentation, operations, and research, for more than thirty years. A prime motivation for ice nucleation research in the past has been to produce aerosols which function to form the maximum amount of ice crystals at temperatures warmer than $-20^{o}C$. For precipitation enhancement purposes, a nucleant which realizes its maximum activity at relatively warm temperatures below $0^{o}C$ is most desirable. This allows the seeding effect to take place in portions of clouds, where the natural nucleation process is deficient.

Of equal importance to the ice nuclei effectiveness, but less well understood or considered in the design or conduct of weather modification experimentation, are the rates of ice crystal formation by various silver iodide aerosols. This factor was recognized in early nucleation studies as the "time lag" of ice nucleation. The rate processes involved in nucleation and ice crystal formation will influence the subsequent rate of development and fallout of precipitation. Therefore, an understanding of such rate processes is necessary to avoid misinterpretation and improper application of laboratory derived composite effectiveness values.

Nucleation effectiveness and rates are not totally unrelated, in that they both will reflect the mechanism for ice crystal formation. This mechanism is in turn related to the physical and chemical characteristics of the nuclei, as well as the environmental conditions. To

the present time, no technique has been demonstrated to study these inter-relationships in a cloud environment which permits nuclei to function naturally. It has not been thought possible to study the ice nucleation mechnanisms of silver iodide aerosols, except by controlled or forced means.

One purpose of this study is to demonstrate that it is possible to study the complex behavior of silver iodide aerosols in an isothermal cloud environment by drawing an analogy to the principles of chemical reaction kinetics. This should lead to a better understanding of the inter-relationships involved in the nucleation process and allow better application of laboratory results to the atmosphere. In addition, this new technique should find application in the study of nucleation in natural and seeded atmospheric clouds which can be probed by cloud physics aircraft.

Another purpose of this study is to introduce an improved ice nucleant for weather modification use, which can be produced by a simple modification to existing solution combustion generating systems. The study of mixed silver halides as ice nuclei at the CSU Cloud Simulation and Aerosol Laboratory was initiated on the basis of evidence that AgI-AgCl (silver iodide-silver chloride) and AgI-AgBr (silver iodide-silver bromide) aerosols, in various molar ratios, would display a better efficiency of ice crystal formation at temperatures closer to $0^{o}C$ than AgI aerosols presently used. The AgI-AgCl aerosols were chosen for full characterization here. This necessarily includes the determination of effectiveness, rates, and mechanisms of ice crystal formation as a function of nuclei size and composition, and also cloud characteristics.

The facilities described in chapter four and the kinetics approach discussed in chapter three have been used to achieve this.

1.2 Specific Objectives

The general purposes of this study may be separated into three specific objectives. These are:

1) introduce mixed aerosol phase change kinetics as a viable approach to the study of ice nucleation, and apply its principles to data from the CSU isothermal cloud chamber.
2) demonstrate the inter-relationships between effectiveness, rates of ice crystal formation, mechanisms for ice crystal formation, and nuclei chemistry, occurring in nucleation by AgI-AgCl nuclei.
3) generate and test mixed silver iodide-silver chloride aerosols to prove or disprove preliminary evidence of their superior effectiveness compared to commonly used AgI aerosols; in particular, those from the AgI·NH_4I-acetone-water solution combustion system.

1.3 General Approach

This study introduces, for the first time, an approach to the determination of ice crystal nucleation mechanisms based on principles of chemical kinetics. This kinetics is not to be confused with non-equilibrium thermodynamics (sometimes referred to as "kinetics"), the classical approach to studying ice nucleation rates and mechanisms. In kinetics, the measured rate of formation can be used to define the mechanism of formation if kinetic parameters are properly controlled. Considering the isothermal cloud chamber as being analogous to a chemical reactor after the introduction of an ice nucleating aerosol, our

product is then ice crystals. With appropriate control of kinetic parameters such as temperature, nuclei concentration, vapor concentration, and droplet concentration, ice nucleation mechanisms are then defined. The analogy and principles of kinetics are discussed in depth in the third chapter. The knowledge of the nucleation mechanism along with a standard procedure for determining the ice nucleating effectiveness of an aerosol, and a simple means of altering aerosol chemical composition, allows the investigation of the inter-relationships among these characteristics.

The production of AgI-AgCl aerosols is thermodynamically possible by the addition of ammonium perchlorate (NH_4ClO_4) to the $2AgI \cdot NH_4I$-acetone-water solution combustion system for aerosol generation. The reaction is described as follows:

$$AgI + NH_4ClO_4 \rightarrow AgCl + 1/2\ I_2 + 1/2\ N_2 + O_2 + 2H_2O;\ \Delta H = -56.6\ kcal.$$

The negative heat of reaction (Δ) indicates that the reaction would be exothermic. If produced, the AgCl would survive since it is even more stable than AgI. It is likely that the AgI and AgCl will combine to form solid solution aerosols. This means that Cl atoms will replace some I atoms in the crystal lattice. Different composition aerosols were produced by varying the mole percentage (with respect to AgI) of NH_4ClO_4 added to the solution. Increments of ten percent were used, starting at zero percent, until nucleation effectiveness (ice crystals per gram AgI) was optimized in the 960 liter isothermal cloud chamber. Chlorine to iodine molar ratios in the aerosols were determined by neutron activation analysis (see 4.1.5) to confirm the production of AgCl. The NH_4ClO_4 is also likely to eliminate any complexing hygroscopic contaminants from the AgI as well, thus

$$NH_4ClO_4 + KI \rightarrow KCl + 1/2\ I_2 + 1/2\ N_2 + O_2 + 2H_2O;\quad \Delta H = -72.0\ kcal.$$

Solution combustion was performed on the above mentioned solutions using the CSU standard test generator.

II. LITERATURE REVIEW

2.1 Chemistry of AgI Aerosols Used for Weather Modification

The first solution combustion system for the production of AgI aerosols was developed by Vonnegut (1949). The method involved the combustion of acetone-water solutions of silver iodide, using ammonium iodide (NH_4I) as a solubilizing agent. After vaporization the AgI cools and solidifies into relatively pure submicron aerosols. The NH_4I, on the other hand, decomposes upon combustion and what remains is probably too volatile to survive (St. Amand et. al, 1971). Subsequent experimentation and generator development led Vonnegut (1950) to recommend the use of alkali iodides as solublizing agents for silver iodide in acetone. That the aerosols produced were not silver iodide, but complexes of silver iodide (2AgI·NaI, 2AgI·KI) was not recognized until several years later (Vonnegut, 1957). Mixtures and complexes of silver iodide and alkali iodides are hygroscopic, undergoing transitions to various hydrates (Burkhardt et. al, 1970; St. Amand et. al, 1971a) in a humid atmosphere. The final result is an insoluble, although highly modified, AgI particle left within a solution droplet. The ice nucleus activity of such aerosols has been found to be very inferior to uncomplexed AgI aerosols at temperatures warmer than $-12^{\circ}C$ (Garvey, 1975). The reason for this is probably a solubility effect, although it is uncertain whether the dissolution of AgI is complete or simply etching of ''active sites'' on the surface (Mossop and Jayaweera, 1969). In any case, the original system using ammonium iodide as the solublizing iodide was re-adopted for weather modification experimentation using solution combustion systems (Donnen et al., 1972). Exceptions were the Colorado River Basin Pilot Project of the Bureau of Reclamation (Elliott

et al., 1978) and the Israeli Rainfall Enhancement Program (Gagin and Nueman, 1974).

Pyrotechnic generation of AgI aerosols has become popular since its introduction by workers at the Naval Weapons Center in China Lake, California (St. Amand et al., 1970). In most pyrotechnics, the silver iodide is produced by the reduction of silver iodate (Finnegan et al., 1962) as follows:

$$AgIO_3 + 2Al \rightarrow AgI + Al_2O_3.$$

Endless variations of $AgIO_3$, plus aluminum for heat, magnesium for clean burning at high altitude, an additional oxidizer (KIO_3, KNO_3 for example), and a binder, have been produced for use in weather modification. Pyrotechnics are particularly useful in cumulus cloud modification since they allow accurate delivery of nucleating aerosols by aircraft. Following the inadvertent discovery of the positive influence on nucleation effectiveness of a chlorinated epoxy resin fuel binder in the Navy TB-1 formulation, Nuclei Engineering Corporation attempted to duplicate the results by adding 3% hexachlorobenzene (C_6Cl_6) to the TB-1 formulation. This new formulation produced AgI aerosols with the highest ice nuclei effectiveness ever achieved in the warm temperature region ($>-12^{\circ}C$) by pyrotechnic production (Sax et al., 1979). The reason for the enhanced ice nucleus activity of this aerosol had not been conclusively related to the presence of chlorine. There is some evidence however, that it is related to the production of silver chloride, as discussed in the following section.

2.2 Reasons for the Ice Nucleating Ability of AgI Aerosols

There are at least two accepted reasons why AgI aerosols have the ability to nucleate ice, and to varying degrees. The first, epitaxial

growth from a surface crystal structure similar to that of ice, was the basis of Vonnegut's original choice of this substance as a likely ice nucleant. Secondly, it appears that the presence of impurity centers or defects on the nucleant surface (Fletcher, 1960, 1969), favorable to the adsorption of water in structural clusters, can be of equal importance. The actual process is very likely a combination of these factors.

Considering the latter, silver iodide is a hydrophobic substance whose surface interaction with water is weak. Corrin et al. (1964) demonstrated that water vapor adsorption by silver iodide decreased as its purity increased. Silver iodide, made by reacting pure silver with pure iodine, did not adsorb water and showed no nucleating tendencies down to $-15^{\circ}C$. The sites upon which water adsorbs on AgI are really impurity sites (Corrin et al., 1967). These are formed during the production and aerosolization of AgI. Silver iodide used in combustion generators is commonly contaminated during its manufacture by adsorption-precipitation of hygroscopic by-products, such as alkali nitrates or excess alkali iodide as follows:

$$AgNO_3 + NaI(KI) \rightarrow AgI + NaNO_3(KNO_3).$$

Likewise, silver iodate, the source of AgI in pyrotechnics, is commonly contaminated with by-products and reactants of their manufacturing process (personal communication with Dr. William Finnegan). For example,

$$AgNO_3 + NaIO_3(KIO_3) \rightarrow AgIO_3 + NaNO_3(KNO_3).$$

Davis et al. (1975) have also shown, by coincident x-ray diffraction and ice nuclei effectiveness studies of AgI aerosols, generated by the combustion of the $2AgI \cdot NH_4I$-acetone-water system at various flame tem-

peratures, that a trace of NH_4I must remain on the surface of the nuclei for high ice nuclei activity.

Defect sites have also been found to be polar sites (Edwards and Evans, 1961). When one ion (I^-) is replaced by another (Cl^-), the surface charge distribution may be altered, essentially changing the nature of active sites.

The epitaxial effect in nucleation by silver iodide has been discussed by Zettlemoyer et al. (1961) and Vonnegut and Chessin (1971). That epitaxial catalysis is improved by any modification which brings the lattice constant of the nucleant to a closer match with that of ice, follows from a nucleation catalysis theory based on the elastic distortion that results because the lattice constant of silver iodide is 1.5% larger than that of ice (Turnbull and Vonnegut, 1952). In such a theory, the mismatch between the structures of ice and AgI is responsible for the 2.5°C supercooling necessary to cause bulk water to freeze in its presence. Vonnegut and Chessin (1971) demonstrated that by the coprecipitation of silver bromide with silver iodide, metastable solid solutions are formed (Br atoms are substituted for as many as 30% of I atoms in the AgI crystal lattice) which can cause bulk water to freeze at a supercooling of only 1.3°C. This coincided with the reduction of the lattice constant by up to 0.5%. They pointed out, however, that they may have also changed other physical and chemical properties of the surface. This would influence water adsorption, and water cluster formation is a precursor to the epitaxial effect (Zettlemoyer et al., 1961).

Although the exact importance of each factor discussed is still uncertain, mixed silver iodide-silver chloride would seem a likely can-

didate as an efficient ice nucleant since it might have a better epitaxial match to ice than pure AgI (similar to AgI-AgBr) and the Cl^- might produce surface defect sites more favorable to water cluster formation (personal communication with Dr. A C. Zettlemoyer). It is possible that such a mechanism is responsible for the high activity of the NEI TB-1 pyrotechnic formulation. Heats of formation calculations of possible reactions occurring in the combustion of this formulation show that the formation of silver chloride is possible thermodynamically as follows:

$$4AgIO_3 + 2AgI + C_6Cl_6 \rightarrow 6AgCl + 3I_2 + 6CO_2; \Delta H=-493.3 \text{ kilocalories.}$$

If formed, AgCl would survive the generation process (AgCl is more stable than AgI) and solid solutions or intimate mixtures of AgI and AgCl would be produced in aerosol form. Sax et al. (1979) found preliminary evidence of chlorine in the TB-1 (with C_6Cl_6) aerosol by energy dispersive x-ray analysis. This strongly suggested a study of the nucleating properties of purposely generated AgI-AgCl aerosols.

2.3 Laboratory Determination of the Ice Nuclei Effectiveness of Aerosols

There are several approaches to the determination of the ice nucleation activity, or effectiveness, of an aerosol. The absolute value of effectiveness at a given temperature will depend on the method used, which may allow only a given mechanism for ice formation (see section 2.4) to procede. In addition, all methods suffer from the production of varying degrees of unrepresentativeness to natural atmospheric cloud conditions, and control over such conditions can be highly variable.

The first attempts to measure ice nucleation effectiveness of aerosols utilized simple cold boxes in which a supercooled cloud was formed by injecting moist air (Schafer, 1946; Vonnegut, 1949). Temperature

control was not very accurate in such chambers, varying by 2°C or more over the depth of the cold box. Also, wall effects (diffusion of water vapor and nuclei) were very large and the cloud environment could be severely disturbed by the ice crystal counting technique.

Rapid expansion cloud chambers of the type described by Warner (1957) followed the cold boxes as the accepted method of determining the ice nucleus activity of both natural and artificial nucleants. The technique was to overpressurize and cool a small (several liter) chamber. Upon release of the pressure, the temperature would drop temporarily to a value determined by the overpressure, creating a supercooled cloud. Wall effects were reduced by treating the walls with glycol, and a sugar solution was utilized for counting. However, the method ignored the time dependence (rate) of the nucleation process and high transient supersaturations were created by rapid cooling.

The membrane filter technique, described by Bigg et al. (1963) and later modified and improved by Stevenson (1968) and others, utilizes the ability of membrane filters to capture aerosol particles. The filter is processed in an ice thermal diffusion chamber. In such a device, the supersaturation of water vapor can be controlled by controlling the temperature difference between the filter surface and an ice surface above the filter. Supersaturation is an important parameter in the nucleation process. Its value can determine the effectiveness of many nucleants (Huffman, 1973; Anderson and Hallet, 1976) and must be carefully controlled. Although very popular, this method measures nucleating ability from the vapor only, ignoring the interaction between nuclei and droplets, and the influence of the membrane substrate on the nucleation activity of aerosols has been criticized (Fukuta, 1966; Schaller and Fukuta, 1979).

The ability of aerosols to freeze supercooled droplets has also been studied by several investigators. Gokhale (1965), Gokhale and Goold (1968), and Vali (1968) have thoroughly investigated the freezing of millimeter sized water drops suspended on a substrate. Sax and Goldsmith (1972) studied this phenomenon with 20 to 80 micron droplets freely suspended in air.

Other studies of nucleation effectiveness have utilized portable continuous ice nucleus counters. Langer (1973) and Pasarelli et al. (1974) studied the nucleation effectiveness of various aerosols in the NCAR ice nucleus counter. Used in its normal operating mode, this instrument contains rather large temperature gradients and sustained water supersaturations. This likely forces condensation on nuclei, which might not occur naturally. The short residence time of aerosols in the chamber (few minutes) is also a problem.

Despite the variety of techniques possible, only large cloud chambers have been used to routinely calibrate the effectiveness of silver iodide aerosol generators and pyrotechnics used in weather modification experimentation. Three facilities in the United States have participated in this calibration. They are, the Naval Weapons Center (Odencrantz, 1969), the South Dakota School of Mines and Technology (Donnan et al., 1971), and CSU's Cloud Simulation and Aerosol Laboratory (Steele and Krebs, 1967; Garvey, 1975; Grant and Steele, 1966). Only the CSU facility remains in operation. Cloud chambers can best represent the processes in natural clouds if the temperature, supersaturation, and droplet size and concentration are well controlled. Large size also minimizes wall effects and allows one to deal with large samples of

nucleating material generated from actual field generators. Too often, laboratory studies deal with silver iodide aerosols which may differ from those used in the field, due to the production technique used. The CSU isothermal cloud chamber has the above mentioned advantages over other methods. Contrary to statements by other investigators (Schaller and Fukuta, 1979), there is no evidence that this method suffers from transient high supersaturations during sample introduction, or fails to produce clearly defined or stably sustained supersaturations with respect to ice. These are eliminated by the present methods of sample dilution and cloud air introduction discussed in chapter four. The isothermal cloud chamber can justifiably be said to represent a slowly settling stratus cloud at water saturation. The slow expansion cloud chamber described by Garvey (1975), appears to have the most promise in describing the nucleation activity of aerosols in "dynamic" cloud situations, with small water supersaturations and larger cloud droplet sizes.

2.4 Ice Nucleation Mechanisms

Although the physical mechanisms for ice formation by AgI aerosol have, in general, been agreed upon, the nomenclature is rather ambiguous. For this study, four mechanisms, or modes of function, will be considered and defined as follows:

vapor deposition–the transformation of water vapor directly to the ice phase on nuclei to form an ice embryo which will grow.

condensation freezing to embryos–the deposition of water vapor to the liquid phase on nuclei followed by freezing to form a viable ice embryo.

condensation to droplet freezing-the complete condensation of water vapor onto a nucleus to form a droplet which subsequently freezes.

contact freezing-the freezing of cloud droplets after direct contact by an ice nucleus.

The mechanism of immersion freezing (penetration of a drop by an aerosol particle, followed by freezing) is not included here, as there is no evidence that such an energetically improbable (due to surface tension effects) process occurs naturally, or that the result would be any different than in contact nucleation.

The concept of vapor deposition ice nucleation was envisioned in the early days of ice nucleation. A thermodynamic theory for deposition was developed by Fletcher (1958a), showing that the rate of ice nucleation is an increasing function of nuclei size and the supersaturation with respect to ice, and a decreasing function of temperature. This theory predicts that deposition on submicron silver iodide is , for all practical purposes, impossible under realistic atmospheric conditions (Sax, 1970). The theory, however, may be quite inadequate in quantitatively describing the nucleation behavior of aerosols, since it applies macroscopic ideas to molecular regions (Sax, 1970; Pruppacher and Klett, 1978). Numerous studies have confirmed the qualitative predictions of the theory, but have shown that AgI aerosols have a finite nucleating ability, although the process appears quite inefficient at most temperatures important to weather modification for precipitation enhancement. Using very small particles (<100 A^{o} radius), produced by reacting iodine vapor with a silver aerosol and deposited on a gold surface, Edwards and Evans (1960) showed that deposition at water saturation did not occur at

temperatures warmer than -18.5°C, and only for 0.5% of the aerosol at that temperature. Gerber (1972) found size cutoffs for vapor depositional activity by AgI aerosol (thermally generated from an AgI-amine complex and deposited on a Goetz aerosol spectrometer foil), at water saturation, of 500 A° diameter at -20°C and 1500 A° diameter at -16°C. Anderson and Hallet (1976) found a similar size cutoff for nucleation from the vapor at water saturation and below onto dislocation (growth) steps of single crystal silver iodide substrates, only the nucleation occurred even at -5°C. They did not, however, distinguish between vapor deposition and freezing following capillary condensation onto their cleaved surfaces; the second mechanism mentioned previously. Schaller and Fukuta (1979) were the first to study vapor deposition onto freely suspended thermally generated AgI aerosols, by using a wedge shaped ice thermal diffusion chamber. Their results displayed the expected supersaturation and temperature dependences and gave -9°C as the nucleation threshold (1.3% nucleation in one minute) at water saturation for 0.3 micron mean diameter aerosol.

It is difficult to find any specific experiments on the mechanism of condensation freezing to embryos. This is a result of the difficulty of separating this mechanism from vapor deposition nucleation. The two are often combined in the term "sorption nucleation". Such behavior was evident in the work of Anderson and Hallett (1976), Gerber et al. (1970), and Edwards and Evans (1968). It has been treated theoretically by Fletcher (1959). Preliminary studies at CSU have revealed that very small quantities of hygroscopic contamination on AgI aerosol can encourage this mechanism, which can be fast and efficient at warm temperatures and water saturation, in contrast to deposition.

Condensation to droplets followed by freezing on 'pure' AgI particles requires supersaturations with respect to water. Edwards and Evans (1960), and Mossop and Jayaweera (1969) concluded that 'pure' AgI cannot function in this way at the small supersaturations encountered naturally. However, Schaller and Fukuta (1979), in their study of freely suspended AgI aerosols, found the necessary supersaturations to be small, although larger supersaturations enhanced nucleation. As with much past work on mechanisms, however, discrepancies might be explained in terms of the different particle sizes used, or experimental methods employed. In this case, the aerosols used by Schaller and Fukuta were not size representative of the typical field generator effluent. They were much larger, and more favorable for condensation at lower water supersaturations. As discussed earlier, condensation to droplet-freezing also becomes very likely, even at water saturation, for mixed AgI-alkali iodide aerosols (St. Amand et al., 1971) and has been confirmed for the AgI·NaI complex by Mossop and Jayaweera (1969).

The concept of contact nucleation was discussed by Vonnegut (1949) as one hypothesis to explain the production of ice crystals for several tens of minutes following aerosol injection into his cold chamber. At that time he rejected this as being the rate determining step. Edwards and Evans (1960) on the other hand, showed that their small AgI aerosols were 200 times more efficient as freezing nuclei than as depositional nuclei and attributed this to collisions with cloud droplets. Gokhale and Goold (1968) found surface nucleation of millimeter sized droplets by AgI particles to be possible, even at $-5^{o}C$, while the nucleation ability of such particles submerged in droplets was poor. Limiting the mechanism to contact nucleation only by allowing cloud size droplets to

pass through an aerosol region, Sax and Goldsmith (1972) confirmed thermally generated AgI as an efficient contact nucleator. Cooper (1974) and Fukuta (1975) have given possible theoretical explanations for this behavior, while Alkezweeny (1971), Isaac (1972) and Young (1973) have modeled the rate of ice crystal formation in clouds by contact nucleation.

The transport of aerosol to supercooled droplets in cloud can occur by one or more processes, ie., Brownian diffusion, diffusiophoresis, thermophoresis, inertial impaction, electrophoresis, and turbulent coagulation. A description and discussion of these processes, particularly in the isothermal cloud chamber, will be reserved for Chapter 3. After collision, nucleation is not certain. Sax and Goldsmith found a steep temperature coefficient to the efficiency of the nucleation collision process, decreasing rapidly at warmer temperatures. Most researchers have explained this in terms of the active site theory of freezing nucleation. Fletcher (1970) suggested that there might be a competition occurring between the rate of freezing of droplets and the rate of dissolution of AgI particles as well. Matthews et al. (1972) specifically discussed rates of solution in cloud sized droplets and displayed theoretically, the short time available for freezing by small AgI particles at warm cloud temperatures.

The majority of the studies previously mentioned examined the mechanistic behavior of AgI aerosols by isolating given mechanisms. Also, little work was performed using the same aerosols as are used for field experimentation. To do so is essential due to the sensitivity of the nucleation process to nuclei chemistry and surface properties. The importance of simultaneously occurring mechanisms in the formation of

ice crystals in supercooled clouds could only be postulated from previous studies. A proper way to answer this question is to examine nucleation behavior in laboratory clouds or natural clouds which allow natural competition for ice crystal formation. Several laboratory studies using large cloud chambers, and in a few cases natural clouds, have debated the importance of given mechanisms in the formation of ice by AgI aerosols. The advantage is the resultant ability to more accurately predict a nucleant's behavior under any given cloud conditions. The problem, however, is in determining simply from ice crystal production, exactly what mechanism or mechanisms are functioning.

At least three methods have been utilized to delineate mechanisms in competitive cloud situations. Weickmann et al. (1970) and Davis and Auer (1972) separated contact nucleation and vapor deposition nucleation by actual field generator aerosols in the CSU isothermal cloud chamber and an orographic cap cloud respectively, by analysis of ice crystals for double structured frozen droplet centered crystals (Auer, 1970). This structure has been associated with an origin as a frozen droplet, thus contact nucleation, by the above authors. Wieckmann et al. reported that all aerosols tested act primarily as contact nuclei at temperatures of $-17^{\circ}C$, while Davis and Auer reported that increases in ice crystal concentration in seeding with AgI from the $2AgI \cdot NH_4I$-acetone-water combustion system could be entirely explained by a collision nucleation mechanism at $-12^{\circ}C$. A second method has been discussed by Katz and Pilie (1974) and Katz and Mack (1980) for use in large cloud chambers. They used fluorescent tracer particles within cloud droplets and observations of replicas of ice crystals produced from thermally generated AgI to determine the percentage of ice crystals that had

frozen droplet centers. They concluded that only 2-5% of the crystals formed were the result of contact nucleations at water saturation. However, low concentrations of constantly evaporating cloud droplets and an impractical nucleant reduce the significance of their findings. Properly performed, this technique shows promise. Their work did definitely display that ice crystals with circular centers are not unique to contact nucleation by AgI aerosols, casting much doubt on the first method discussed. The final common method for distinguishing between contact nucleation and a vapor mechanism is by comparison of ice crystal appearance rates to theoretical collision rates. Blair et al. (1973) attempted such a calculation for the aerosol from the AgI·NH_4I-acetone-water system in their facility, but found only that a simple collision model was inadequate to explain their results. Davis (1974) and Garvey and Davis (1975) were much more innovative in their use of ice crystal production data from the CSU isothermal cloud chamber. Recognizing that contact nucleation is strongly dependent on particle size and droplet concentration, they noted differences in ice crystal formation rates with changes in these parameters, using the 2AgI·NH_4I-acetone-water system for particle generation. The changes observed agreed qualitatively with the concept of contact nucleation and on this assumption, they obtained excellent agreement between experimentally determined and theoretically calculated coagulation rate constants at all temperatures.

The above evidence shows that there is still much contradiction in the literature concerning the mechanisms important for ice formation by aerosols used for weather modification. This question must be answered in order to transfer laboratory results to the atmosphere. The field would benefit from a technique for the definitive determination of the

importance of various mechanisms in competitive cloud situations. The kinetics approach given in the following chapter is such a technique. With kinetics principles, the data of Garvey and Davis definitively identified nucleation by contact, with the theoretical calculations simply supplying confirmatory evidence.

2.5 Rates of Ice Crystal Formation

While it has long been recognized that there is a strong dependence of the nucleation ability of particles on temperature, the dependence on time has received for less attention. The time factor in contact nucleation has been quite evident (Edwards and Evan, 1960; Isaac and Douglas, 1972) and was discussed in section 2.4. The formation of ice crystals by any mechanism, however, is a rate process, reflecting physical and chemical barriers to nucleation. In the past this has been termed the "time lag" of ice nucleation, encompassing all the time dependences and delays which may occur between aerosol introduction into a supercooled cloud and the appearance of ice crystals. The "time lag" in ice nucleation by atmospheric aerosols was investigated by Warner and Newnham (1958), who found the rate of appearance and fallout of ice crystals decreasing exponentially with a time constant of about 15 minutes. Fletcher (1958b) interpreted these results in terms of a time dependent nucleation of a spectrum of nuclei "active" over a range of temperatures. This, however, assumes depositional behavior. Isaac and Douglas (1972) point out that the results could easily be explained by invoking contact nucleation by sufficiently small aerosols. Warburton and Heffernan (1964) reported on a similar "time lag" by AgI-NaI complex aerosols. Their time constants were shorter than those of Warner and Newnham. In both cases, however, the mixing chambers used undoubtedly

contained supersaturations as a result of the cloud introduction procedure and no consideration was given as to which mechanisms might be operative. Anderson and Hallett (1976) noted a completely different "time lag" in nucleation from the vapor onto a "pure" AgI surface, requiring a definite time lapse before ice crystals appeared.

It is quite apparent that ice crystals do not form instantaneously following aerosol introduction to a supercooled cloud. Fletcher stated in hi 1958 article that "no precise meaning is attached to the specification of 'the number of nuclei active at temperature T' unless a time is also specified." It is not likely that this has been an important operational consideration during the ensuing twenty years. This study will stress the importance of this factor in nucleation by AgI aerosols and display the utility of a knowledge of ice crystal formation rates in understanding the function of nuclei in clouds.

III. THEORETICAL CONSIDERATIONS

3.1 A Chemical Kinetics Approach As Applied to the Experiment

From a chemical standpoint, kinetics deals with the rates of chemical reactions, with all the factors which influence the rates of reactions, and with the explanation of the rates in terms of reaction mechanisms. Kinetics measurements furnish informational input. The mechanisms are derived models to explain this information.

Some definitions are necessary. The reaction rate is defined as the rate of change of concentration of a substance involved in a reaction. The functional relation between rate and concentration is called a rate expression. These are differential expressions of the general form,

$$\frac{dC_A}{dt} = f(C_A, C_B, \ldots C_N).$$

Here, C_A is the concentration of the particular product or reactant which is being followed to measure the rate of reaction. In many instances, the rate of decrease in concentration of a reactant is found to depend on the product of concentration terms,

$$\frac{dC_A}{dt} = K\, C_A^a\, C_B^b \ldots C_N^n.$$

K is referred to as the rate constant and a, b, and n are orders of the reaction with respect to each reactant. The net order of reaction is given by the sum of these exponents. A rate expression is of practical importance since it can be applied to calculate reaction times and yields. Also, it can afford an insight into the mechanism by which the reaction proceeds. The reaction may be complex on a molecular scale, but the form of the empirical rate law will suggest the particular path via which the reaction takes place.

Examination of past data on rates of appearance of ice crystals in the isothermal cloud chamber suggested that it might be possible to draw an analogy to chemical reaction kinetics and analyze and interpret these data kinetically and to delineate mechanisms for ice crystal formation. In this analogy, the cloud chamber is seen as a reaction chamber with ice nuclei, cloud droplets, and water vapor as reactants and ice crystals as the final product. The form of kinetics studied here might properly be termed phase change kinetics in a mixed aerosol system. The reaction equation is,

$$N + V + D \xrightarrow{K'} IC$$

where N, V, D, and IC are nuclei, vapor, droplets, and ice crystals respectively. The mechanisms for ice crystal formation may be summarized in the diagram below.

vapor deposition: N→IE→IC→ (collected IC)
condensation freezing to embryos: N→IE→IC→ (collected IC)
condensation to droplet freezing: N→[O]→IC→ (collected IC)
contact freezing: N→[O]→IC→ (collected IC)

Here [O] refers to a frozen droplet and IE to an ice embryo. All of these can occur in the isothermal cloud chamber. Vapor deposition can occur at any value of supersaturation above ice supersaturation. It therefore can occur at water saturation, at which the chamber is held. Condensation freezing to embryos can occur for any nuclei with hygroscopic surface contamination or a soluble component. If too much of a soluble component is present, the nuclei will become immersed in a solution droplet (condensation to droplet freezing). Contact between nuclei and droplets will always occur to some extent. Its importance in ice crystal formation will depend on the existence of other formation

mechanisms and their rates in comparison. Thus, all types of nucleation mechanisms may be studied in the isothermal cloud chamber. Only the behavior of nucleants at supersaturations with respect to water are not approachable.

For each series of processes, the rate of appearance of ice crystals will be dependent on the slowest component process. It is likely that this will be the first step in each case. That is, ice embryo formation, growth of a dilute solution droplet, or nuclei contact with droplets would be the rate determining or slowest step in the sequence. The immediate appearance of ice crystals after insertions of various aerosols in the chamber in the past has shown that the other processes are not rate determining. The elimination of such factors makes the experimentally determined kinetics easier to interpret. The rates associated with each mechanism will then be dependent, for a given nucleus, only on the concentrations of nuclei and vapor (vapor deposition, condensation freezing) or nuclei and droplets (contact freezing). The respective rate expressions are,

$$\frac{dC_N}{dt} = -K' \, C_N^n \, C_V^v \qquad (3.1.1)$$

$$\frac{dC_N}{dt} = -K'' \, C_N^n \, C_D^d \; . \qquad (3.1.2)$$

However, the isothermal cloud chamber is held at water saturation at a given temperature and droplet concentration is maintained fairly well during any given test. Therefore these quantities are constants and all processes will be psuedo n-th order. That is, they will display n-th order kinetics because the concentrations of the other reactants are

held constant. This is a handy simplification which the isothermal cloud chamber provides for in a kinetic study.

Solving the above differential equations with C_V and C_D constant and n=1 gives,

$$C_N=C_{NO}\ \exp[-K' C_V t] \tag{3.1.3}$$

$$C_N=C_{NO}\ \exp[-K'' C_D t] \tag{3.1.4}$$

C_{NO}: initial nuclei concentration.

There is no physical reason to believe that n will be any other number. Reactions that are higher order or non-integer order with respect to a single component generally involve a decomposition, collision between component molecules, or autocatalysis of reactant by product to form product. None of these can occur in nucleation in the isothermal cloud chamber. The second equation is just the equation for nuclei depletion by Brownian coagulation with droplets if K_B is substituted for K''. The formation of ice crystals in either case will follow a simple exponential law. A particle size distribution complicates matters due to size dependencies in nucleation, but evidence is that rates of nuclei depletion (ice crystal formation) are exponential in nucleation from the vapor onto a distribution of particles, and the resultant rate law in a contact process is exponential if the effective particle size distribution is sharply peaked and normal. A plot of the natural logarithm of C_N/C_{NO} versus time would then be a straight line.

Two or more of the ice crystal formation processes can occur simultaneously. Two simultaneous processes may be distinguished from experimental data by analogy to two parallel first order chemical reactions

producing the same product, as displayed, for example, by Frost and Pearson (1953). To complete the analogy, the nuclei producing ice crystals by each mechanism must be considered as different species. This is not a physically unreasonable assumption on the basis of the size cut-offs for the vapor dependent nucleation mechanisms discussed in section 2.4 and the fact (as will be shown) that the rate of contact nucleation is controlled by Brownian collection of aerosols by droplets in the ICC. The rate of collection of aerosols by Brownian motion becomes very small for aerosols greater than 500 A^{o} in diameter. In such a case the logarithmic plot of nuclei depletion will be a curve (assuming $K' \neq K''$). If one mechanism does not overwhelm the other in producing ice crystals, it is possible to fit two straight lines to the data and determine the percent production of ice crystals for each mechanism. This is possible because the net depletion of concentration is the sum of two exponential functions. The slower process (smaller slope) can be extrapolated back to time zero and eliminated from the first slope to obtain the rate of depletion by the faster process. Figure 1 is an example. If K_2 gives K', then $K_1 + K' = K''$ and K' is responsible for $(e^{-.50} \times 100)\%$ of the nuclei depletion to form ice crystals. If more than two mechanisms are functioning, it will be more difficult, but not impossible, to distinguish them from the kinetics.

To distinguish between a vapor dependent process and a droplet dependent process, one need only to examine the change in slopes with the change in one concentration at a given temperature. By raising or lowering the liquid water content (see section 4.1.1), droplet concentration can be changed in the isothermal cloud chamber. K' will not change with droplet concentration. Absolute vapor concentration can be

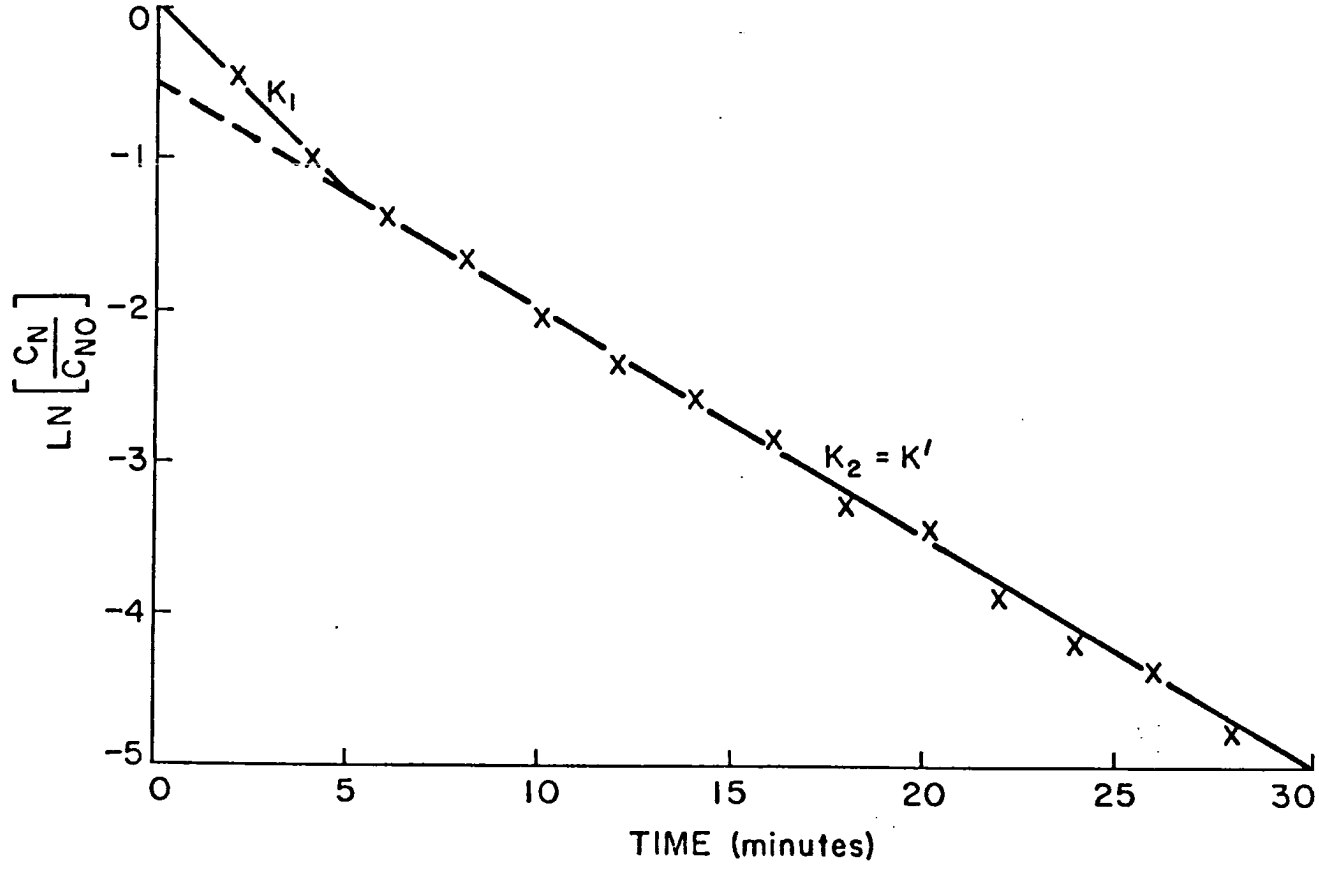

Figure 1. Analytical Separation of two first order chemical processes producing the same product.

changed only by changing temperature. It should be possible to distinguish between the condensation freezing and deposition mechanisms by correlating the kinetics, nuclei chemistry, and the effects of changing particle sizes. When the mechanisms are distinguished, the K values for each component process will be transferable to the atmosphere at water saturaton. Only K'' will need to be adjusted to account for varying droplet sizes and concentrations. This theoretical first order kinetics treatment thus suggests an experimental method for studying rates and mechanisms of ice nucleation. A kinetic analysis of data should be simple as long as the processes beyond nucleation in the diagram of page 23 are fast compared to nucleation and there are no artifacts introduced by the use of a particle size distribution. Indeed, size classification would be most desirable in a proper kinetic study, but was not available for this research.

The assumption of first order in the present discussion was a matter of convenience for a description of mixed aerosol phase change kinetics, as well as a reflection of expectations and observations prior to the analysis. However, similar methods could just as well be used on data which displays second order kinetics and so on, or any combination of such. The analogous theory exists in many kinetics texts (see, for example, Moore, 1972) for determining what order or combination of orders a data set displays. In general, this entails plotting the respective expressions versus time which would give a linear plot in each possible situation. The proper data, if examined properly, supplies the facts concerning which mechanisms are functioning. The proper data is the concentration or fraction of reactant or product (ice crystals) as a reaction (nucleation) proceeds.

3.2 Kinetics Determined From Aerosol-Droplet Collision Theory

It has been mentioned that some past data from the isothermal cloud chamber (hereafter referred to as the ICC) has shown the formation of ice crystals by the aerosols from the $2AgI \cdot NH_4I$ - acetone - water system to be fairly slow. Collisions between nuclei and cloud droplets then, most certainly occurred and may have been the primary mechanism for ice crystal formation as concluded by Davis (1974). The addition of NH_4ClO_4 to this system was not expected to introduce chemical changes in the aerosol that would change the dominant mechanism for ice crystal formation. In light of these facts, it seemed appropriate to develop a theoretical kinetics model based on aerosol - droplet collisions, for comparison with the experimental kinetics. This would provide added evidence concerning the experimentally derived mechanisms for ice crystal formation. Since this is performed solely for confirmatory purposes, simplifying assumptions are made, many of which are derived from the extensive theoretical work of Davis (1974).

In section 2.4, the various possible methods for the transport of aerosols to cloud droplets were listed. Brownian diffusion of aerosol particles to cloud droplets is particularly important for particles less than 1000 A^o in diameter. It can be quantified by the well-known equation,

$$\frac{dC_P}{dt} = -K_B \, C_P \, C_D \qquad (3.2.1)$$

where C_P: concentration of aerosol particles (m^{-3})

C_D: concentration of cloud droplets (m^{-3})

K_B: Brownian coagulation coefficient (m^3 sec^{-1}).

Diffusiophoresis is the transport of aerosol particles due to concentration gradients in a non-uniform, but isothermal, gas mixture. The aerosol particles will move in the direction of the diffusive flux of heavier gas molecules. Consequently the effect is to draw the particles toward condensing droplets and away from evaporating droplets. Since droplets in the ICC are constantly evaporating, the diffusiophoretic effect prevents collisions. There appears to be little dependence on particle size (Goldsmith and May, 1966). Young (1974) has theoretically compared the aerosol transport rate by Brownian diffusion and diffusiophoresis for 10 μm cloud drops growing at 0.3 % supersaturation. He found the former to dominate for particles less than 800 A^{o} in diameter under such conditions.

Thermophoresis describes the transport of aerosol particles as a result of thermal gradients in the carrier gas. Since warm air molecules have a higher kinetic energy than cold air molecules, the resultant transport is toward evaporating droplets and away from condensing droplets. Thus there is a competition between thermophoresis and diffusiophoresis. Davis (1974) investigated the theoretical resultant transport of AgI particles in the ICC by these two effects. Computations for mean particle diameters of 130, 190 and 490 A^{o}, and mean droplet concentrations of 2090 and 9410 cm^{-3} showed that the net transport is dominated by thermophoresis (toward droplets), but in all cases is two orders smaller in magnitude compared to Brownian diffusion. Mean particle diameters and droplet concentrations used in the present research are within the range of these reported values and thus, this transport process is considered negligible.

Inertial impaction occurs when particles with differing velocities collide with each other. St.-Amand, et al. (1971b) showed this factor to be small in comparison to Brownian diffusion for small water droplets and typical silver iodide generator aerosols, which have mean diameters generally well below 1000 A^{o}. This factor is negligible in this research as well.

It is difficult to assess the relative importance of electrical effects on the collection efficiency of submicron aerosols by cloud droplets due to the sparse knowledge of charge distributions on supercooled cloud droplets and AgI aerosols. Past attempts to measure the charge on supercooled droplets in the ICC have failed to detect a charge. Electrophoresis is thus not considered to play any role in the collision process between droplets and aerosol particles in the ICC.

The influence of turbulence on the coagulation rate has been discussed and demonstrated by Greenfield (1957) and Isaac and Douglas (1972). It becomes important only for particles greater than about 2000 A^{o} in radius and is ignored here.

The primary transport process in the ICC is thus Brownian diffusion. Using the expression for K_B as given by Isaac and Douglas (1972),

$$K_B = (RT)\ (3kN)^{-1} \times [R_P^{-1} + R_C^{-1} + 0.9L(R_P^{-2} + R_C^{-2})] \times (R_P + R_C) \qquad (3.2.2)$$

where,

R: universal gas constant (J $mole^{-1}$ K^{-1})

T: temperature (K)

k: coefficient of viscosity of air (N s m^{-2})

L: mean free path of air molecules (m)

N: Avogadro's number

R_P, R_C: radius of particle, cloud droplet (m) and

L can be calculated from

$$L = (k\pi^{1/2}) \ (2 \ P \ d_a)^{-1/2} \qquad (3.2.3)$$

P: pressure ($N \ m^{-2}$)

d_a: density of air ($kg \ m^{-3}$).

Equations (3.2.1), (3.2.2), and (3.2.3) are used together to describe the theoretical collection of aerosol particles by cloud droplets. Additional aerosol losses to collection by ice crystals and self coagulation (see section 5.1) are considered negligible. Solving (3.2.1) gives,

$$\left(\frac{C_P}{C_{P0}}\right)_{BD} = \exp(-K_B \ C_D \ t) \qquad (3.2.4)$$

where C_{P0} is the initial nuclei concentration. When multiplied by 100, the natural logarithm of (3.2.4) plots on the same scale as the experimental kinetics plot.

Values from (3.2.4) are not directly comparable to the experimental results without the consideration of two additional factors induced by the experimental technique. These are the cloud introduction airflow and chamber wall effects. The cloud airflow evaluates nuclei from the chamber at an increasing rate with decreasing temperature (a higher airflow is required at colder temperatures). This particle size independent dilution can be described mathematically by the equation,

$$-\left(\frac{dC_P}{dt}\right)_{AD} = \frac{\alpha}{v} C_P \qquad (3.2.5)$$

where

α: dilution rate (liters sec^{-1})

v: chamber volume (liters).

Solving (3.2.5) gives,

$$\left(\frac{C_P}{C_{P0}}\right)_{AD} = \exp\left(-\frac{\alpha}{v} t\right). \qquad (3.2.6)$$

Multiplication by 100 and taking natural logs once again allows this effect to be plotted on the same scale as a kinetic plot.

The quantification of diffusional loss to the walls is a more difficult task. Davis (1974) used the expression given by Fuchs (1964) for the rate at which aerosol particles diffuse to the walls of a storage vessel in which there is some convection. This is,

$$\left(\frac{dC_P}{dt}\right)_{WD} = \frac{-A_{SC}}{V_C} \cdot \frac{D_P}{\Delta} \cdot C_P \qquad (3.2.7)$$

where,

Δ: thickness of the stagnant air layer near the chamber walls (m)

D_P: thermal diffusion coefficient of the AgI particles (m^2 sec^{-1})

A_{SC}: surface area of the chamber test volume (m^2)

V_C: chamber test volume (m^3).

D_P can be calculated by the Einstein relationship, $D_P = KBT$, where K is Boltzmanns's constant, B is particle mobility given by,

$$B = (6\pi\nu R_p)^{-1} \left[1 + A\frac{L}{R_p} + Q\frac{L}{R_p}\exp\left(-\frac{bR_p}{L}\right)\right] \qquad (3.2.8)$$

ν: kinematic viscosity of air ($m^2\ s^{-1}$)

A,Q,b: empirical constants

and T is the absolute temperature in degrees K. Common values for A, Q, and b are 0.864, 0.29, and 1.25 respectively (Davies, 1966). The chamber volume is 0.96 m^3 and surface area is 4.8 m^2. Thus,

$$\left(\frac{dC_p}{dt}\right)_{WD} = -5.0 \times 10^{-2} \times \frac{D_p}{\Delta} C_p. \qquad (3.2.9)$$

While the calculation of D_p is fairly straightforward, the wall loss is highly dependent on Δ, a quantity whose value for the ICC has not been accurately determined. Δ is the distance from the wall where the coefficients of molecular and convective diffusion are equal. Davis references several authors who have measured Δ at between 0.05 and 850 μm for various unstirred volumes. He inferred a value of 200 μm for the ICC based on previous experiments at CSU on the decay of similar generator effluent in another large container. However, he pointed out that this value of Δ may not be accurate for cloud conditions, especially at warmer cloud temperatures with higher absolute vapor density. Since this theoretical comparison is considered a minor aspect of this study, no effort was made to experimentally determine more accurate values of Δ for the ICC. Solving (3.2.9) gives,

$$\left(\frac{C_p}{C_{PO}}\right)_{WD} = \exp(-2.5 \times 10^4\ D_p\ t) \qquad (3.2.10)$$

which can be plotted on a kinetic plot in a similar fashion to Brownian coagulation and airflow effects.

Summing the slopes of the three kinetic plots produced from (3.2.4), (3.2.6), and (3.2.10) will give the kinetic plot for the theoretical transport of aerosol particles to cloud droplets in the presence of the airflow and wall diffusion dilution mechanisms. This is then directly comparable to the experimental plot determined from the production of ice crystals.

IV. INSTRUMENTATION AND EXPERIMENTAL PROCEDURES

4.1 Facility Instrumentation and Techniques

4.1.1 Isothermal Cloud Chamber

The CSU isothermal cloud chamber (ICC) has previously been described in approximately the present configuration by Garvey (1975). A few modifications and recalibrations were performed during this research.

1) the installation of a Particle Measurement Systems forward scattering spectrometer probe (FSSP)
2) chamber cross-sectional dewpoint calibration
3) cloud introduction airflow recalibration
4) the installation of an acoustic sensing ice crystal counting device.

The FSSP enabled an accurate determination of droplet concentrations and sizes, and variations of these with temperature and time. Spatial variations of these parameters and cloud uniformity were inferred from the dewpoint calibration. A suspected error in the assumption of a constant cloud introduction airflow (Garvey and Davis, 1975) led to the recalibration of this rather important parameter. The acoustic counter is a first step toward the goal of replacing the present slide counting technique with a continuous technique that will not disturb the cloud.

The chamber configuration is diagrammed in Figure 2. The cloud is continuously replaced by atomization of distilled water with a Monaghan 670 ultrasonic nebulizer. Cloud droplets are mixed with cold air and allowed to equilibrate thermodynamically by rising through the center standpipe. Liquid water content (LWC) can be varied from 0.3 gm^{-3} to

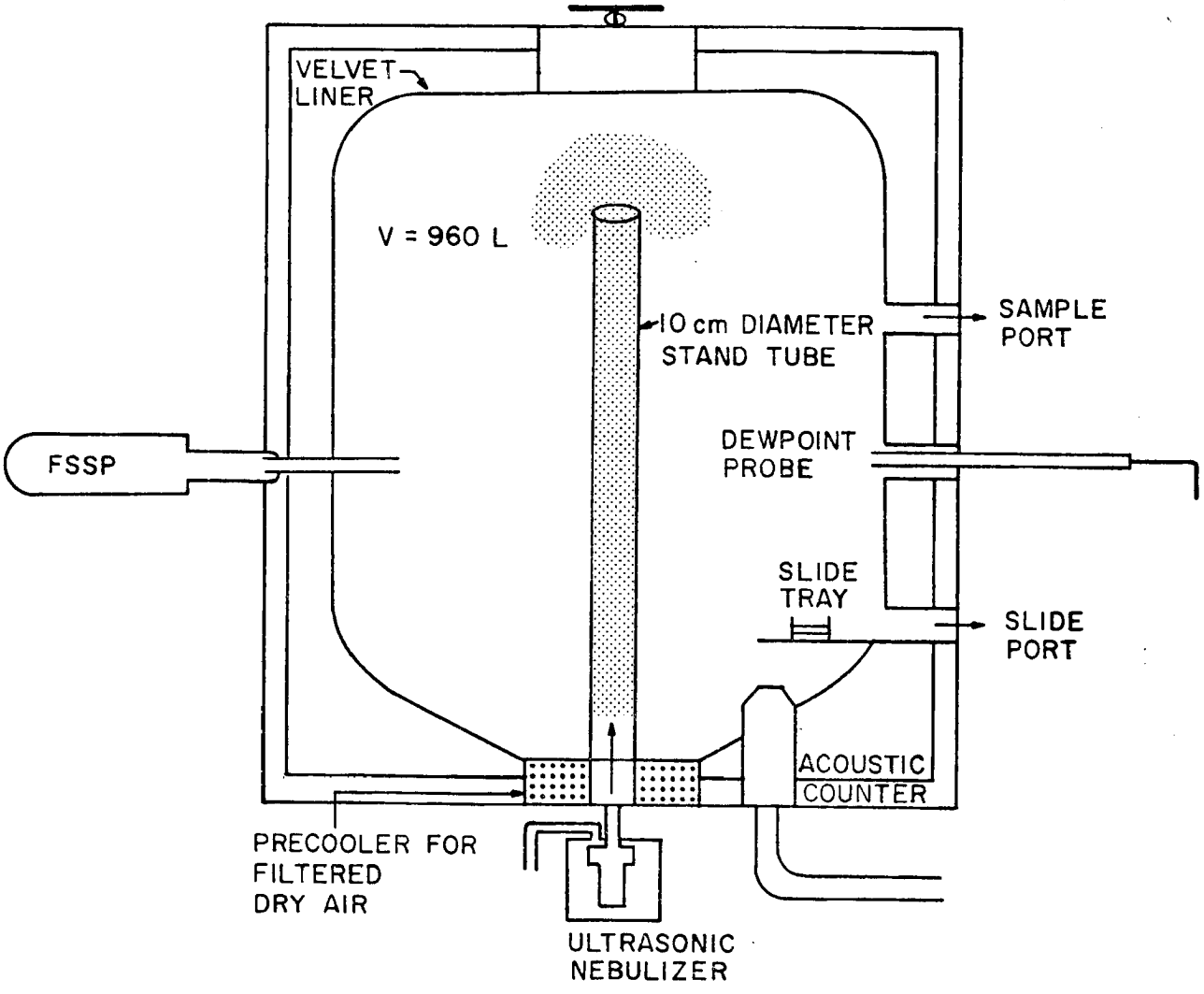

Figure 2. Schematic of the CSU Isothermal Cloud Chamber.

3.0 gm^{-3}. Temperature within the 960 liter experimental volume (monitored by an array of thermocouples) can be maintained to within $\pm$ 0.2°C of that desired over a range from 0°C to -16°C. Time response is limited by the 35 second recording period of the chart recorder. Gradients of as much as 0.5°C have been noted at -20°C.

The cloud density is controlled by varying the rate at which cloud droplets are introduced into the ICC. It is monitored continuously near the chamber wall, using a Cambridge dew point hygrometer. The technique employed is to evaporate a cloud sample and measure its dewpoint temperature. The difference between the saturation mixing ratio corresponding to this temperature and that corresponding to the cloud temperature is the LWC. It is important to maintain fairly uniform cloud density throughout the chamber. An extended dew point probe was designed to examine any variations of cloud density. For a LWC of 1.5 gm^{-3}, the variations in time can be approximately $\pm$0.15 gm^{-3}. In a cross-section between the wall and the standpipe at -12°C, the LWC was found to be 1.5 $\pm$0.15 gm^{-3} during a number of passes. The cloud is thus very uniform. For a LWC of 0.5 gm^{-3}, the variations in time can be $\pm$0.10 gm^{-3}. Multiple passes at -12°C with this cloud density showed, however, that the LWC is 0.5 gm^{-3} to within six inches of the standpipe, but increases to 0.8 gm^{-3} at the standpipe. Deviation can range from $\pm$0.10 gm^{-3} at the wall to $\pm$ 0.20 gm^{-3} at the center. The cloud character is thus less steady at 0.5 gm^{-3} LWC, as inferred from the dewpoint hygrometer.

To maintain cloud density at a given temperature an airflow into, and thus out of the ICC is necessary. Garvey and Davis (1975) assumed a constant airflow of 40 liters per minute. This was incorrect. A

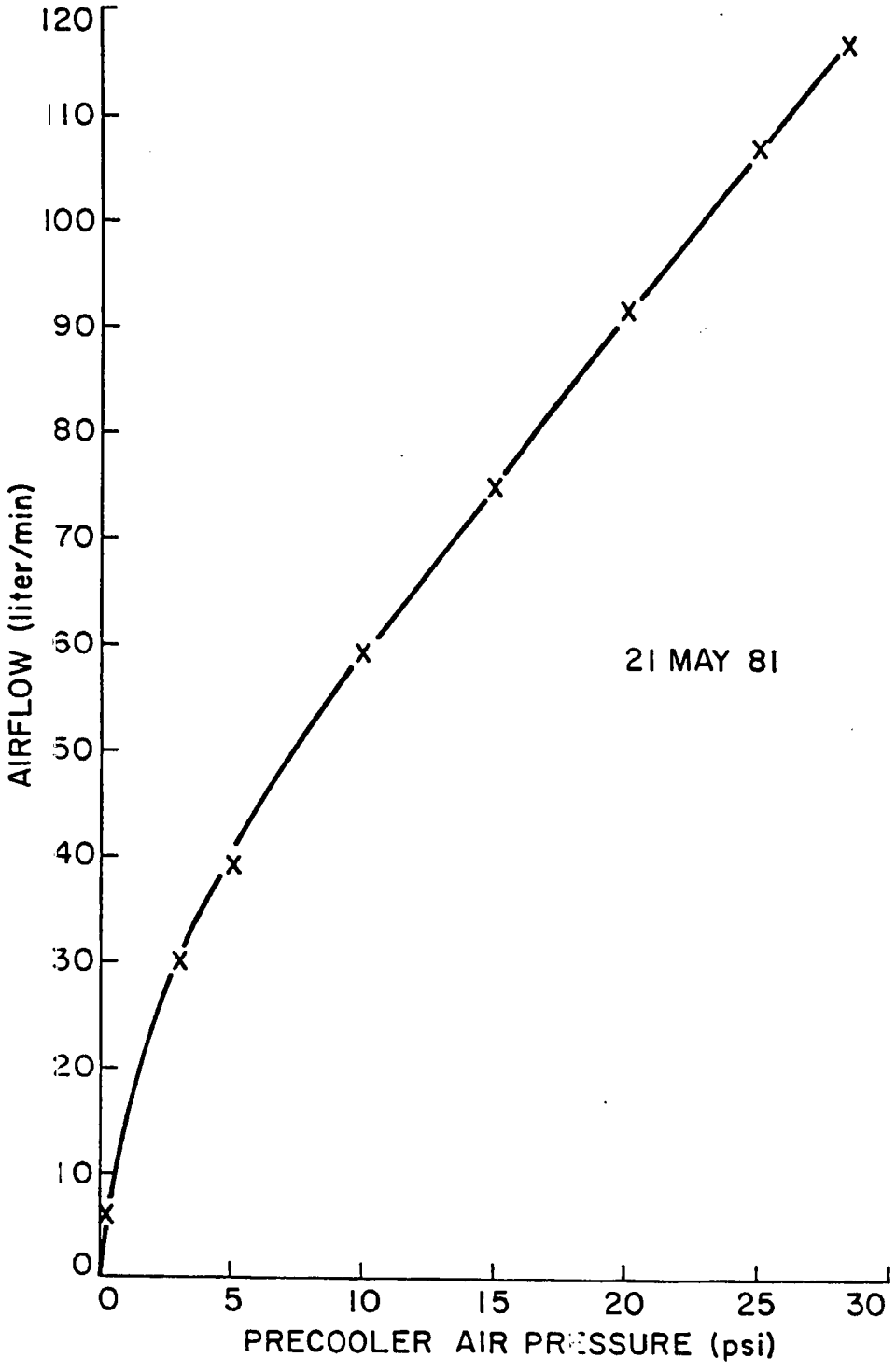

Figure 3. Cloud introduction airflow versus precooler air pressure for the determination of the airflow dilution factor.

calibration was performed using a gas flow meter. The results appear in figure 3, in the form of precooler air pressure versus airflow. It can be seen that the airflow can range as high as 116 liters per minute, which is attained at -20°C. The airflow at any temperature is noted by simply reading the precooler air pressure. The strong temperature dependence of this variable leads to different nuclei dilution rates as discussed in section 3.2, and must be considered in interpreting the experimental kinetics and absolute effectiveness values as well. This is discussed in section 4.4.

Droplet size distributions determined from 1-10 minute averages of FSSP data appear in Appendix A for all temperatures, and liquid water contents of 0.5 gm^{-3} and 1.5 gm^{-3}. These are given as the percent of total droplet concentration per size bin. The FSSP measures the amount of light scattered into collecting optics during particle transit through a focused laser beam (Knollenberg, 1976). The auxiliary 2 to 15 micron diameter size range was used to size droplets into one micron width bins. Number concentrations and normalized percent size distributions were formed by noting that,

$$\frac{\text{total\#droplets}}{\text{cm}^3} = \frac{\text{LWC} \times 10^{-6}}{\Sigma f_i m_i}$$

where, f_i: fraction of total droplets in size bin i.

m_i: mass of a droplet of radius r_i.

and an integrated mean bin radius calculation is used to determine r_i,

$$r_i = \left[\frac{(r_b^4 - r_a^4)}{4(r_b - r_a)}\right]^{\frac{1}{3}}$$

r_a and r_b being the extreme values of a bin. LWC was taken as the value given by the dewpoint probe. This was considered more accurate than assuming a flow rate for the FSSP to obtain numbers per cm^3. A modified

sampling tube (1.5 mm diameter) was utilized to accelerate droplets through the focused laser beam and achieve statistical concentrations. Raw data was corrected on the assumption of parabolic flow. Tests showed no sampling error as a result of possible evaporative losses while in transit within the tube. It is noted that there is little significant change in the droplet size distributions with temperature, except at the high and low ends of the temperature spectrum, where it peaks more sharply. Also, the 0.5 gm^{-3} LWC clouds have more sharply peaked distributions with a smaller mean droplet size. In no case are the distributions peaked as strongly as the distribution obtained several years ago by collection of droplets on soot coated microscope slides (shown also in Appendix A). Figure 4 displays the total droplet concentration versus temperature. There is an indication of a concentration minima in the $-12^{o}C$ to $-14^{o}C$ temperature range, but considering daily variations, values of 4250 cm^{-3} and 2000 cm^{-3} might be chosen as representative of the 1.5 gm^{-3} and 0.5 gm^{-3} clouds respectively, over the $-6^{o}C$ to $-20^{o}C$ temperature range.

The acoustic ice crystal counter will not be discussed here, as it is still in the testing and calibration stage and did not provide data for this research.

4.1.2 Vertical Dilution Tunnel

This part of the facility has been described and characterized in detail by Garvey (1975). The CSU standard test generator was operated below the tunnel, which was operated in both the natural draft and maximum fan displacement (114,000 cfm) modes for this research. Sample collection is performed at the first rooftop platform with a 4.25 liter

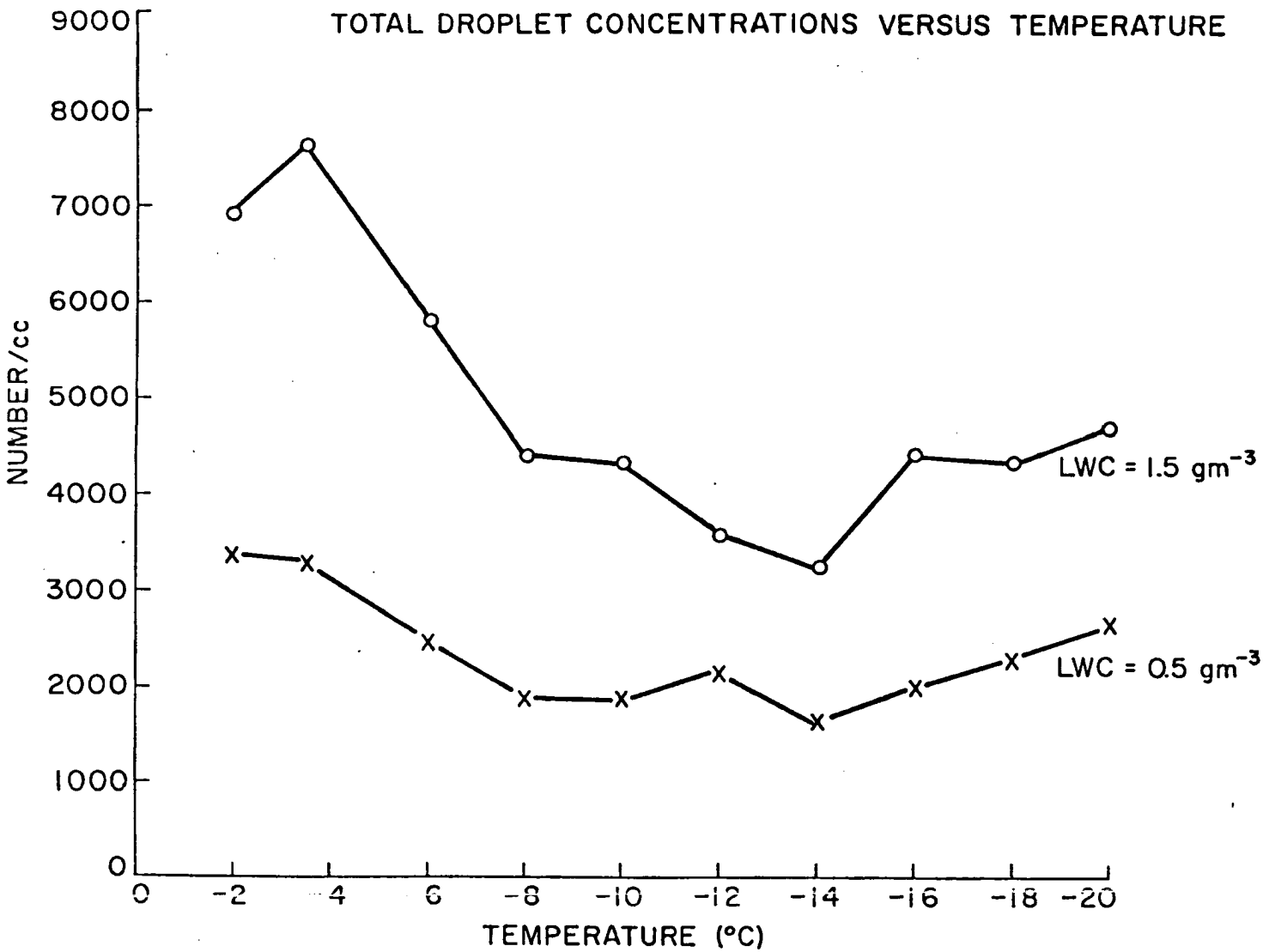

Figure 4. Total cloud droplet concentrations versus temperature for liquid water contents of 0.5 gm^{-3} and 1.5 gm^{-3} (by FSSP).

syringe. Samples can be diluted with dry (-30°C dewpoint) air before insertion into the cloud chamber.

4.1.3 Electrostatic Precipitator

Particle size determination was a necessity for this research. A commercial classifier was not available, so a simple electrostatic precipitator was designed for aerosol collection onto a substrate which could be analyzed by scanning electron microscopy (SEM). A description of the precipitator and a calculation of its theoretical collection efficiency are given in Appendix B. Before applying such corrections to particle size distributions determined by SEM analysis, it was necessary to compare with observations of deposition patterns on the substrate to determine the validity of such theoretical calculations for the designed precipitator. This is discussed in section 5.2. Aerosols were collected in the wind tunnel at a position below the syringe sampling site. A 0.005 inch thick tin sheet was used as a precipitation substrate.

4.1.4 Scanning Electron Microscope

Aerosol samples collected by electrostatic precipitation were analyzed at the scanning electron microscope facility of the CSU anatomy department. The microscope used was a Hitachi HHS-2R with capabilities to 100,000X (100 A^{o} resolving power). Energy dispersive x-ray analysis for composition was simultaneously available. Substrate samples were coated with approximately 150 A^{o} of conductive AuPd (gold-palladium) coating after mounting with copper tape onto microscope stubs. This value was quoted from calibration curves for the Technics Hummer V sputter coater used for deposition, and must be subtracted from the size distributions measured from photomicrographs. Representative samples were taken across the width of the collection substrate

and photomicrographs were taken at 50,000X (200 A^{o} per millimeter) for particle sizing. Particles were sized into 100 A^{o} bins by visual ruler estimation.

4.1.5 Neutron Activation Analysis

Neutron activation analysis of aerosol samples collected on nucleopore filters was performed at the Rhode Island Nuclear Science Center. This was necessary to obtain a quantitative assessment of the amounts of AgCl actually produced by generation of different solutions. The technique used is to bombard a sample with a neutron beam to force acceptance and unstable isotope formation by the atoms. The gamma ray emissions by various isotopes of elements during their subsequent decay can be displayed by a spectrometer. The mass of a given element can be fairly accurately determined by comparison to the emission peak amplitude of a known mass of the same element. In this manner, iodine to chlorine ratios were determined for the aerosols used in this research. This will be the same as the AgI/AgCl ratio, and from this the efficiency of conversion of Cl to form AgCl can be determined, and correlated with ice nucleation effectiveness. The assumption is made that NH_4Cl is not formed upon cumbustion. This substance decomposes at 220°C (while AgCl solidifies at 455°C) and thus is not likely to be formed during condensation following combustion.

4.2 Ice Nuclei Effectiveness Determination

Effectiveness in the ICC is determined by the total number of ice crystals which grow and fall out per gram AgI. This is calculated from the cumulative number of ice crystals falling onto microscope slides (examined in a cold box microscope) by the following equation:

$$E = N_{IC} \times \frac{A_C}{A_V} \times \frac{R_D}{R_G} \times \frac{D_S}{V_S} \qquad (4.2.1)$$

N_{IC}: total # of ice crystals collected per slide viewing area

A_C: chamber cross-sectional area (cm^2)

A_V: microscope viewing area (cm^2)

R_D: wind tunnel dilution rate (liters/min)

R_G: AgI generation rate (g/min)

D_S: syringe dilution factor

V_S: syringe volume (liters).

Slide counts are averaged per viewing area, with five viewing areas per slide removed (generally at 3-5 minute intervals after aerosol injection). A_c, A_v, and V_s are constants given by,

$$A_c = 8.35 \times 10^3 cm^3$$

$$A_v = 2.01 \times 10^{-2} cm^2$$

$$V_s = 4.25 \text{ liters.}$$

R_G will depend on the particular solution burned (due to density and flow rate differences) and is determined periodically by measuring solution density and flow rate out of the generator nozzle. R_D depends on airflow during generation. Values used for several years were used for this research. They are,

$$R_D = \begin{cases} 1.0 \times 10^5 \text{ liters min}^{-1} & \text{natural draft airflow} \\ 3.23 \times 10^6 \text{ liters min}^{-1} & \text{maximum fan airflow.} \end{cases}$$

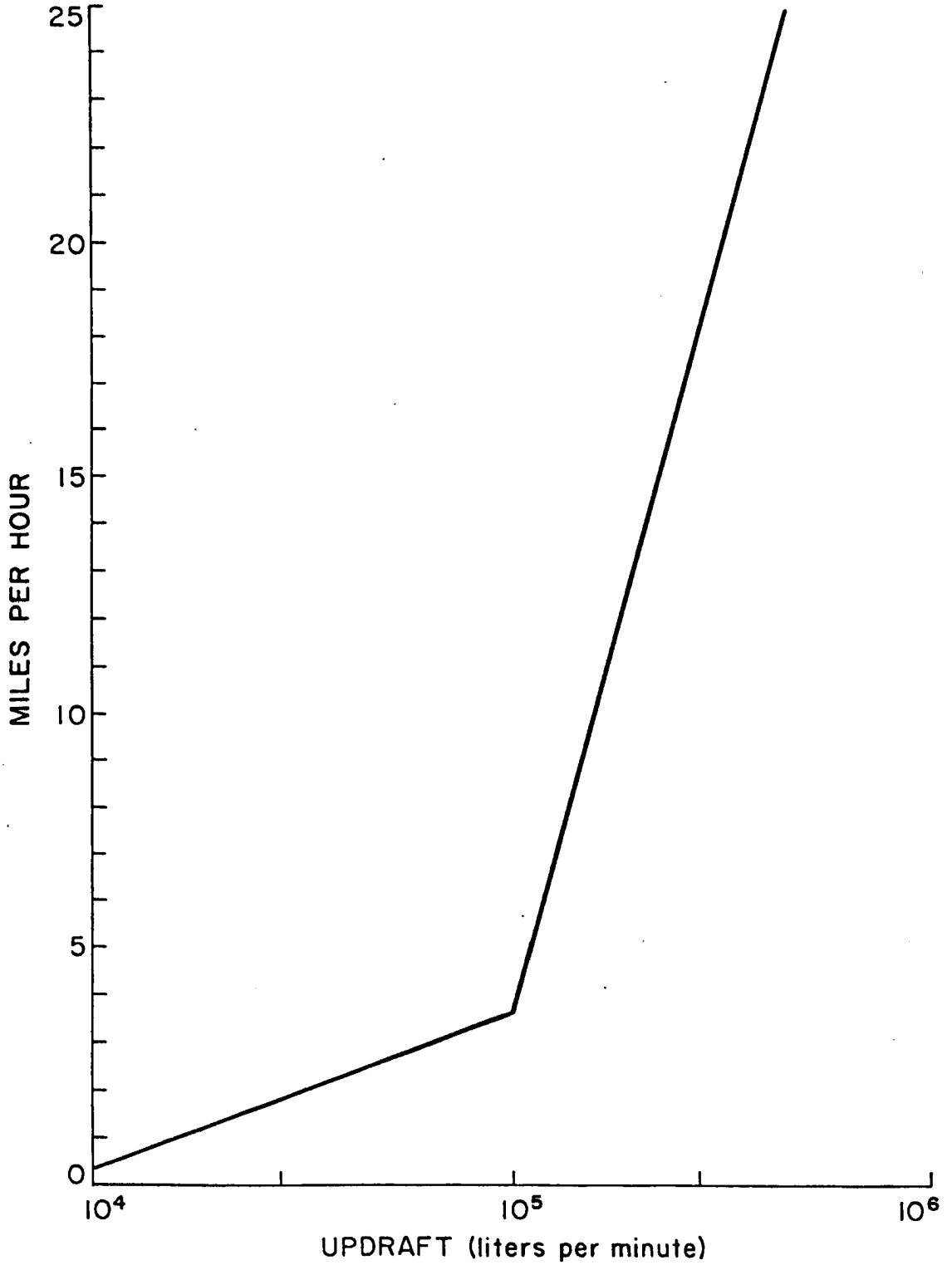

Figure 5. Wind tunnel dilution factor(liters per minute) as a function of updraft velocity(miles per hour) measured with a hot wire anemometer.

It was recognized that R_D might vary considerably under natural draft conditions. This could only be confirmed recently when a hot wire anemometer became available. Figure 5 displays the relation between vertical wind velocity in the tunnel, and dilution factor, as calculated from tunnel dimensions and a laminar flow assumption. The arrows indicate the range of values recorded since the anemometer was installed. It is obvious that the natural draft dilution factor can vary a great deal, a factor which must be considered in evaluating the results of this study, and certainly in future testing.

D_S accounts for the syringe dilution necessary to permit nucleation to proceed without depleting cloud liquid water severely. Respective dilution multiplication factors are, 8.64, 74.7, and 646, for one, two and three dilutions with dry air. Only at the warmest temperatures (-5^oC, -6^oC) was no dilution employed in this research. This situation introduces warm humid air to the chamber, bringing about the opportunity for unrealistic condensation behavior, and the results must be examined carefully.

4.3 Analysis of Rates of Ice Crystal Formation

4.3.1 Graphical Representaton of Rates of Ice Crystal Formation

As mentioned, ice crystals are counted in the ICC by the microscope slide technique. Slides are removed at three minute intervals after injection until there are less than 5-10 ice crystals per viewing area. Slides are then removed at five minute intervals until less than one crystal appears per viewing area on two consecutive pulls. In this manner, a cumulative ice crystal count is obtained. From this data, a normalized plot of ice crystal formation can be otained by computing the % production of ice crystals versus time. This allows the comparison of the rates of ice crystal appearance in different tests at the same, and different, temperatures.

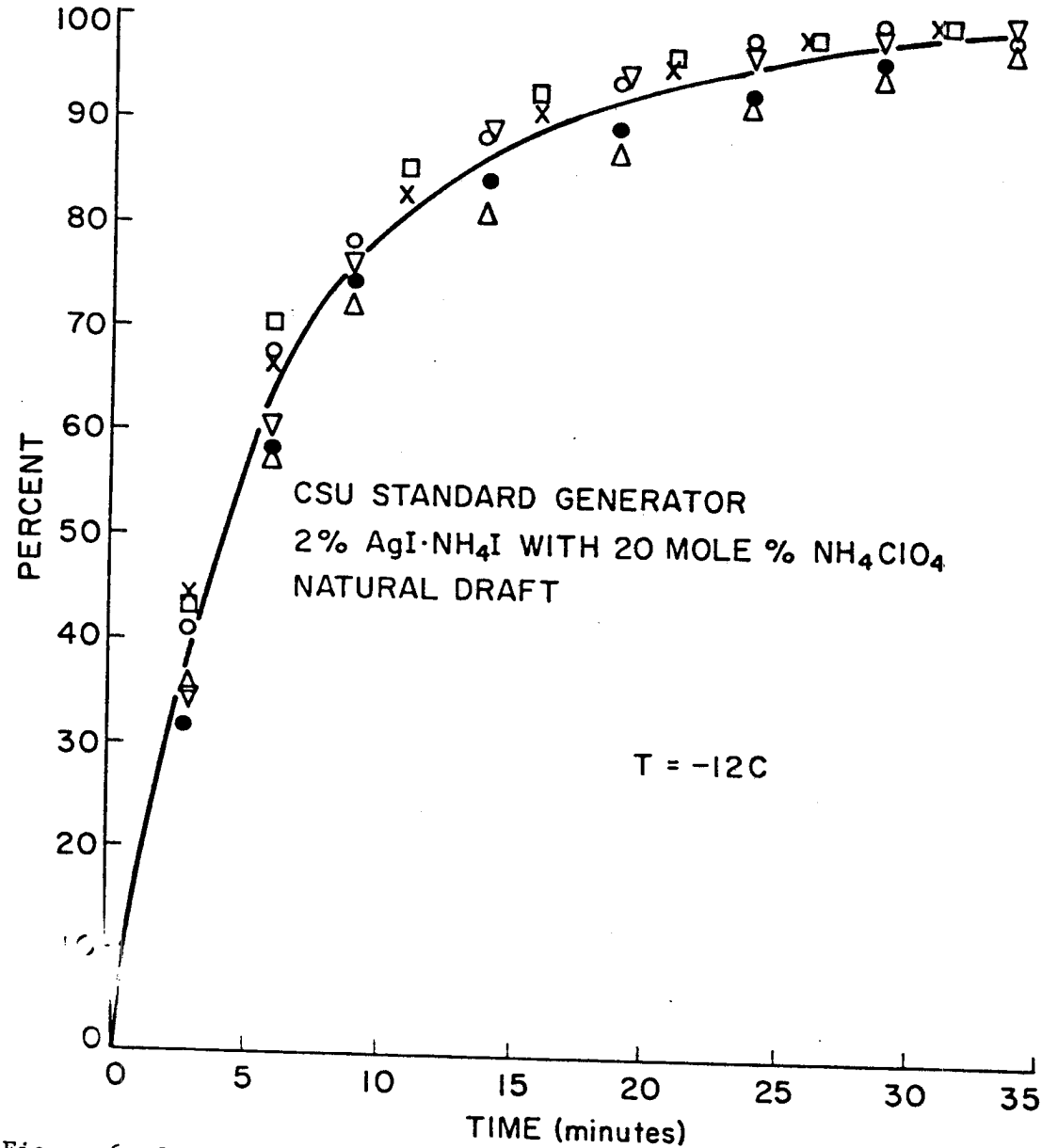

Figure 6. Comparison of the average rate of ice crystal formation (denoted by solid line) to the component rates at $-12^{o}C$ and a LWC of 1.5 gm^{-3}. Component rates are denoted by various symbols.

Since multiple tests for effectiveness are run at a given temperature, it was necessary to combine the respective plots to obtain an average plot. This was done simply by averaging ice crystal formation at any time arithmetically. Figure 6 is an example of the separate experimental curves and the average curve. Obviously some error may be involved here. However, experimental limitations justify such simplification. Different tests produce different numbers of ice crystals at any given temperature (a factor of two would not be highly unusual). Therefore, due to the existence of a detectability limit (≈40 ice crystals/liter) by the present ice crystal counting technique, the computed % production of ice crystals will vary among tests, being most representative for higher cumulative ice crystal counts. Also, concentrations and sizes of aerosols generated under natural draft dilution conditions can vary for the reasons discussed in section 4.2. This will affect both rates and yield in any nucleation process. Therefore, until generation techniques are improved (constant dilution rate or a size classification and concentration control capability), and until a more sensitive ice crystal detection technique is designed, arithmetic averaging of ice crystal formation data seems wisest. However, until improvements are made, the sensitivity of kinetic analysis of this data will be limited. Fine details may be masked.

4.3.2 Experimental Kinetics Plots

Disregarding other external nuclei dilution mechanics, the percent of nuclei depleted by nucleation will be equal to the present of ice crystals formed. In other words,

$$\% \text{ ice crystals} = [100 - (\frac{C_N}{C_{NO \text{ nucleated}}} \times 100]\ \% \qquad (4.3.1)$$

$$100 \times (\frac{C_N}{C_{NO \text{ nucleated}}} = (100 - \% \text{ ice crystals formed}). \qquad (4.3.2)$$

The first order kinetics plot is then obtained by plotting the natural logarithm of this result versus time. It will appear as in figure 1 with Ln(100-%) replacing $Ln(C_N/C_{No})$ and a y-intercept of 4.605.

4.4 Data Correction for Dilution Mechanisms

In section 3.2 airflow dilution and wall diffusion were discussed as inadvertent factors which influence the transport of nuclei to droplets in the ICC. These machanisms however will influence the rate of nuclei depletion in any process of ice crystal formation from injected aerosols. The experimental data cannot be fully interpreted unless these factors are subtracted from experimental data. Only the correction due to airflow is performed in the results however. Wall effects are excluded because of the assumption of their constancy with temperature and liquid water content (droplet concentration) for a given particle size distribution. In any case it is impossible to know which part of the particle size distribution produces ice crystals at a given temperature, and thus be able to determine the magnitude of the wall effects. Values given by Davis (1974) indicate that this is a small factor compared to airflow dilution. It becomes less important for higher airflows and faster rates of ice crystal formation. The importance of this factor could be better determined in future kinetics studies by proper size classification of aerosol particles.

Airflow dilution is strongly temperature dependent and liquid water content dependent. Since the airflow was not calibrated until the later stages of this research, it was assumed to be approximately constant over a period of time at a given temperature or liquid water content. Table 1 gives the values of the kinetic slope correction (α/v) for airflow at all values of temperature and liquid water content used in this research. Addition of these values to the values of the slope

Table 1.
KINETIC SLOPE CORRECTION FOR AIRFLOW

TEMPERATURE(^{o}C)	LWC (GM^{-3})	α/v (SEC^{-1})
- 6	1.5	.0417
- 8	1.5	.0484
-10	1.5	.0615
-12	1.5	.0771
-12	0.5	.0391
-16	1.5	.0984
-20	1.5	.1160
-20	0.5	.1160

of the respective experimental kinetics plots will give the slope of the corrected kinetic plot. These new plots will thus always have less negative slopes than the experimental plots and true changes in kinetics with temperature and liquid water content will be displayed.

Effectiveness must also be corrected for nuclei which are depleted before they can initiate ice crystals. This correction is made using an analogy to chemistry once again. If A is the number concentration of nuclei which would form ice crystals in the absence of airflow dilution at any time, then two reactions are occurring to deplete A.

$$A \xrightarrow{k_1} \text{ICE CRYSTALS (IC)}$$

$$A \xrightarrow{k_2} \text{ICE CRYSTALS LOST TO DILUTION.}$$

The governing rate law (assuming first order behavior) is then,

$$-\frac{dA}{dt} = K_1 A + K_2 A = (K_1 + K_2)A$$

so that,

$$A = A_0 \, e^{-(K_1 + K_2)t} \tag{4.4.1}$$

where A_0 is the initial number concentration of effective nuclei.

Now,

$$\frac{d(IC)}{dt} = K_1 A. \tag{4.4.2}$$

Substituting (4.4.1) gives,

$$\frac{d(IC)}{dt} = K_1 \, A_0 \, e^{-(K_1 + K_2)t}. \tag{4.4.3}$$

Integrating gives,

$$IC = \frac{K_1}{K_1 + K_2} A_0 \, e^{-(K_1 + K_2)t}. \tag{4.4.4}$$

Letting $t = \infty$, the actual (corrected) number of ice crystals produced per gram of AgI is,

$$A_0 = \frac{K_1 + K_2}{K_1} (IC)_{\text{total}}. \tag{4.4.5}$$

Here, $(K_1 + K_2)$ is just the experimentally measured rate (negative slope of experimental kinetics plot) constant and K_1 is the airflow adjusted rate constant.

4.5 Experimental Procedure

The exact procedure for achieving the study objectives was fairly straight-forward. The aerosols from the various solutions were tested for effectiveness, multiple times across full temperature spectra in the ICC, after natural draft dilution in the wind tunnel. This progressed until ice nuclei effectiveness was optimized. The aerosol from the solution with 20 mole % NH_4ClO_4 were chosen for a complete kinetics analysis, although all data was treated as described in section 4.3.2, a truly complete kinetic analysis was not possible due to time restrictions. Also, this aspect of the research was not fully formulated at the start of the program, but evolved with it. It should be considered as an initial demonstration of the power and applicability of the technique.

To facilitate the kinetics study, the 20 mole % NH_4ClO_4 solution aerosols were tested multiple times at a cloud liquid water content of 0.5 gm^{-3}, in addition to the standard 1.5 gm^{-3} used for all aerosols. This was performed at cloud temperatures of $-12^{\circ}C$ and $-20^{\circ}C$. Kinetic changes with changes in droplet concentrations is the primary means for distinguishing between droplet dependent or vapor dependent mechanisms. Given a mechanism for ice crystal formation, particle size can play an important role in both effectiveness and rates of formation. A proper kinetic study of the characteristics of a given nuclei should then include an evaluation of the effects of particle size changes. This was

achieved in two ways. A smaller mean sized particle distribution was produced by maximum fan generation of aerosol. This causes the generator flame to burn hotter and minimizes aerosol coagulation prior to sampling. A larger mean sized aerosol was produced by increasing AgI content to 6 weight percent in the solution. Full temperature spectra, including liquid water content changes, were performed in each case.

V. RESULTS AND DISCUSSION

5.1 Aerosol Analysis

5.1.1 Composition

Preliminary compositional studies using KEVEX analysis on the SEM were successful in detecting silver, iodine, and chlorine in the expected mixed aerosols. The neutron activation technique was performed on single samples only, due to time constraints. These samples were of the aerosols generated from the solutions with 20, 30, and 40 mole percent NH_4ClO_4. Samples were collected on nucleopore filters of 0.4 micron pore size, for time periods ranging from four to ten minutes. This insured the collection of all particle sizes without a significant bias in collection efficiency toward any particular size. The resulting iodine to chlorine mass ratios and chlorine to iodine molar ratios are given in table 2.

Table 2.
NEUTRON ACTIVATION ANALYSIS RESULTS FOR SOLUTION COMBUSTION AEROSOLS

SOLUTION	MASS RATIO (gm I/gm Cl)	MOLAR RATIO (mole Cl/mole I)
2% $AgI.NH_4I$ w/ 20 mole % NH_4ClO_4	19.33±1.33	0.185±0.012
2% $AgI.NH_4I$ w/ 30 mole % NH_4ClO_4	12.78±0.45	0.280±0.010
2% $AgI.NH_4I$ w/ 40 mole % NH_4ClO_4	8.33±0.32	0.429±0.016

The background iodine, chlorine, and silver concentration, determined from a blank filter, were negligible (less than .01% of that collected). The actual mole % of Cl atoms replacing I atoms in the crystal

lattice is given by, mole % Cl = $\frac{\text{molar ratio}}{1 + \text{molar ratio}}$ x 100. These values are 15.6, 21.9, and 30.0% respectively for the aerosols analyzed in table 2. These results, although from single samples, show that the conversion of chlorine from NH_4ClO_4 to form AgCl is about 75% efficient. Some chlorine may have been lost as gaseous HCl for example. The assumption that all of the chlorine is associated with AgCl and not the highly volatile substance NH_4Cl was not tested in this research. X-ray powder pattern analysis of aerosol samples for identification of mixed AgI-AgCl would certainly be desirable in the future. This would also provide the structural information to determine epitaxial changes with composition that could be correlated with effectiveness data.

5.1.2 Particle Size

Inspection of electrostatic precipitator collection foils and initial photomicrographs made it quite apparent that aerosol collection was nearly 100% efficient, contrary to theoretical calculations. Figure 7 displays particle concentration per square millimeter of foil as a function of distance within the precipitator and corresponding particle size distributions for the aerosol from combustion of the solution with 20 mole % NH_4ClO_4. There is a slight depositional dependence on particle size, large sizes being collected most efficiently, contrary to theory. Size distributions were measured from samples taken at the plus signs. This biased particle size to a slightly larger size than existed and biased concentrations to slightly lower values than existed. A fifth sampling position would have been desirable. The higher efficiency of the precipitator is likely due to the violation of laminar flow within the collection area and a higher than estimated electric field strength. Particles produced by propane combustion were eliminated from the parti-

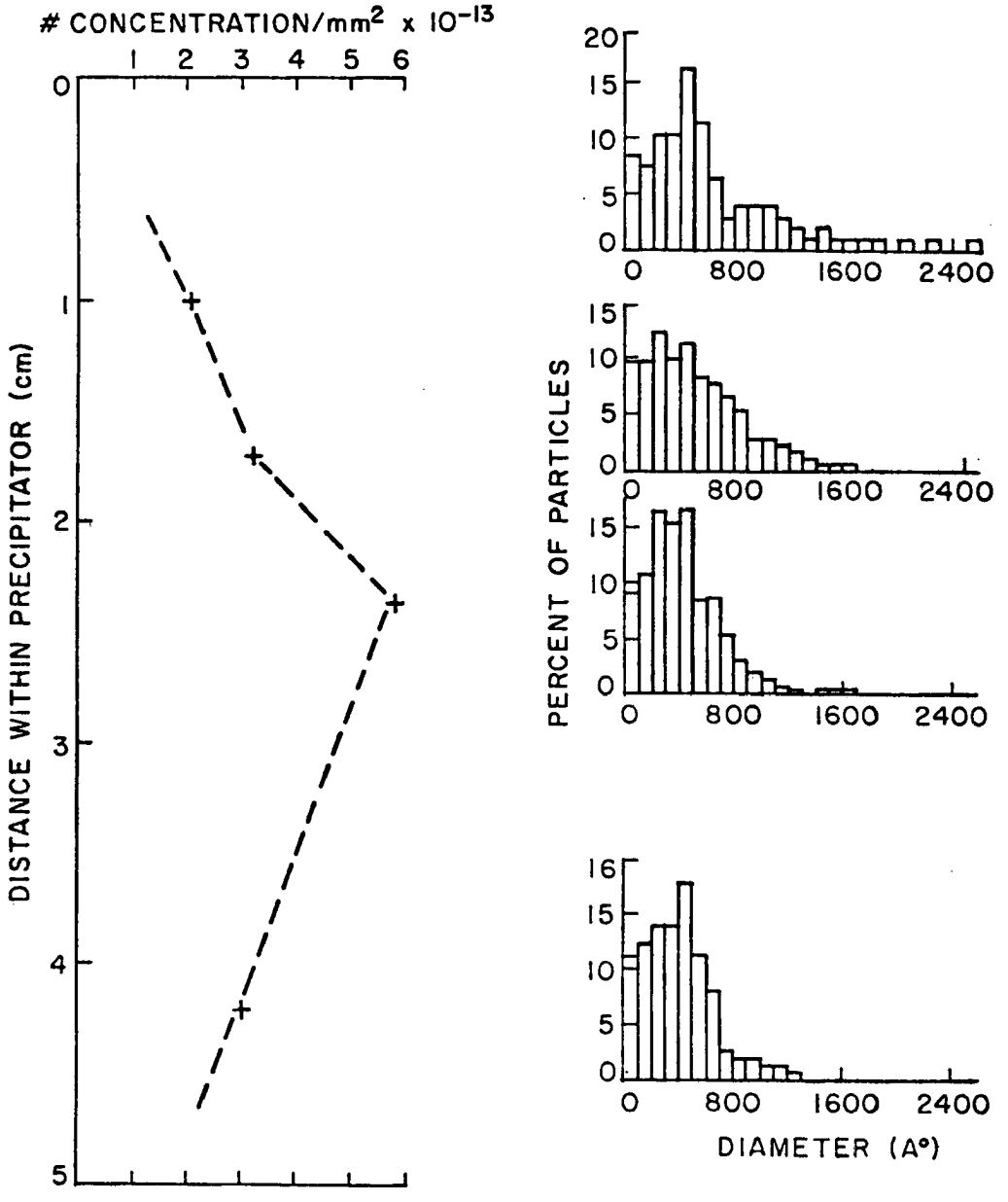

Figure 7. Typical concentrations and particle size distributions within the electrostatic precipitator.

cle size distributions, but represented only 6% of the particles, with no particular size bias.

Figures 8, 9, and 10 display the particle size distributions of aerosols generated from the various solutions used in this research. The distribution of aerosols from the solution with 10 mole % NH_4ClO_4 was not measured, but would be expected to be very similar to the distributions of figure 8. There is a general trend toward a broader peaked distribution and loss of smaller particles as the mole percentage of NH_4ClO_4 in solution is increased. Increasing the AgI content in the acetone generator solution to 6 weight % obviously has the effect of producing an aerosol with a larger mean size. Maximum fan dilution of the aerosol from the solution with 20 mole % NH_4ClO_4 markedly decreases the mean particle size (289.6 A^o versus 521.8 A^o diameter under natural draft dilution) as desired. In nearly every case, particles less than 1000 A^o were single particles, while those greater than 1000 A^o were generally aggregates of smaller particles. It can be expected then, that variable wind conditions under natural draft could alter the resulting particle size distribution to a significant extent.

One might question whether or not the distributions of figures 8, 9 and 10 could change during transport to the cloud chamber in the four liter syringe. A simple test was arranged to answer this question. An undiluted syringe of aerosol from the solution with 20 mole % NH_4ClO_4 was drawn at a low velocity through a nucleopore filter of 0.2 micron pore diameter. Collection efficiencies for all but the largest particles were estimated to be high. Figure 11, the particle size distribution from the filter, may be compared to figure 8b. Although the sample was small, there appears to be minimal coagulation occurring in the

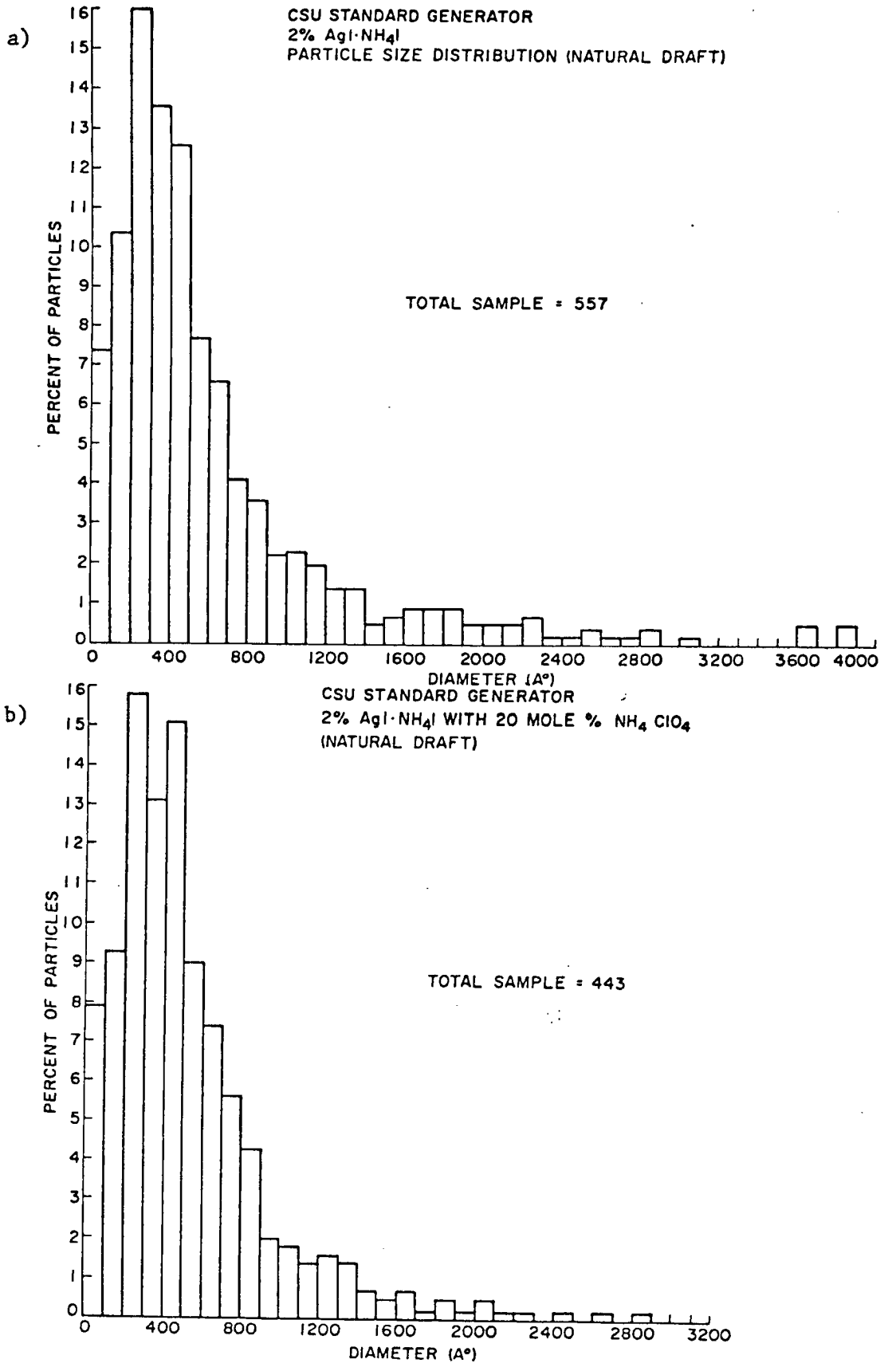

Figure 8. Aerosol particle size distributions produced from the combustion of the $2AgI \cdot NH_4I$-acetone-water (a)) solution and this solution with the addition of 20 mole% NH_4ClO_4(b)).

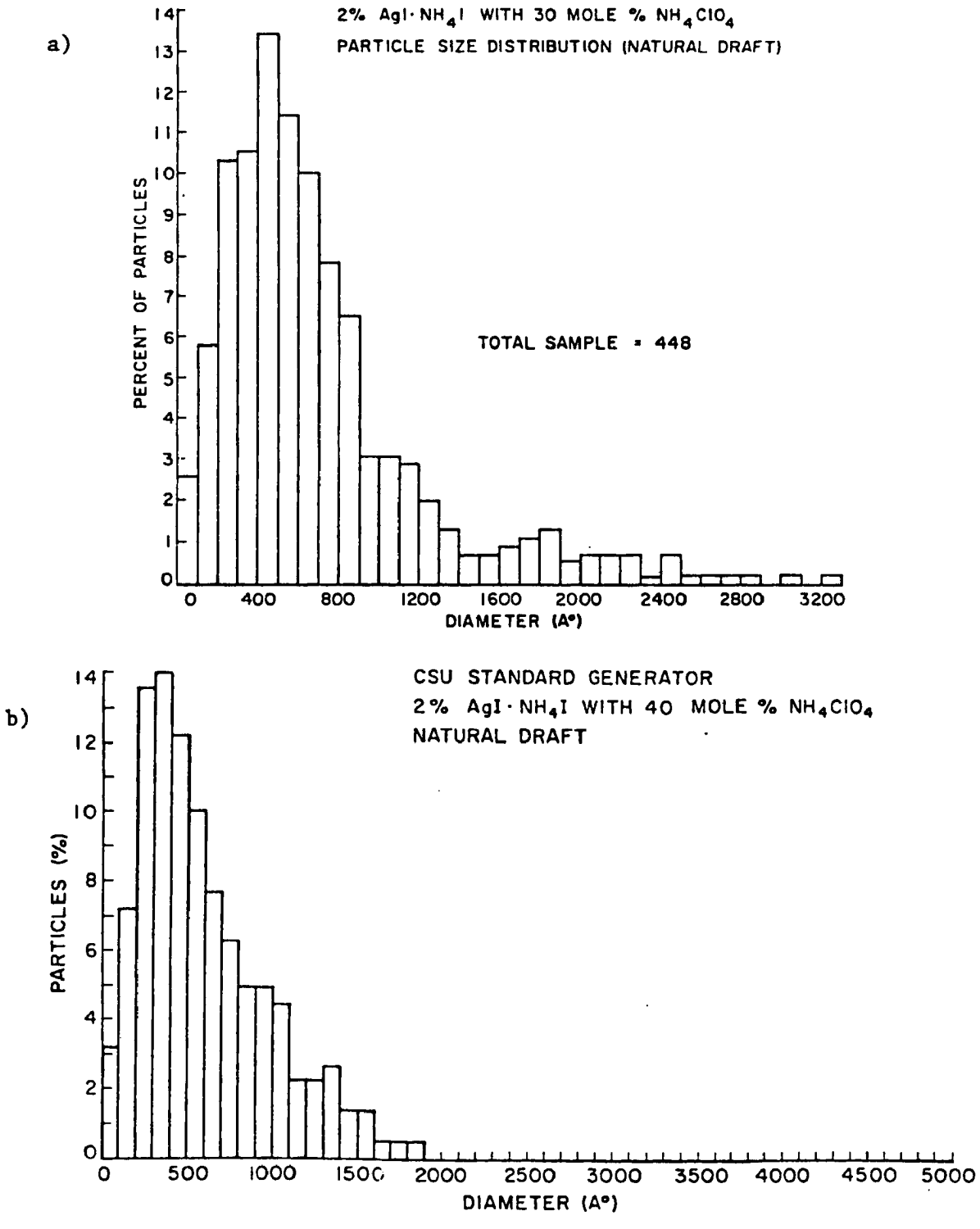

Figure 9. Aerosol particle size distributions produced from the combustion of the $2AgI \cdot NH_4I$-acetone-water solution with the addition of 30 mole% (a)) and 40 mole% (b)) NH_4ClO_4.

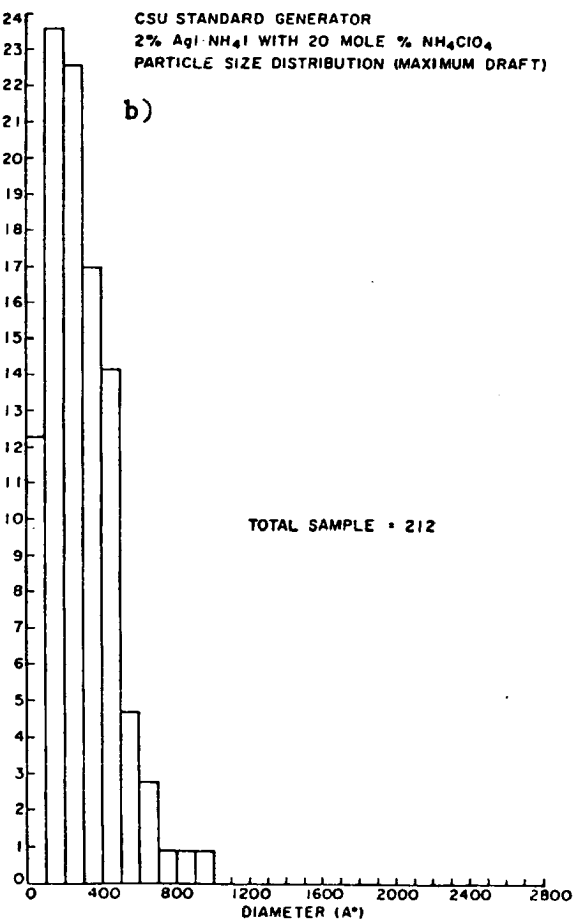

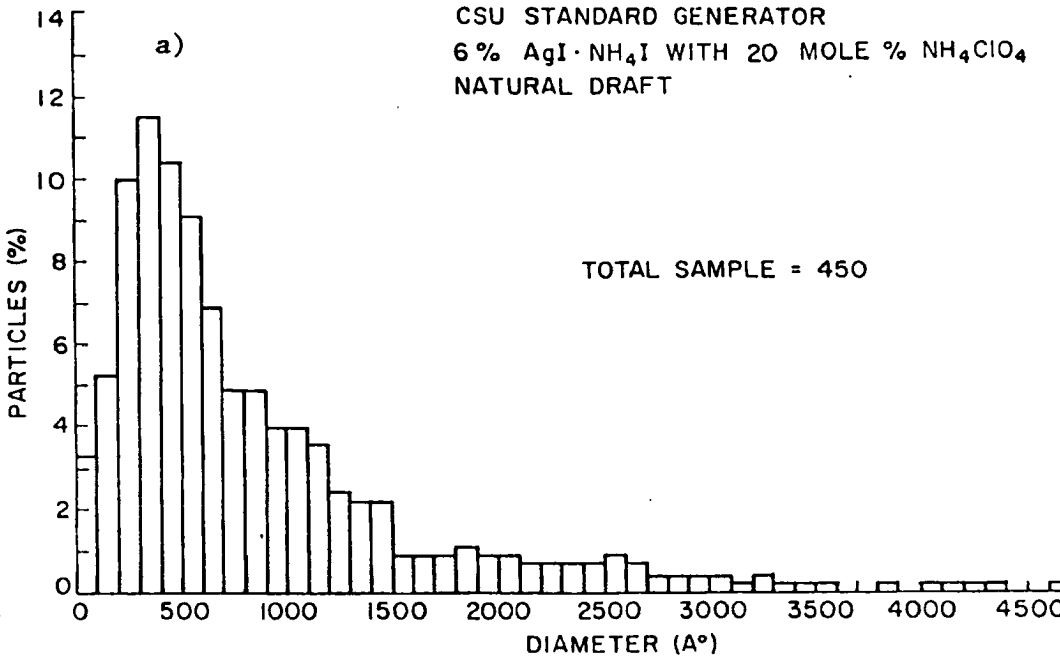

Figure 10. Aerosol particle size distributions produced from the combustion of the $2AgI \cdot NH_4I$-acetone-water with 20 mole% NH_4ClO_4 solution when the AgI content is adjusted to 6 weight% (a)) and when generated with maximum draft dilution (b)).

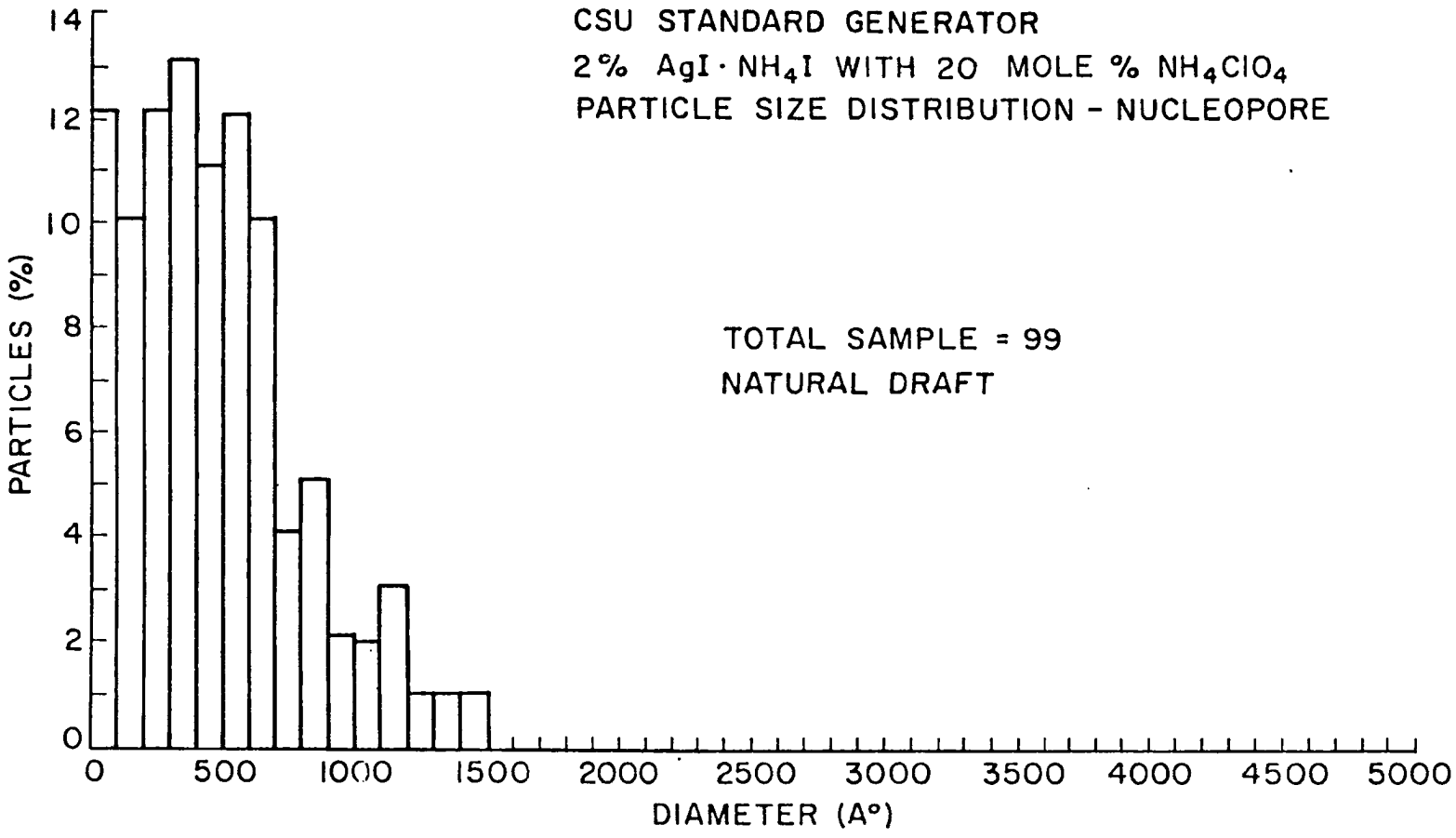

Figure 11. Aerosol particle size distribution produced from the combustion of the $2AgI \cdot NH_4I$-acetone-water with 20 mole% NH_4ClO_4 solution and collected on a nucleopore filter, directly from the syringe.

syringe, even for this situation of maximum particle concentration collected for three minutes after the normal sample injection time.

It is possible to obtain estimates of particle concentrations per gram of AgI by assuming spherical particles and computing mass distributions for each particle size distribution. Some error is definitely introduced by the assignment of spherical diameters to particles greater than 1000 A^{o}, which were generally irregular. However, the computed concentrations will give an indication as to how much of the total particle population is being utilized to form ice crystals at any given temperature. For the aerosol from the solution with 20 mole % NH_4ClO_4 it was calculated that 1.07×10^{15} and 7.3×10^{15} particles per gram are produced under natural draft dilution and maximum fan dilution respectively.

5.2 Ice Nuclei Effectiveness

The results of effectiveness determination for several of the aerosols generated in this research are given in figures 12-16. Original data points appear with solid lines denoting the best estimated fit to arithmetic mean points. Dashed lines refer to the dilution corrected mean effectiveness. These are included here, although the corrections are based on the experimental kinetics presented in section 5.4. All data shown is for a cloud liquid water content of 1.5 gm^{-3} and aerosols generated with natural draft dilution in the vertical wind tunnel.

Immediately noticeable are the differences between the standard $2AgI.NH_4I$-acetone-water solution combustion aerosol effectiveness in figure 12 and the effectivess of aerosols from the combustion of solutions with NH_4ClO_4 shown in figures 13-16. Large improvements in effectiveness in the temperature region from $-16^{o}C$ to the detectable thres-

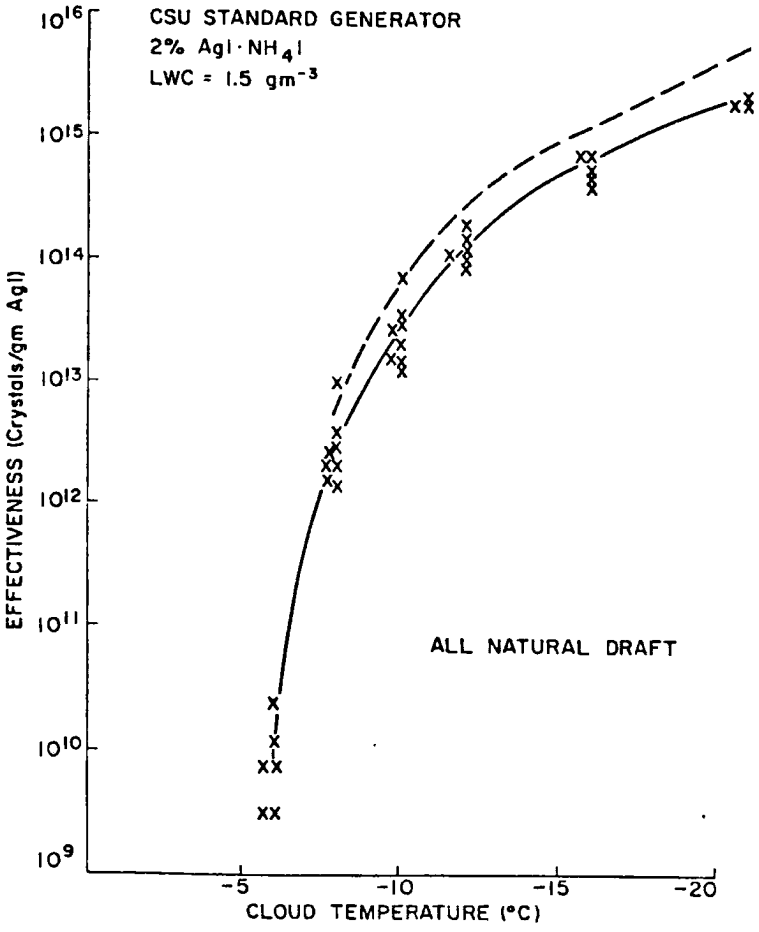

Figure 12. Ice nuclei effectiveness of the aerosol produced from the combustion of the $2AgI \cdot NH_4I$-acetone water solution.

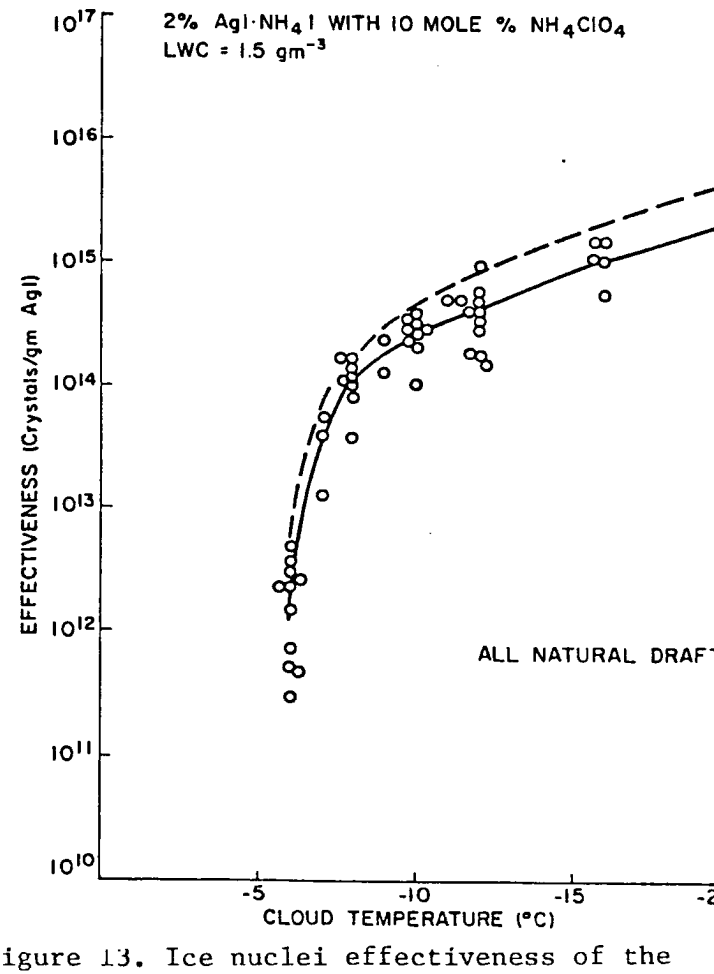

Figure 13. Ice nuclei effectiveness of the aerosol produced from the combustion of the $2AgI \cdot NH_4I$-acetone water solution with the addition of 10 mole% NH_4ClO_4.

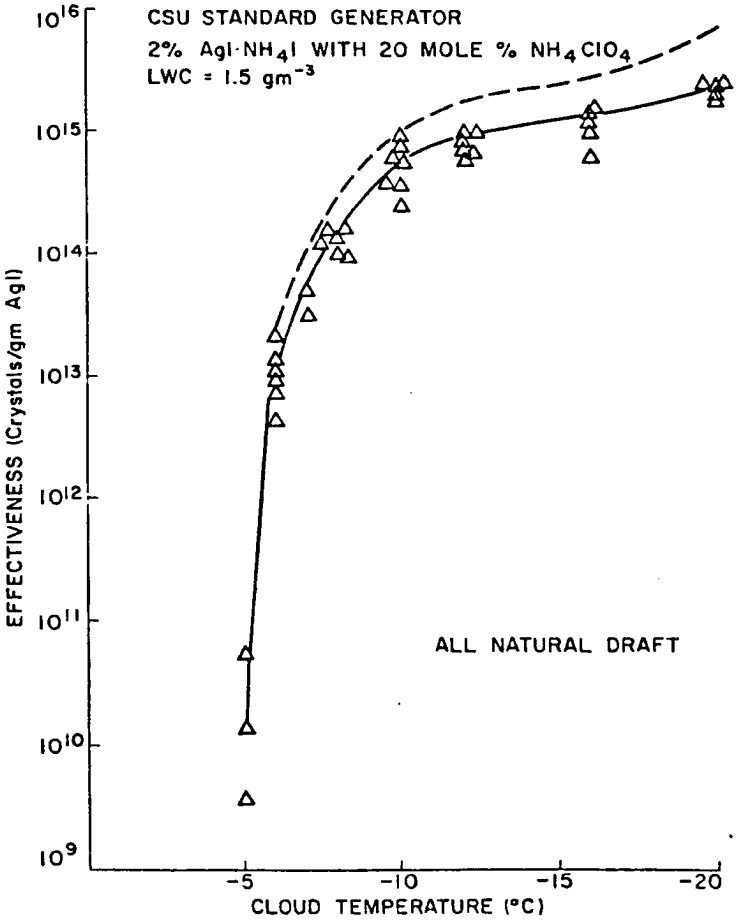

Figure 14. Ice nuclei effectiveness of the aerosol produced from the combustion of the $2AgI \cdot NH_4I$-acetone water solution with the addition of 20 mole% NH_4ClO_4.

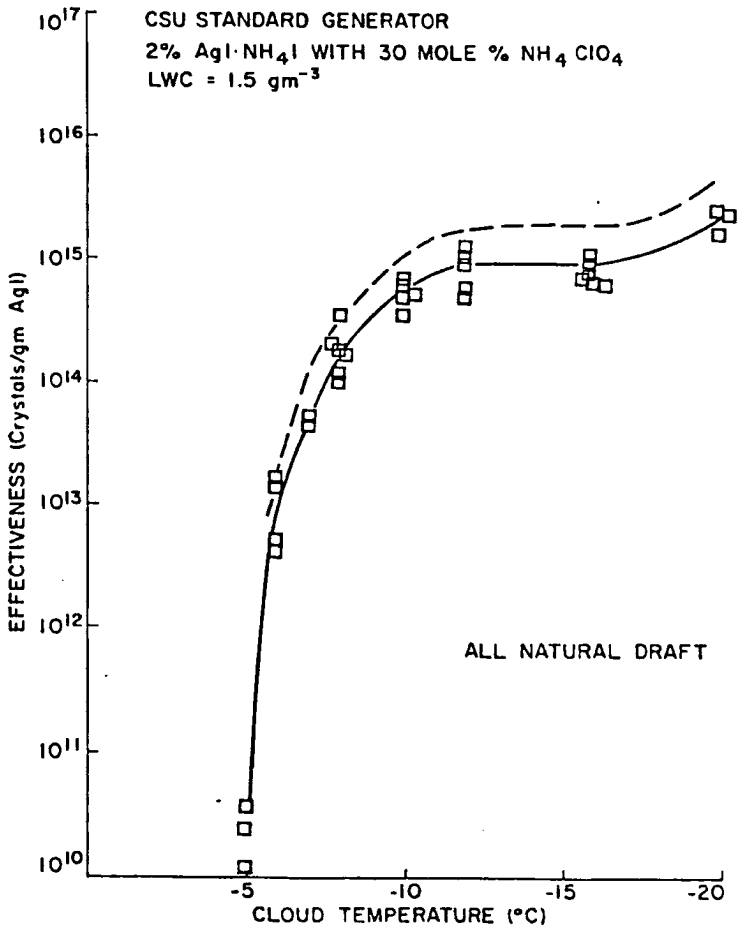

Figure 15. Ice nuclei effectiveness of the aerosol produced from the combustion of the $2AgI \cdot NH_4I$-acetone water solution with the addition of 30 mole% NH_4ClO_4.

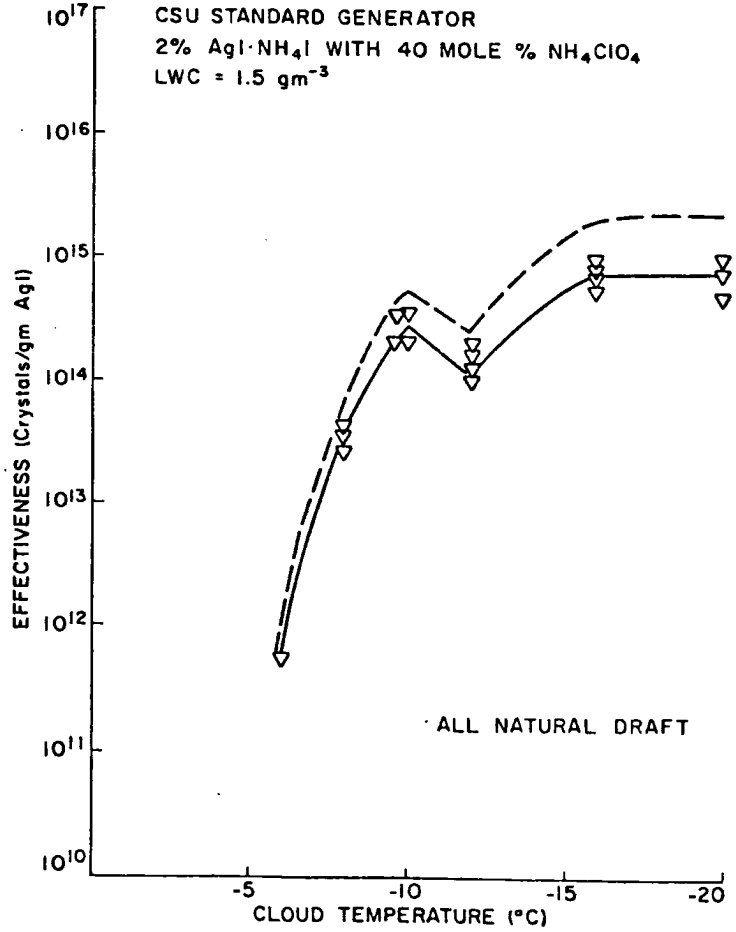

Figure 16. Ice nuclei effectiveness of the aerosol produced frome the combustion of the $2AgI \cdot NH_4I$-acetone water solution with the addition of 40 mole% NH_4ClO_4.

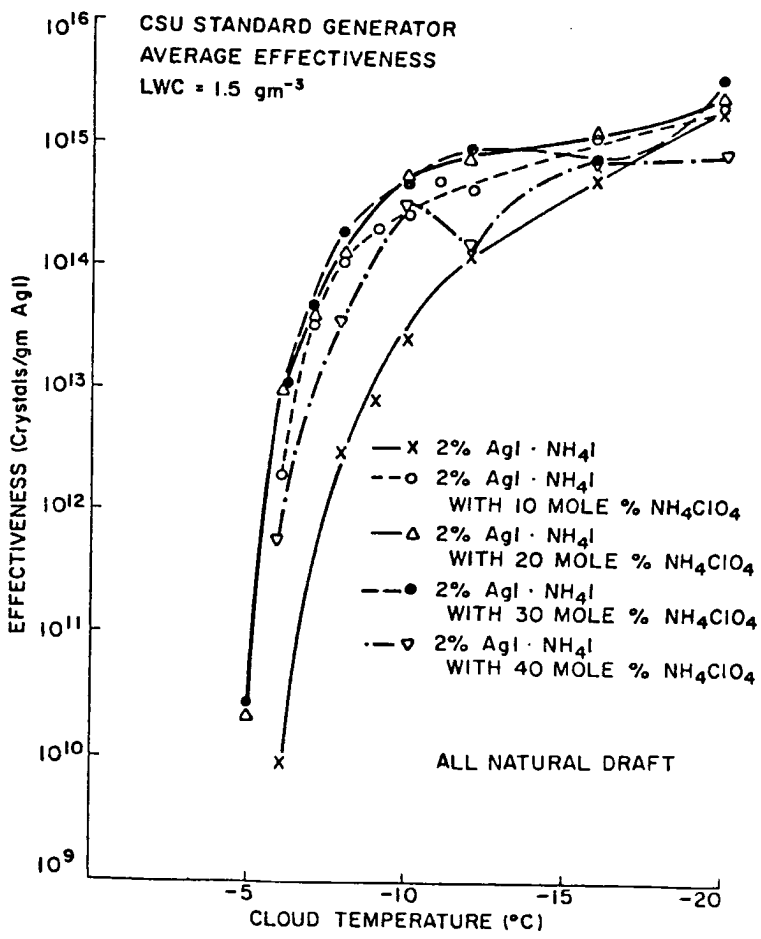

Figure 17. The average effectiveness of all aerosols generated with natural draft dilution.

hold temperature are recognizeable with the addition of just 10 mole % NH_4ClO_4 to the standard solution. The effect is maximized with the replacement of approximately 22 mole % of the iodine atoms (30 mole % NH_4ClO_4) by chlorine atoms in the AgI lattice. Effectiveness is enhanced by one order of magnitude at $-12^{o}C$ to three orders of magnitude at $-6^{o}C$. The effectiveness threshold is improved by a full degree centigrade to $-5^{o}C$. Also, the relative flatness of the efficiency curve at temperatures colder than $-10^{o}C$ is most desirable for applications which desire enhanced ice crystal concentrations only in warmer cloud regions and none at colder temperatures. Of course, ice crystal formation rates must be considered in such a situation as well.

The mean effectiveness curves are displayed in figure 17 so that a trend is recognizeable. The trend displayed with the successive addition of NH_4ClO_4 is consistent with an epitaxy argument for increases in ice nucleation effectiveness. That is, with the addition of too much chlorine, epitaxy will be destroyed because AgCl is not an ice nucleus. This occurs with the addition of 40 mole % NH_4ClO_4 to the standard solution. Some of the drop in effectiveness at this point is due to the larger mean particle size (implying fewer particles per gram), but the particle size distribution for this aerosol is not much different than that of the aerosol from the solution with 30 mole % NH_4ClO_4. The unexplained anomaly in the 40 mole % curve at $-12^{o}C$ probably holds little significance.

It is interesting at this point to compare the mole percentage of chlorine present in the most efficient of the mixed AgI-AgCl aerosols to the mole percentage of chlorine which could possibly be produced from the NEI TB-1 pyrotechnic with hexachlorobenzene. If the 3 weight %

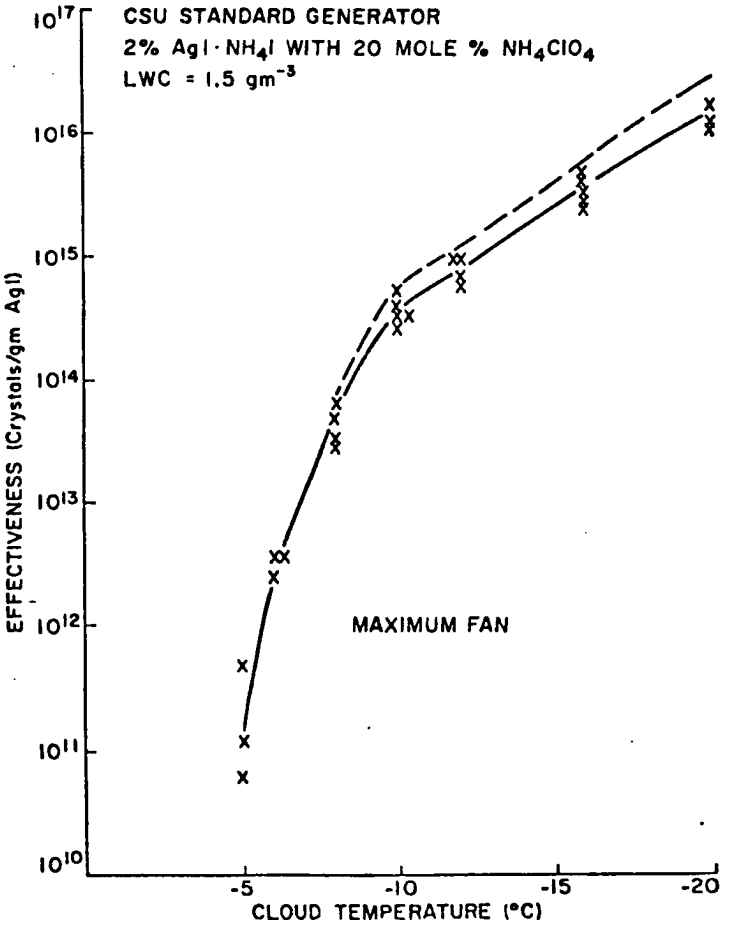

Figure 18. Ice nuclei effectiveness of the aerosol produced from the combustion of the 2 $AgI \cdot NH_4I$-acetone water solution with the addition of 20 mole% NH_4ClO_4 and generated with maximum draft dilution.

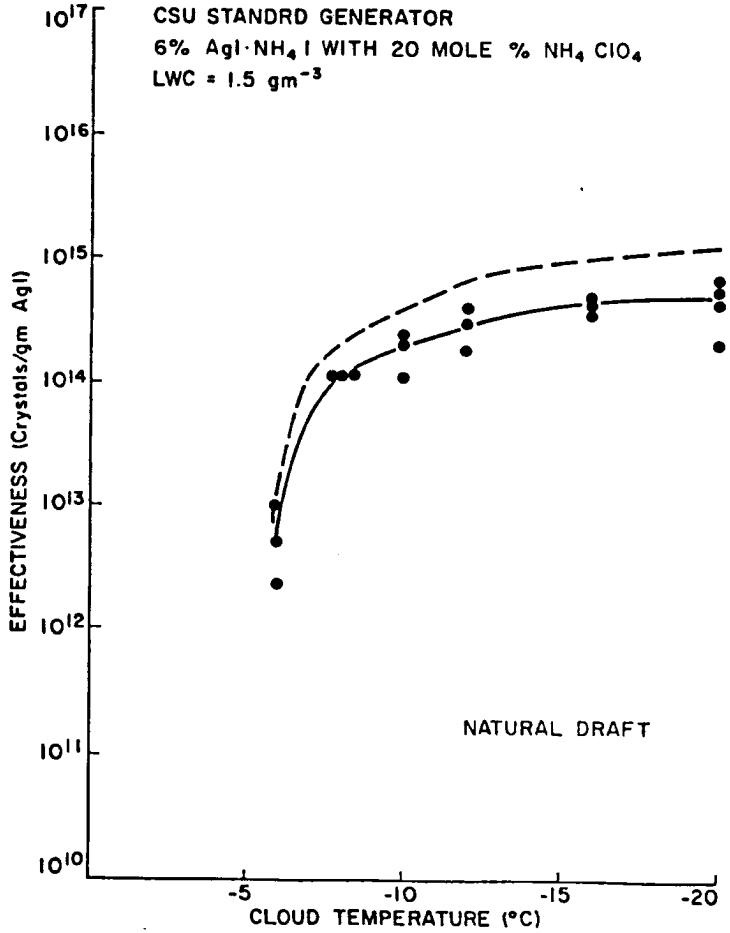

Figure 19. Ice nuclei effectiveness of the aerosol produced from the combustion of the $2AgI \cdot NH_4I$-acetone water solution with the addition of 20 mole% NH_4ClO_4 and the AgI content adjusted to 6 weight %.

C_6Cl_6 addition found to maximize the effectiveness of the NEI TB-1 was to react completely according to the reaction equation given in section 2.2 to form AgCl (leading to solid solutions or intimate mixtures of AgI and AgCl in aerosol form), one can compute that 22.8 mole % of the iodine would be replaced by chlorine atoms. This compares to the approximately 22 mole % replacement in the most efficient aerosol tested in this study. The agreement is impressive, but no quantitative analysis was performed on the NEI TB-1 aerosol for chlorine content.

Figures 18 and 19 display the efficiency curves of the solution system with 20 mole % NH_4ClO_4 generated under maximum draft dilution in the wind tunnel and with 6 weight % AgI respectively for completeness. As expected, more ice crystals per gram AgI are produced by the smaller size aerosols at $-20^{\circ}C$ (a typically efficient temperature for any sized ice euclei) and lower numbers per gram are produced by the larger aerosol.

5.3 Rates, Kinetics and Mechanisms of Ice Crystal Formation

Rate of ice crystal formation data, averaged at each temperature as discussed earlier, is displayed in figures 20-24. It is immediatelly obvious that a long time is necessary (generally 30-35 minutes) for cumulative ice crystal production by these aerosols and that the production rate is apparently exponential in nature. Also, there is little difference between the standard aerosol rates and those of the AgI-AgCl aerosols. This is a strong indication that the new nucleants function in the same manner as the standard AgI nucleant to form ice crystals. This will indeed be shown to be the case. The chemical changes have resulted in a nucleus which functions similarly, but more efficiently to form ice crystals. These rate plots also display an apparent

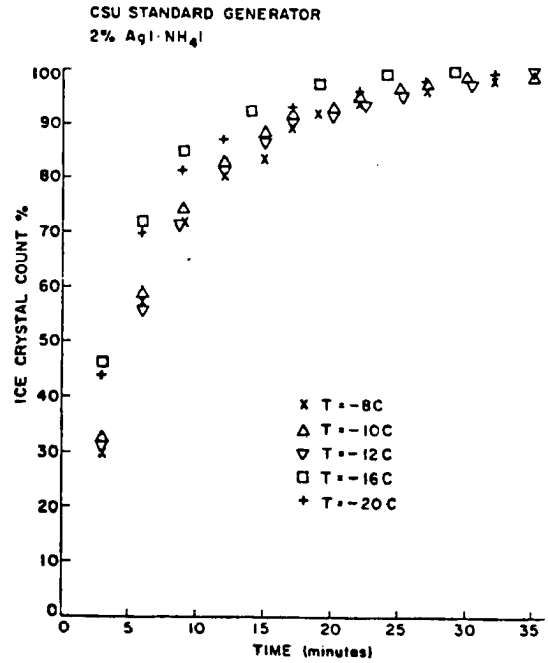

Figure 20. Rates of ice crysta formation by the aerosol produced from combustion of the given solution.

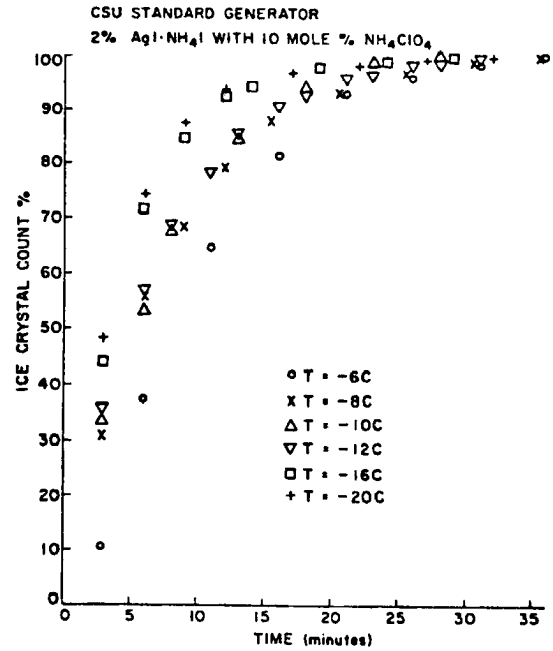

Figure 21. Rates of ice crystal formation by the aerosol produced from combustion of the given solution.

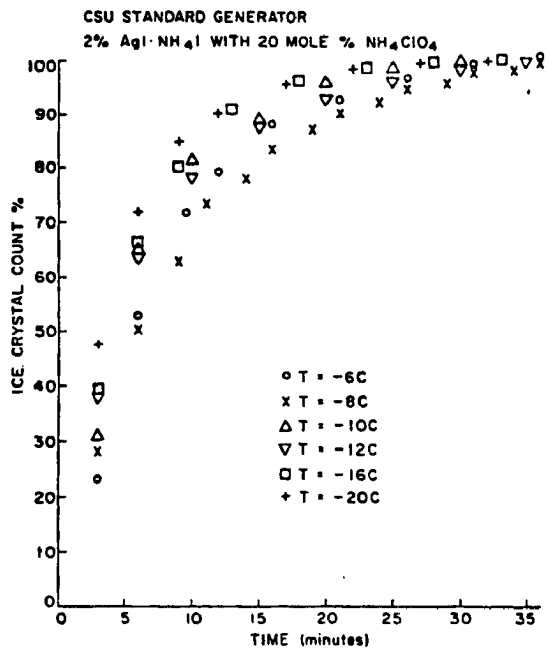

Figure 22. Rates of ice crystal formation by the aerosol produced from combustion of the given solution.

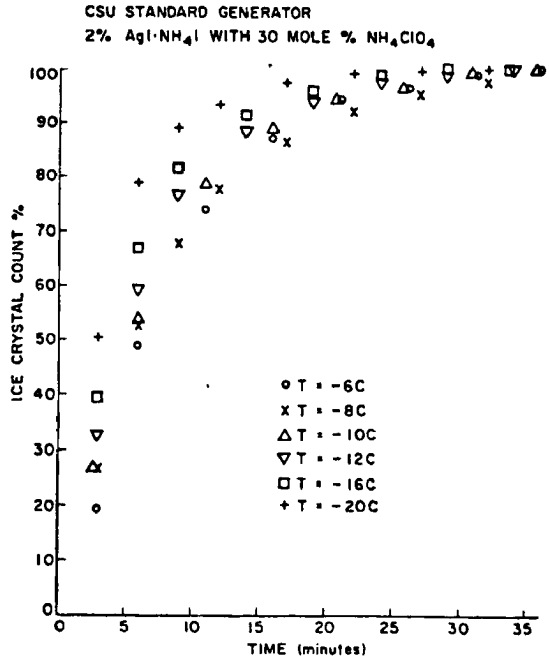

Figure 23. Rates of ice crystal formation by the aerosol produced from combustion of the given solution.

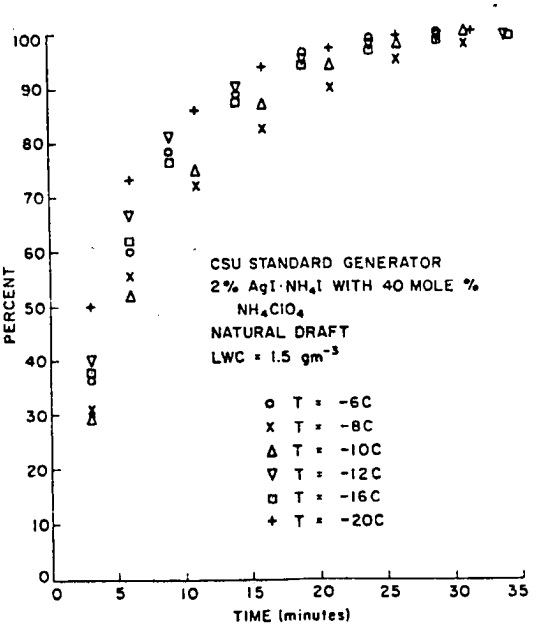

Figure 24. Rates of ice crystal formation by the aerosol produced from combustion of the given solution.

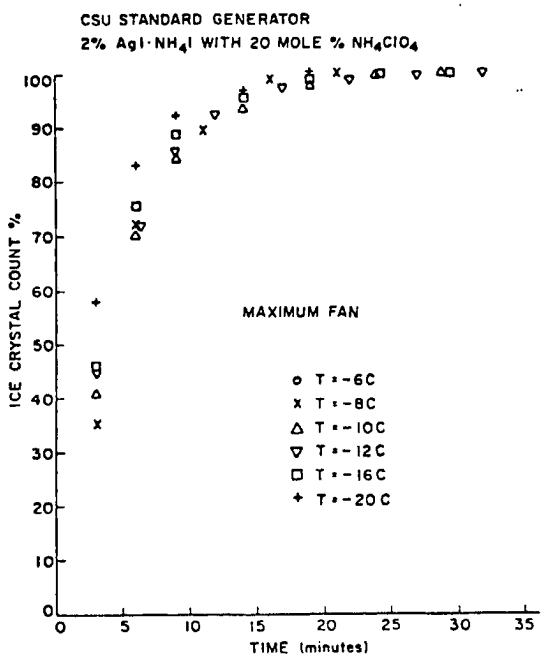

Figure 25. Rates of ice crystal formation by the aerosol of figure 22 generated with maximum draft dilution.

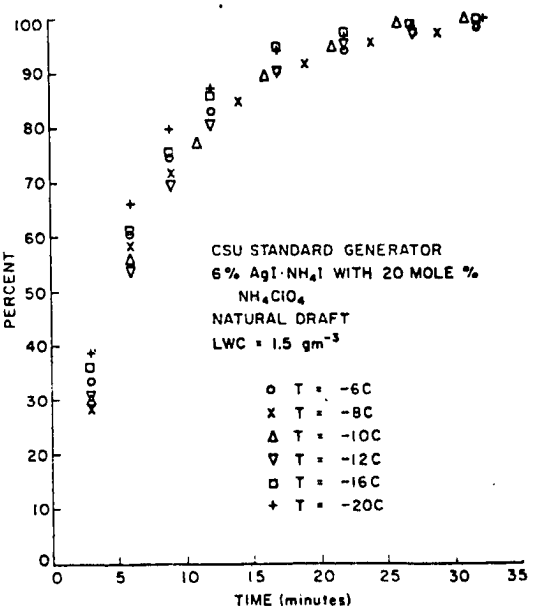

Figure 26. Rates of ice crystal formation by the aerosol produced from combustion of the given solution.

temperature coefficient to ice crystal formation, although the data must first be plotted kinetically and corrected for airflow dilution before such a detail can be confirmed.

Figures 25 and 26 display the ice crystal formation rates for the smaller and larger sized mixed aerosols respectively. There is little change in comparison to figure 22 when a slightly larger mean sized aerosol is used (figure 26). However, the maximum draft aerosol (smaller sized) is inherently faster in producing ice crystals. This is an initial indication that a contact nucleation process is in action. Brownian coagulation theory dictates that smaller particles of the same substance will collide faster with the same droplet distribution.

Kinetics permits a more graphic picture of nucleating characteristics and allows delineation of the gross or macro-mechanism for ice crystal formation. Figures 27-31 display plots of the same raw data of figures 20- 24 in a kinetic fashion. As expected, the plots are linear and with such high correlation, generally, that estimated best fit lines could be drawn through the data rather than least square fits. There were only a few cases where this was questionable. At all temperatures except $-20^{\circ}C$, for all the aerosols, the plots are singular in slope (purely first order) indicating a singular mechanism for ice crystal formation in action. At $-20^{\circ}C$, in every case, a curve is produced which may be separated into two distinct slopes, showing that there are two competing mechanisms producing ice crystals. An overall slower, but more persistent process dominates in the end. These two mechanisms can be separated and percentages and rate constants can be determined as discussed in section 3.1. However, this is best done after the raw data has been corrected for dilution. Before performing the above, it is of

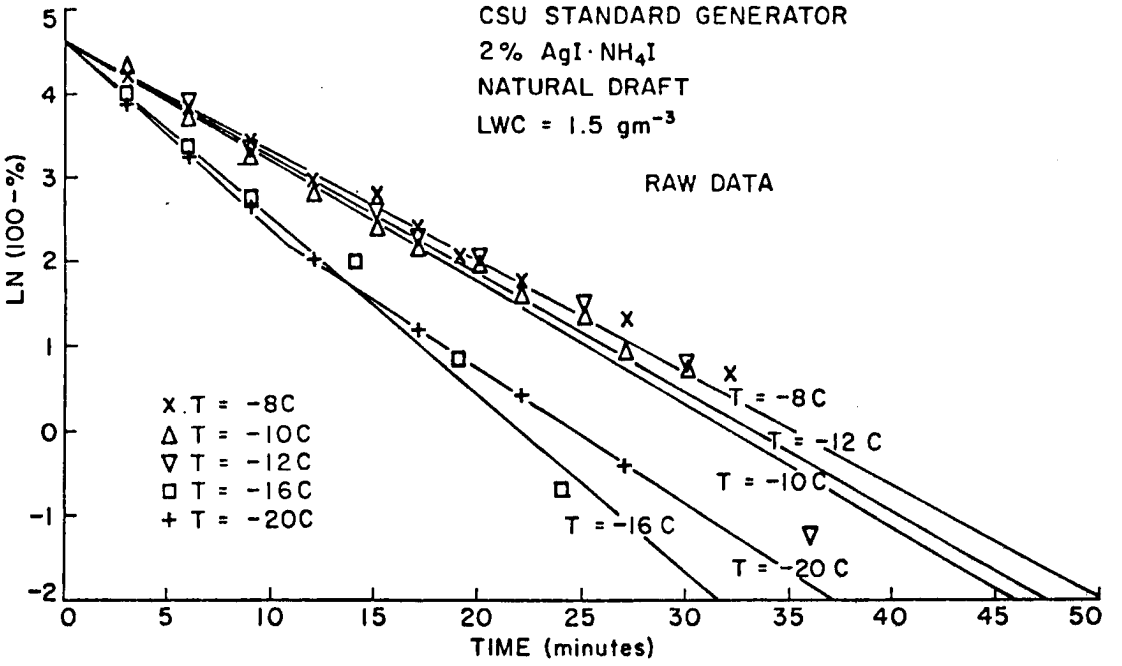

Figure 27. Raw kinetics plot produced from the ice crystal formation rate data of figure 20 ($2AgI \cdot NH_4I$).

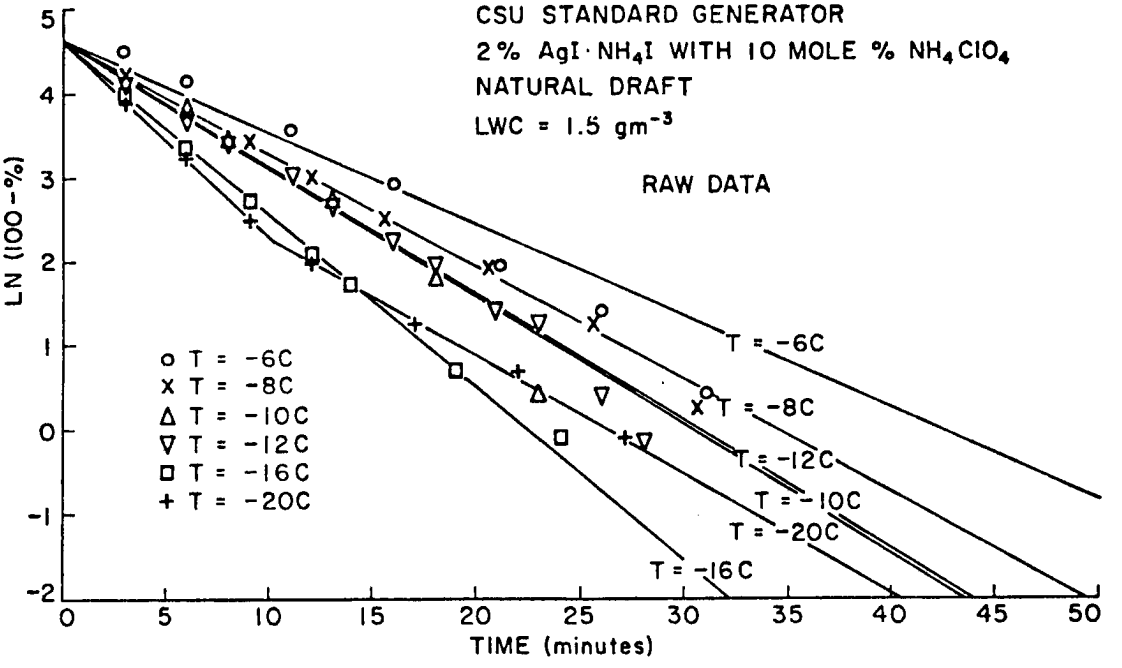

Figure 28. Raw kinetics plots produced from the ice crystal formation rate data of figure 21 ($2AgI \cdot NH_4I$ with 10 mole% NH_4ClO_4).

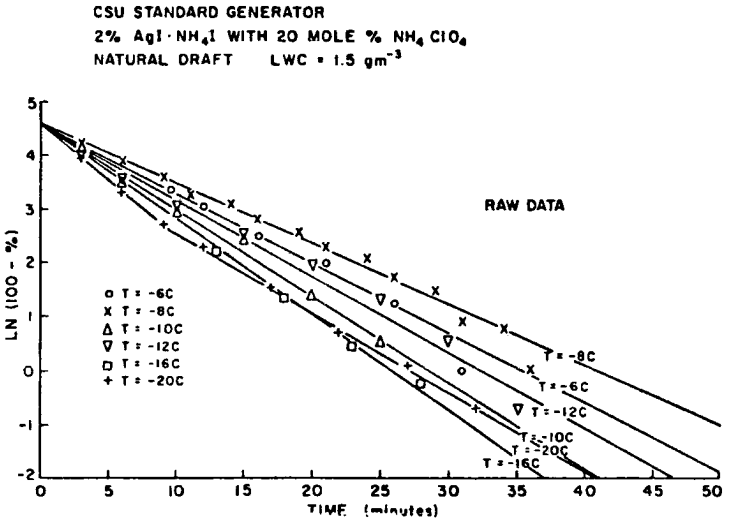

Figure 29. Raw kinetics plot produced from the ice crystal formation rate data of figure 22 ($2AgI \cdot NH_4I$ with 20 mole% NH_4ClO_4).

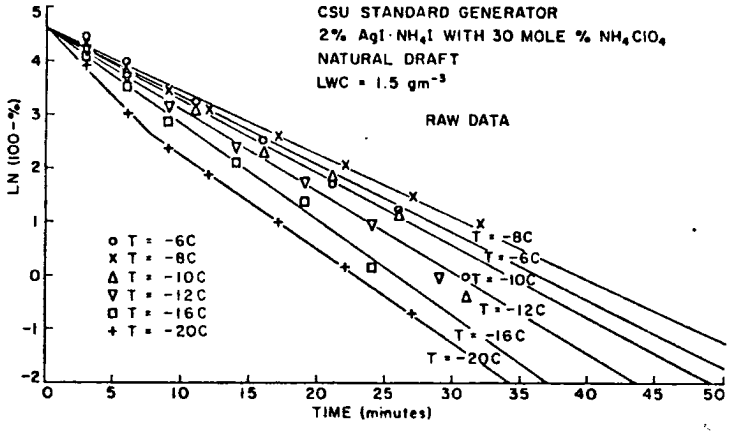

FIgure 30. Raw kinetics plot produced from the ice crystal formation rate data of figure 23.

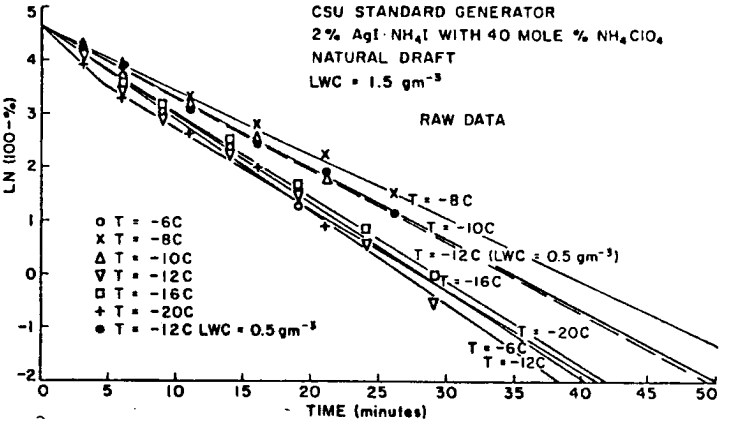

Figure 31. Raw kinetics plot produced from the ice crystal formation rate data of figure 24.

interest to examine kinetic changes in the raw data with changes in liquid water content. As stated, such an analysis will determine whether the singular mechanism for ice crystal formation is droplet concentration dependent or vapor concentration dependent, since absolute vapor concentration and thus saturation ratio is maintained for any liquid water content at a given temperature, while droplet concentration changes drastically. The results of lowering the liquid water content to 0.5 gm^{-3} on the phase change kinetics of the aerosol from the combustion of the solution with 20 mole % NH_4ClO_4 is shown in figure 32. Two temperatures are displayed. These results represent an average of a large number of tests. The slope of the kinetic plot does indeed decrease when the cloud droplet concentration decreases by more than a factor of two. In figure 32a, the change is much larger than can be accounted for by the change in cloud introduction airflow. This is obvious after the data is corrected for airflow as in figure 33. The singular mechanism functioning at $-12^{o}C$ in the ICC is droplet concentration dependent and thus contact nucleation, as indicated by this kinetic analysis. Corrected effectiveness at a liquid water content of 0.5 gm^{-3} is 1.2×10^{15} compared to 1.7×10^{15} at 1.5 gm^{-3}. Thus, as expected in a contact nucleation process, droplet concentration changes only the ice crystal production rate, not the effectiveness. Spot checks at other temperatures revealed that the same situation occurred at all temperatures $-16^{o}C$ and warmer.

One very interesting result which is a consequence of the perfect straight line behavior and collision nucleation mechanism is that the nucleation is strictly by contact as defined. That is, there is no rate affecting delay to freezing following contact. In the case of a two

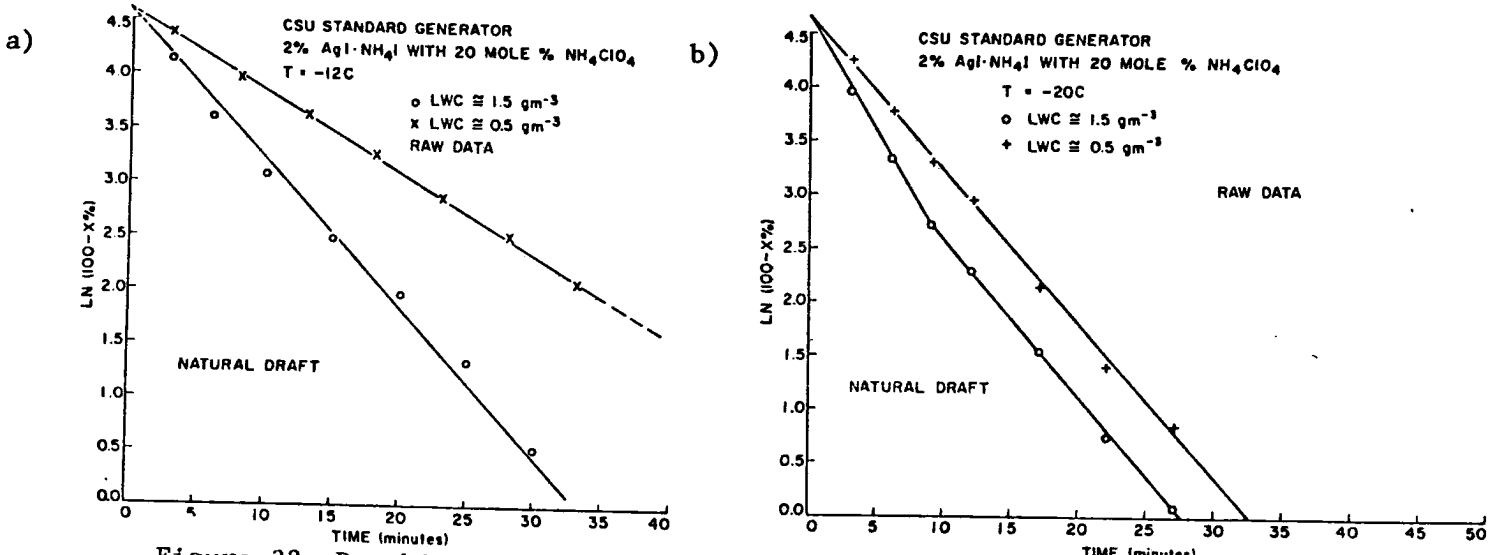

Figure 32. Raw kinetics displaying the dependence on LWC at -12°C (a)) and -20°C (b)).

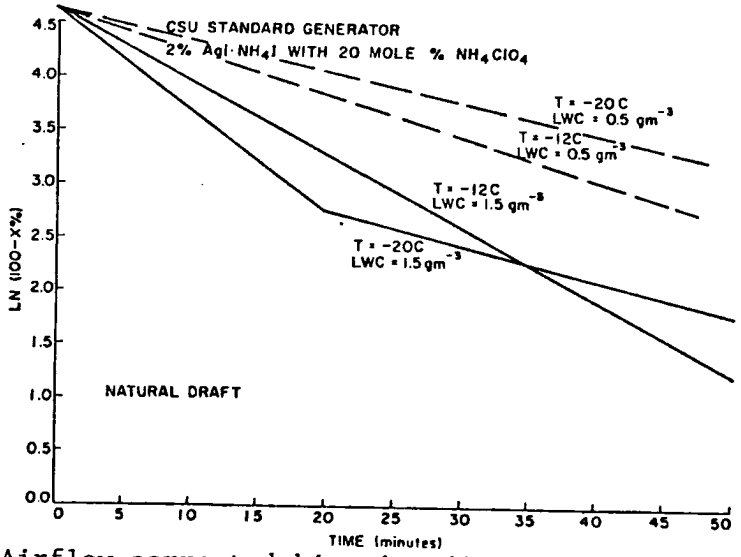

Figure 33. Airflow corrected kinetics displaying the dependence on LWC.

stage process, first involving nuclei collision with droplets, then a time dependent freezing process, an analogy can be drawn to the kinetics of a series first order reaction in chemistry (see for example, Frost and Pearson (1953)). This can be represented as,

$$[N] \xrightarrow{K_1} [O] \xrightarrow{K_2} [IC]$$

where K_1 is the rate constant for collsion, [O] represents a particle on the surface or within a droplet, and K_2 is the rate constant for droplet freezing. Experimentally, the overall process is first order with a singular rate constant K. If $K_1 \gg K_2$, the overall rate constant governing ice crystal formation (K) would be equal to K_2. This is not the case however, because K changes with droplet concentration. K_2 would not. Therefore, $K_1 \ll K_2$ and K_1 is approximately K. Pure contact nucleation is being observed. If the droplet freezing rate was of any importance, the experimental rate plot would not be exponential and kinetics would not be linear. For example when $K_1 = K_2$ the expression for ice crystal production takes on a complicated form and the respective rate and kinetic plots would appear (Frost and Pearson, 1953) as generalized below:

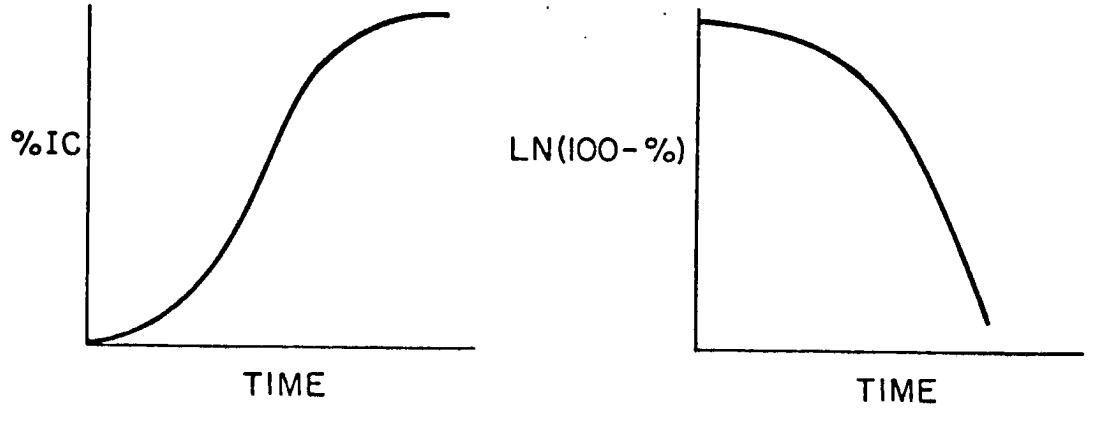

Figure 33d. Generalized plots for a series first order reaction with equivalent rate constants (two stage).

The kinetic plots at two liquid water contents at -20°C (figure 33) display that the persistent process producing ice crystals is independent of cloud droplet concentration, as indicated by the nearly equal slopes. This process in fact, probably dominates ice crystal production in a 0.5 gm^{-3} cloud. Interestingly, this vapor-dependent mechanism is also a singular first order process. This process is believed to be deposition nucleation. Based on chemical considerations alone, one would not expect condensation followed by freezing to occur because of the highly hydrophobic nature of the aerosols produced. Secondly, condensation would certainly occur at warmer temperatures as well. Warmer thresholds for deposition have generally been reported in the literature (Anderson and Hallet, 1976; Schaller and Fukuta, 1979), but the generator effluent aerosols used here are much smaller than particles tested in most past studies. It is certainly reasonable that energetic barriers to viable ice embryo formation might prevent nucleation on these smaller particles until colder temperatures. The appearance of deposition only at -20°C does not necessarily preclude the function of this process at warmer temperatures. However, if this mechanism was of substantial importance at -16°C, it would show up in the data. If it is occurring, its rate is very slow, producing such small ice crystal concentration values as to be unimportant and probably as undesireable as the contact nucleation rate in a low droplet concentration cloud (for most weather modification purposes). The initial slope (high rate constant) at -20°C in the 1.5 gm^{-3} cloud represents a combination of the droplet concentration dependent contact nucleation and the vapor concentration dependent deposition. Extrapolation of the deposition line to the y-intercept reveals that this mechanism accounts for 25% of the total ice crystal versus 75% by contact nucleation.

Kinetically, the delineation of two mechanisms is experimentally sound. A physical explanation or hypothesis for why contact nucleation ends and yet as much as 15% of the ice forming nuclei remain and function by deposition is perhaps in order here. The explanation lies within the understanding of the utilization of various aerosol sizes with time by the two mechanisms. At this temperature, contact nucleation would be expected to be fairly efficient on most particle sizes. Indeed it will be shown that the higher rates and effectiveness of contact nucleation at $-20^{o}C$ and 1.5 gm^{-3} liquid water content as compared to the rates and effectiveness at warmer temperatures is largely due to nucleation by the smaller sized aerosols which do not form ice crystals upon collision at warmer temperatures. Therefore, the composite kinetic plot for contact nucleation would be expected to display a large rate constant. However, after a time, it is only the larger aerosol sizes (with component small rate constants) that are functioning to form ice crystals by contact. In deposition, the particle size - ice crystal formation rate relationship is not well documented or understood. According to the original theory of Fletcher (1958), larger aerosols will function to form ice crystals at the fastest rate. However, the theory was modified by Fletcher (1968), mainly to account for observations of freezing nucleation behavior which showed that given sized particles possess a wide range of nucleation rates. This was explained in terms of particles contaning a distribution of 'active sites' around which ice embryos form. In such a case, larger particles are just more efficient in nucleating ice crystals. Both theories, however, allow for the minimum size requirement which has been observed (see section 2.2).

Thus, the composite kinetics plot for contact at -20°C is dominated by the smaller aerosols and the deposition plot by the larger aerosols. The rates for deposition on the larger sized aerosols are in fact very much faster than for contact. Therefore it is understandable that after a given time, although 15% of the ice nuclei which might function by either mechanism remain, they are effectively eliminated from participating in contact nucleation because deposition is much faster. The separated contact plot at -20°C is thus not the same as that which would result if only contact nucleation was occurring. It is artificially faster due to the competition from deposition.

The above discussion demonstrates the extreme difficulty involved in physically interpreting kinetics on a distribution of aerosols. A definitive and quantitative description of the contact and deposition behavior of an aerosol (at a given temperature and liquid water content) and its size-rate dependencies is one that can only be addressed by proper size classification of the aerosols for cloud chamber studies and coincident measurements in a continuous flow diffusion chamber. This information is not available for actual weather modification aerosols at present, yet is vital not only for understanding nucleation, but for proper use of these nucleants in field operations.

The corrected kinetics plots for all of the aerosols from the test solutions appear in figures 34-38. If transformed again to rate plots, they would represent the actual experimental ice crystal formation rates in the ICC. All of the -20°C depostion plots may be extrapolated to allow comparison of the percent ice crystal production by deposition and contact separately. No particular relationship was seen between the percent of ice crystals due to deposition and the suspected trend in

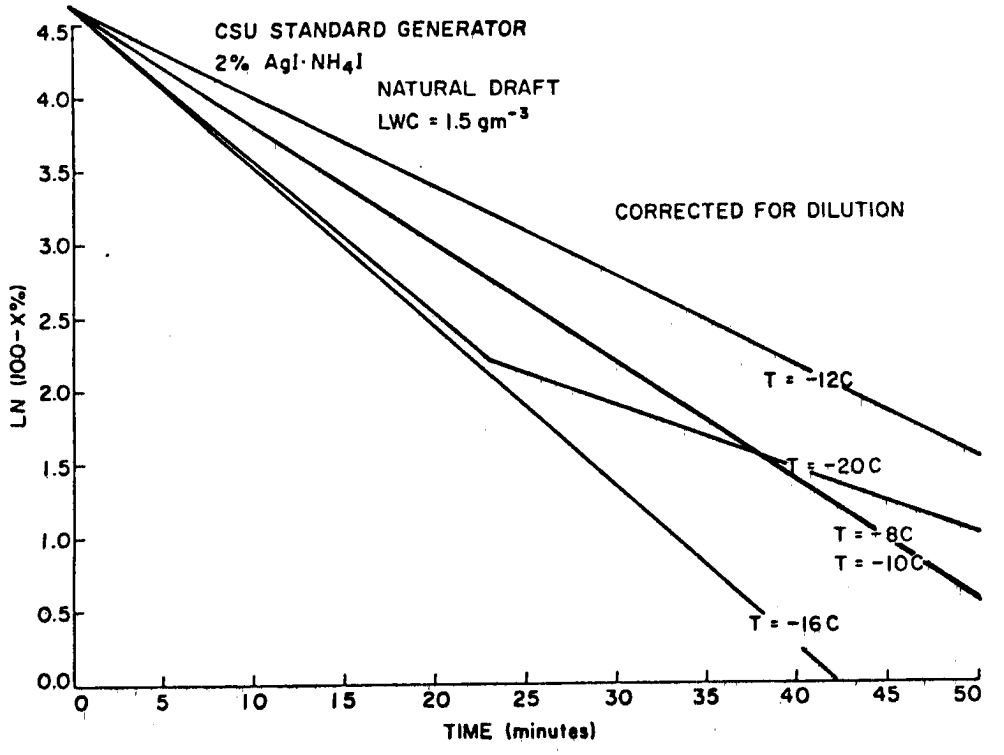

Figure 34. Kinetics plot of figure 27 corrected for airflow dilution.

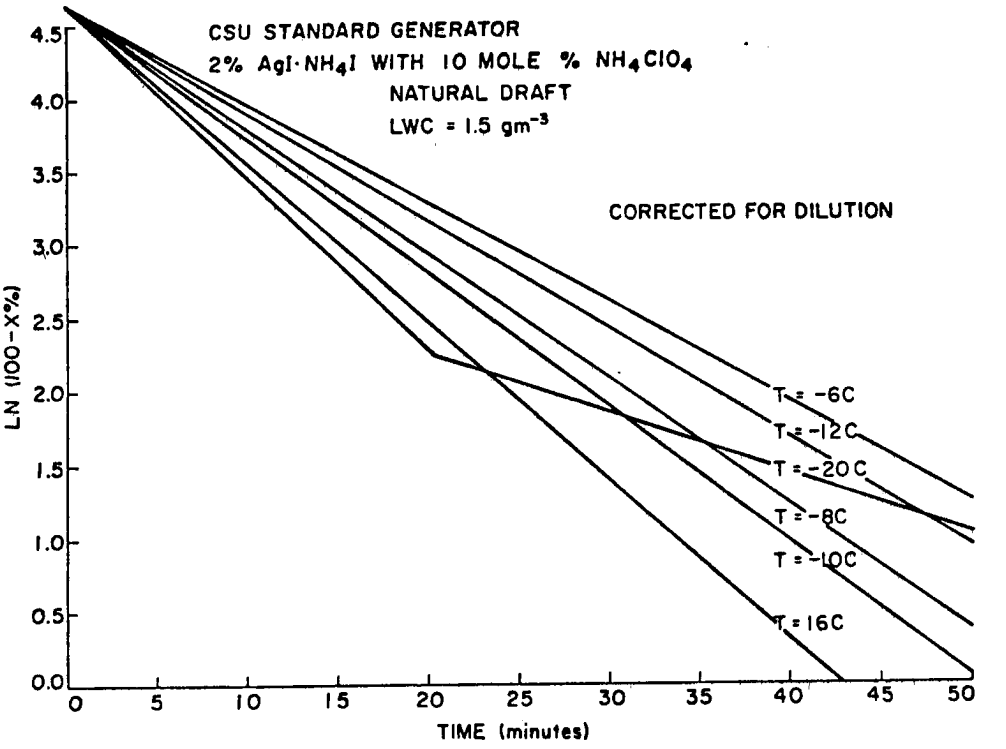

Figure 35. Kinetics plot of figure 28 corrected for airflow dilution.

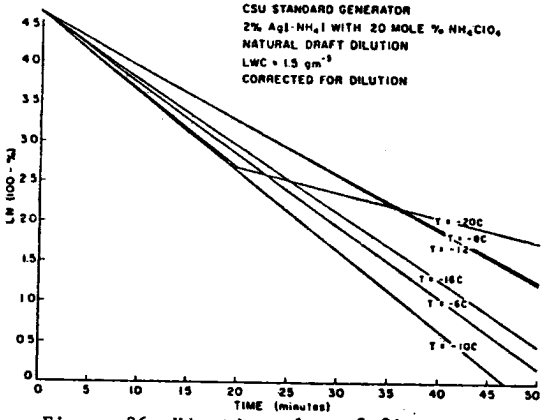

Figure 36. Kinetics plot of figure 29 corrected for airflow dilution.

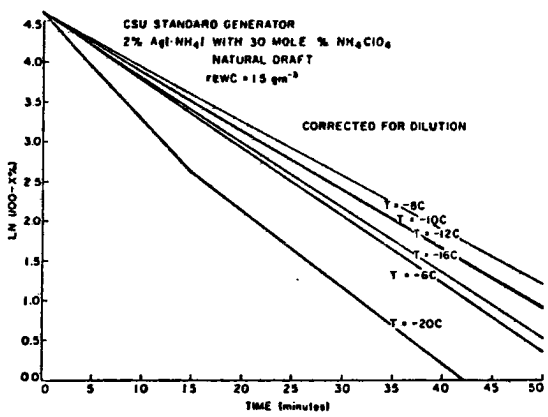

Figure 37. Kinetics plot of figure 30 corrected for airflow dilution.

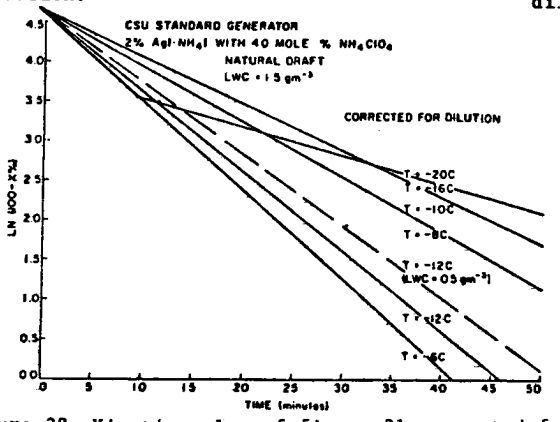

Figure 38. Kinetics plot of figure 31 corrected for airflow dilution.

epitaxy. This is probably because the epitaxial effect is not as great a factor at -20°C. More apparent is a correlation between some function of particle size and the percent ice crystal production due to deposition. Table 3 shows the behavior of mean particle diameter and the percent of particles greater than 500 A°, with respect to the percent deposition for all aerosols at -20°C.

Table 3.
AEROSOL SIZE AND THE PERCENT OF ICE CRYSTALS FORMED BY DEPOSITION

AEROSOL SOLUTION	AEROSOL MEAN DIAMETER(A°)	AEROSOL % >500 A°	% ICE CRYSTALS (DEPOS.)
NATURAL DRAFT, LWC = 1.5 gm^{-3}			
STANDARD	616.0	38.6	23.6
w/ 10 MOLE % NH_4ClO_4	-----	----	23.6
w/ 20 MOLE % NH_4ClO_4	521.8	37.2	21.8
w/ 30 MOLE % NH_4ClO_4	702.2	57.0	56.3
w/ 40 MOLE % NH_4ClO_4	600.0	49.6	48.4
6% AgI·NH_4I w/ 20 MOLE % NH_4ClO_4	857.7	58.2	58.0
MAX FAN, LWC = 1.5 gm^{-3}			
STANDARD			
w/ 20 MOLE % NH_4ClO_4	289.6	10.6	13.2

Mean diameter shows some correlation, but it is not strong. The 500 A° minimum particle size was chosen for comparison with the results of Gerber (1972) on pure AgI particles. He showed a size cut-off for measureable deposition at 500 A°. Figure 39 displays a plot of the % deposition versus the % particles > 500 A°. The line represents a one to

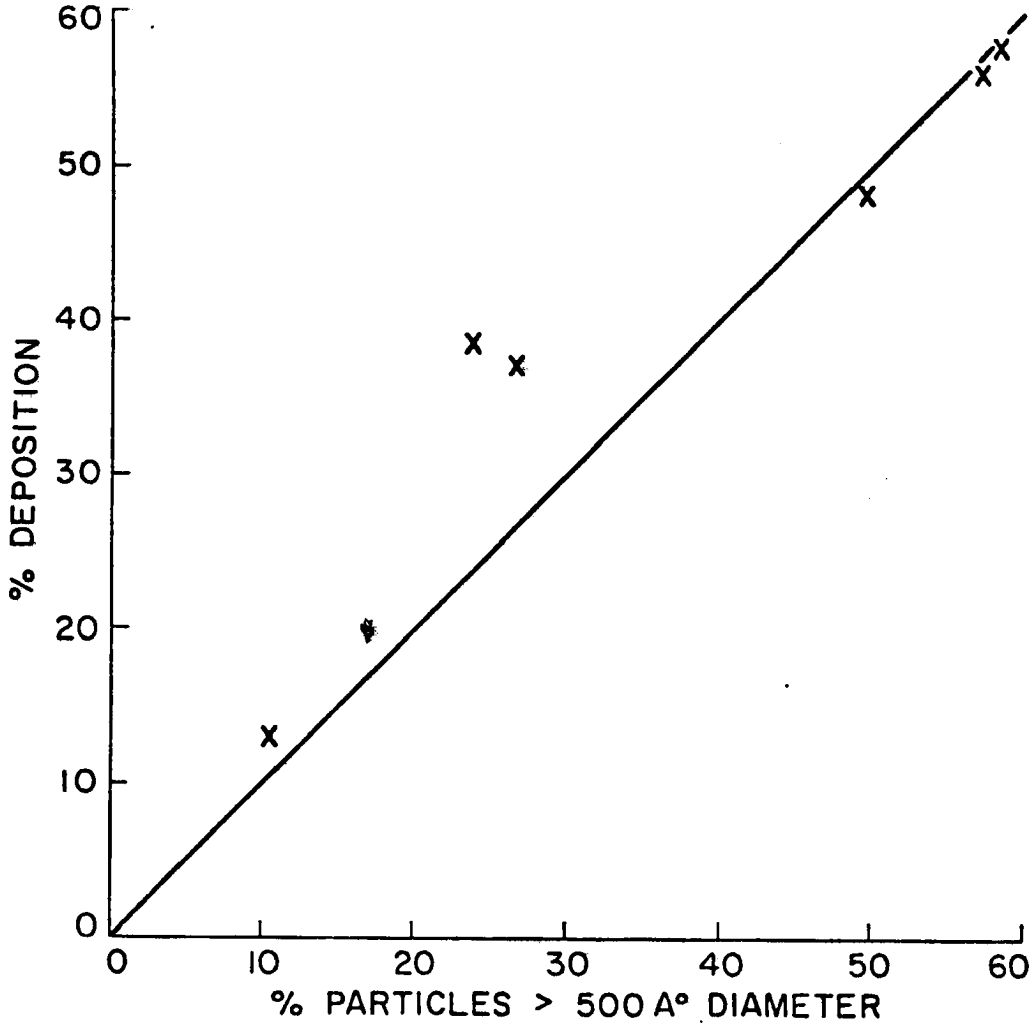

Figure 39. Percent of ice crystals produced by deposition nucleation versus the percent of the particle size distribution greater than 500A° (T = -20°C).

one relationship. Four of the six points fall very near this line. One could speculate that the measured size distributions of the two flyers were not representative of the distributions present during the testing period due to varying tunnel updrafts (leading to different particle sizes generated and different coagulation rates). However, to accept a one to one relationship as presented in figure 39, it must be assumed that all aerosol > 500 A^{o} can and does nucleate ice by deposition. This is not an unrealistic assumption, but until it is addressed in the proper study, the limited data of figure 39 can only be said to suggest that the size cut-off for deposition at near 500 A^{o} measured by Gerber (1972) may be validated here for freely suspended nuclei. It certainly confirms that there is a strong size dependency to deposition nucleation for these aerosols. If these aerosols obeyed the 1600 A^{o} cut-off at $-16^{o}C$ (given by Gerber), deposition would not be distinguishable at this temperature, as was the case in this data set.

More information concerning the deposition nucleation behavior of the mixed AgI-AgCl aerosols is gained from figure 40b, the corrected plot for the 20 mole% aerosol generated under maximum draft in the wind tunnel. It was just shown that the percentage of ice crystals produced by deposition from this small sized aerosol is much less than for the aerosol of the same solution generated under natural draft, in agreement with a size dependency for deposition. Also of note however, is that the rate of ice crystal formation (indicated by the slope = -rate constant in each case) is almost exactly the same (0.032 natural draft versus 0.034 maximum draft). In fact, with the exception of the aerosol from the solution with 30 mole% NH_4ClO_4, the deposition kinetic slopes are nearly constant for all aerosols tested. This observation can quan-

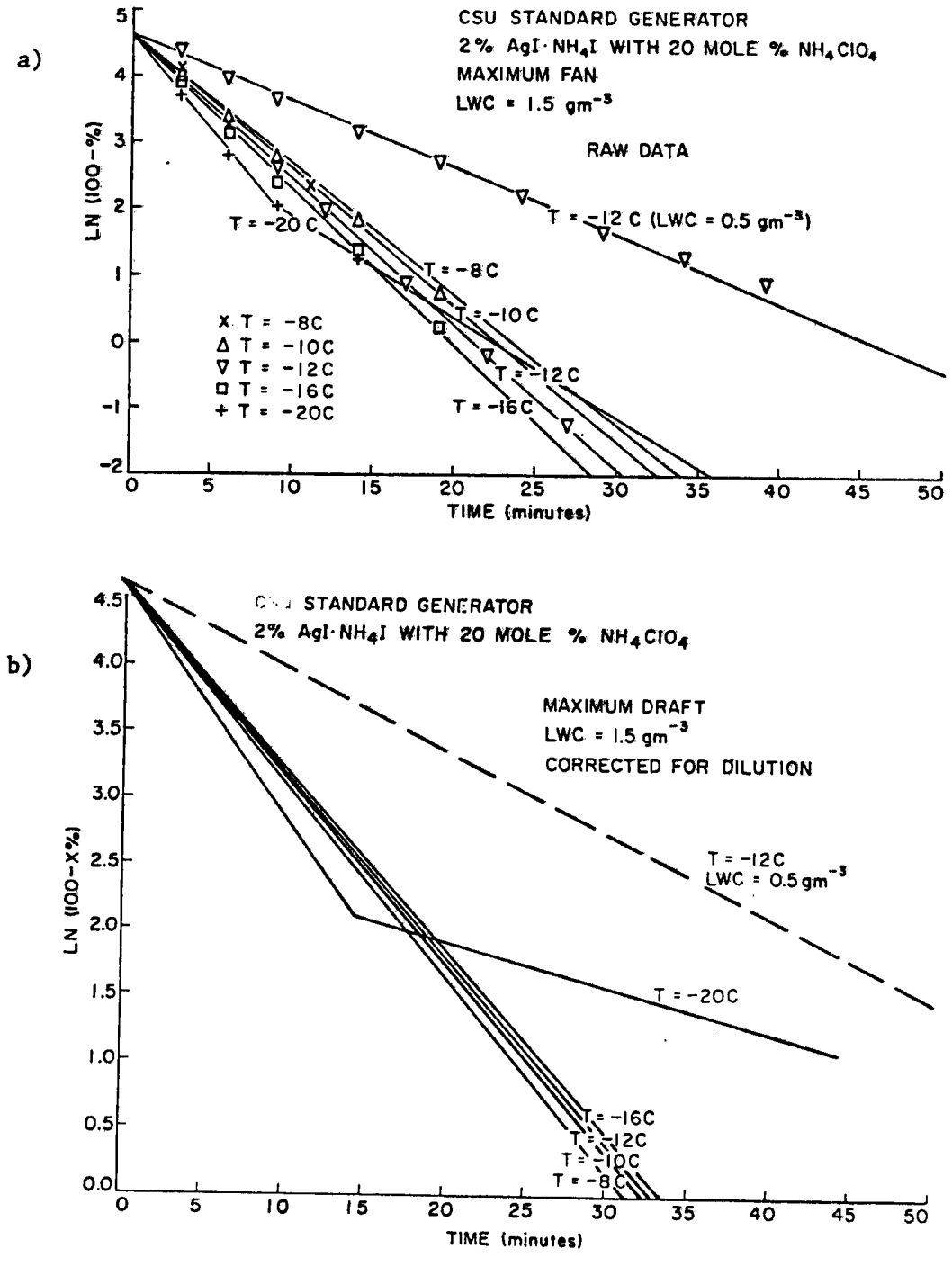

Figure 40. Raw (a)) and corrected (b)) kinetics plots produced from the ice crystal formation rate data of figure 25 (2 $AgI \cdot NH_4I$ with 20 mole% NH_4ClO_4 generated with maximum fan dilution).

titatively fit either deposition theory, with qualifications. If a size dependency of nucleation rate exists, the solution aerosols behave identically because the aggregate particles (> 1000 A^{o}) behave as the largest particle of which they are composed (generally between 500 and 1000 A^{o}), so that the mean size of the aerosols functioning to form ice crystals by deposition never changes to any degree. The more accepted active site theory provides another viable explanation. This is, if the nucleation rate is controlled simply by the distribution of active sites on single particles and this distribution does not change with aerosol composition or degree of aggregation, the nucleation rate would not change, but the concentration of crystals produced would. Once again, more insight could be gained in a properly controlled and parameterized kinetic study.

Attention is now turned to the contact nucleation behavior of the mixed AgI-AgCl aerosols. Confirmation of this ice crystal formation mechanism at temperatures of $-16^{p}C$ and warmer is found in the variation of kinetics with particle size and a comparison to the kinetics determined from aerosol- droplet collision theory. Comparison of figure 40b with figure 36 displays the drastic change in rate constants when the mean aerosol size from combustion of the 20 mole % NH_4ClO_4 solution is decreased by a factor of two under maximum draft dilution. The increase in the rate of production of ice crystals by the smaller size distribution for the same 1.5 gm^{-3} liquid water content is additional hard evidence for contact nucleation. Figure 41 displays the raw and corrected kinetic plots for the aerosol produced when the AgI weight % is increased to 6%. No significant change from the 2% AgI solution aerosol is apparent in the overall rate constants, as determined by the slopes

a)

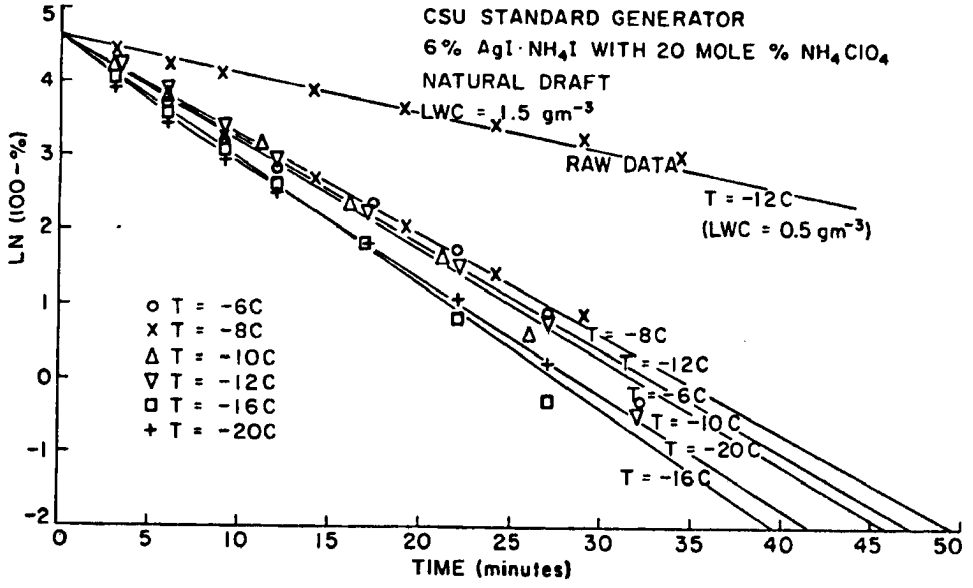

b)

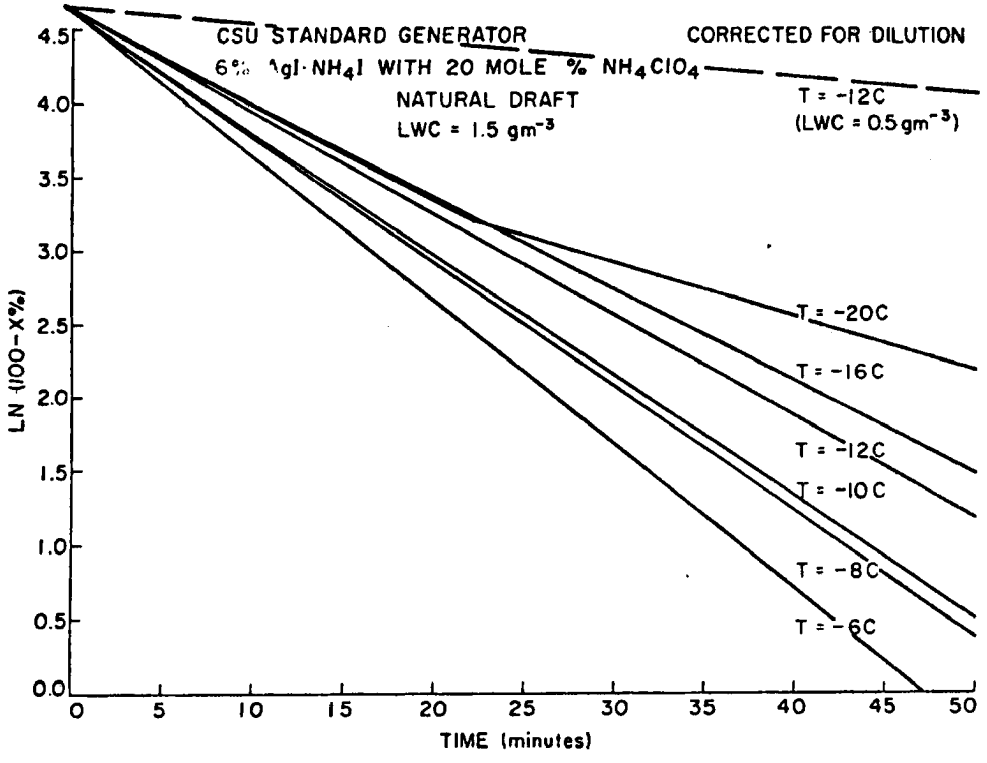

Figure 41. Raw (a)) and corrected (b)) kinetics plots produced from the ice crystal formation rate data of figure 26 (6%AgI·NH_4I with 20 mole% NH_4ClO_4).

of the kinetic plots. This is confusing, but apparently is due to the fact that although the mean particle size is larger, this is largely due to the production of aggregates in small enough concentrations so as not to influence overall rates of ice crystal formation significantly. Brownian coagulation is most sensitive to changes in the smaller sized particles rather than the larger sizes greater than 1000 A^{o}. The basic character of the particle distribution below 1000 A^{o} is maintained when the AgI content is increased to 6% and thus no change in crystal production rates is recognizeable. A change to say, 25% AgI, may have achieved a more substantial change in aerosol size distribution.

The method detailed in section 3.2 was used to produce theoretical kinetic plots for comparison to the experimental ones. Since aerosol and droplet size distributions were masured, equations 3.2.4 and 3.2.10 for Brownian coagulation and wall diffusion were put in summation form to allow computer calculation of these components to the theoretical kinetics for the actual particle distributions. This is more accurate than the use of mean sizes in these calculations. The equations become,

$$\left(\frac{C_P}{C_{P0}}\right)_{BD} = \Sigma_i F_i \Sigma_j \exp(-K_{Bij} C_{Dj} t)$$

$$\left(\frac{C_P}{C_{P0}}\right)_{WD} = \Sigma_i F_i \exp(-2.5 \times 10^{4} D_{Pi} t) .$$

F_i is the fraction of aerosol of size i, and j refers to the droplet size. Only the results of calculations on the aerosols from combustion ofthe solution with 20 mole % NH_4ClO_4 are presented here. Little additional information is gained by plotting more data. Figure 42 displays the theoretical plots of Brownian coagulation, wall diffusional, and airflow dilution losses for the natural draft aerosol at two cloud

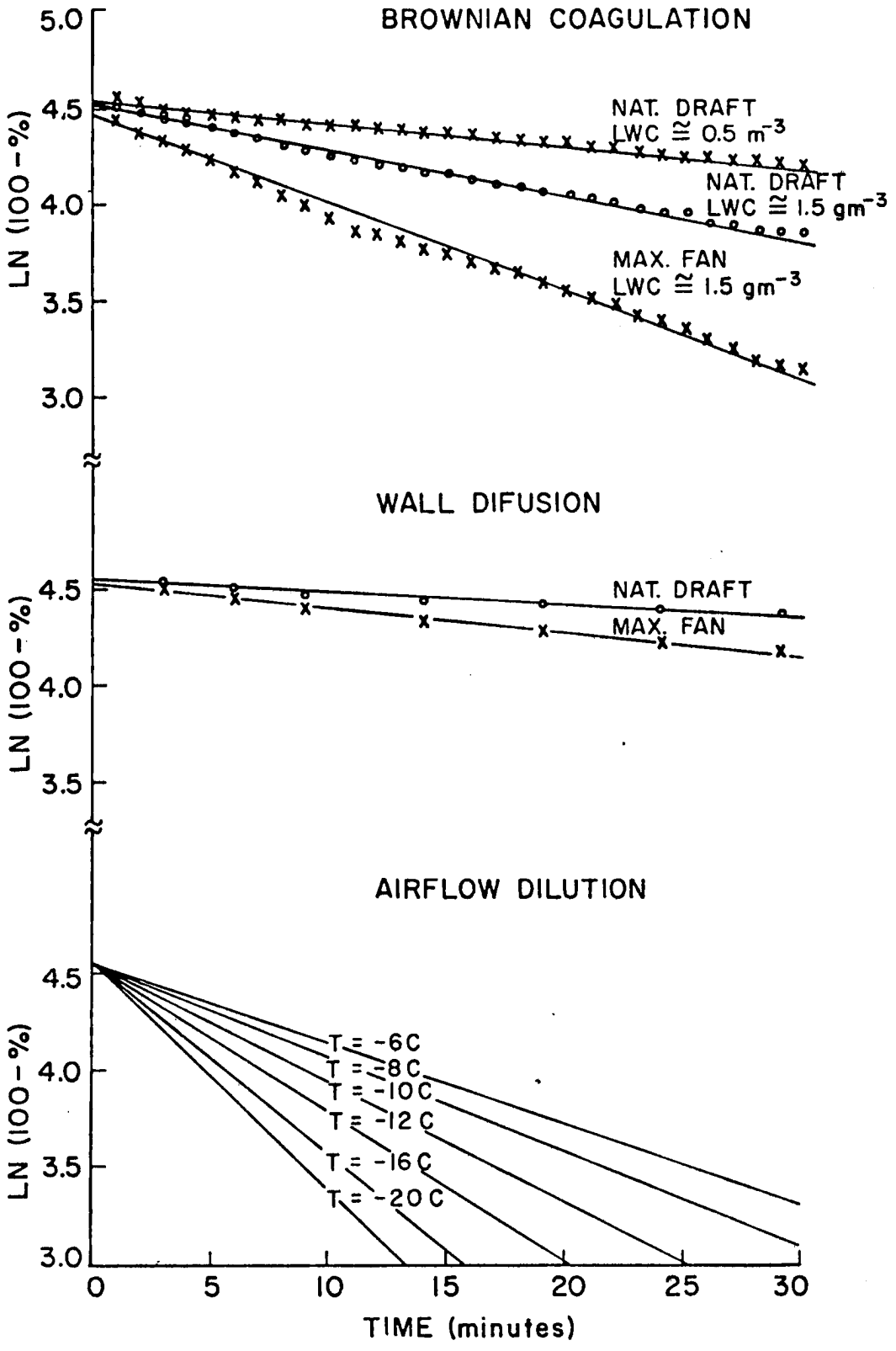

Figure 42. Theoretically produced kinetics plots of the Brownian coagulation, wall diffusion and airflow dilution losses of nuclei.

liquid water contents and the maximum fan aerosol at a 1.5 gm^{-3} liquid water content. Since changes with temperature are basically negligible on the Brownian coagulation and wall diffusion plots, a temperature of $-12^{o}C$ was used. Pressure was taken as 840 millibars. Lines are purposely not drawn to the y-intercept at 4.605 in order to ignore the unrealistically fast coagulation and diffusion in the first minute which is primarily an artifact of the use of a 50 A^{o} mean diameter to represent particles in the first size bin, when in fact there are probably few particles smaller than 50 A^{o} there. Figures 43 and 44 display the resultant theoretical kinetic plots for the natural draft and maximum fan aerosol respectively. They are comparable to figures 29 and 40a. The theoretical plot at a liquid water content of 0.5 gm^{-3} and $-12^{o}C$ for the natural draft aerosol is also included in figure 43 and is comparable to figure 32a. Graphically, it is seen that the experimental plots reflect slightly faster ice crystal formation rates than the theoretical plots in all cases. This can be quantified by comparison of theoretical and experimental contact time constants (equal to the inverse of the slope in each case) as in table 4.

It must be remembered in comparing these values however, that the theoretical results are for 100% utilization of particles to form ice crystals at any temperature. This is not the case experimentally. Also, the accuracy of aerosol and droplet sizing must be considered, as well as the the lack of accurate knowledge of the exact magnitude and temperature dependencies of wall diffusional effects. Therefore, the agreement to within 20 to 40% is actually quite remarkable.

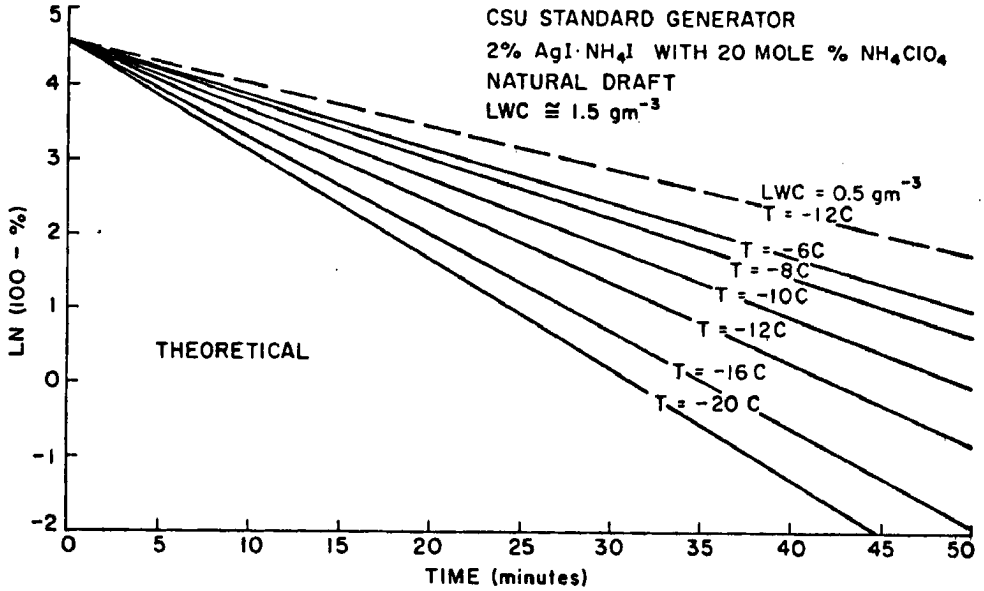

Figure 43. Theoretical kinetics plots for the aerosol from the combustion of the solution with the addition of 20 mole% NH_4ClO_4 and generated with natural draft dilution.

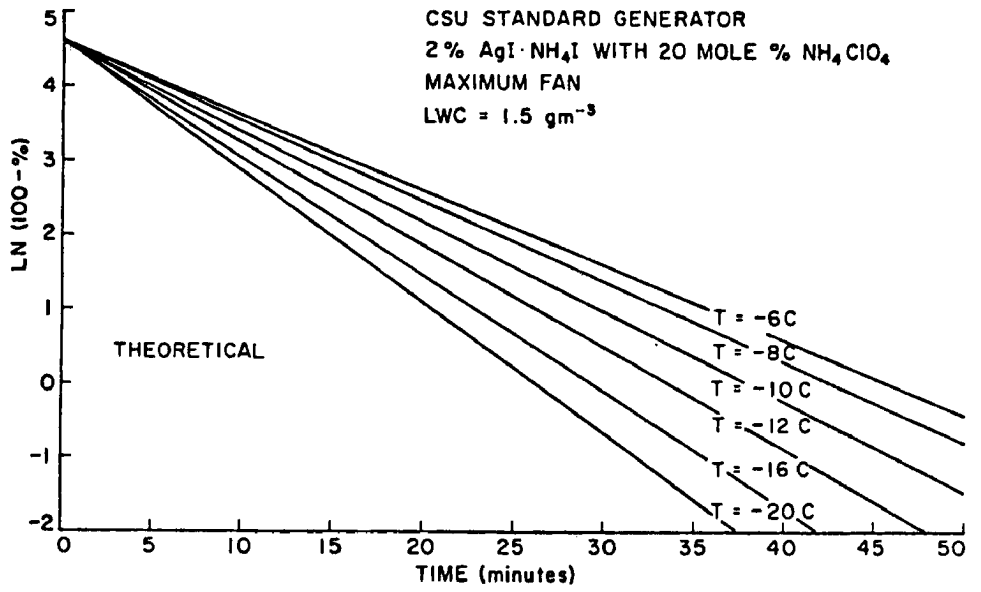

Figure 44. Theoretical kinetics plots for the aerosol from the combustion of the solution with the addition of 20 mole% NH_4ClO_4 and generated with maximum draft dilution.

Table 4.
CONTACT NUCLEATION TIME CONSTANTS

	THEORETICAL (min)	EXPERIMENTAL (min)
NATURAL DRAFT		
(LWC= 0.5 gm^{-3})		
T= $-12^{o}C$	17.1	13.1
(LWC= 1.5 gm^{-3})		
T= $-6^{o}C$	13.7	7.7
T= $-8^{o}C$	12.5	8.8
T= $-10^{o}C$	10.7	6.3
T= $-12^{o}C$	9.2	7.1
T= $-16^{o}C$	7.7	5.5
T= $-20^{o}C$	6.8	2.8
MAXIMUM DRAFT		
(LWC= 1.5 gm^{-3})		
T= $-6^{o}C$	9.9	---
T= $-8^{o}C$	9.3	5.1
T= $-10^{o}C$	8.3	5.0
T= $-12^{o}C$	7.3	4.7
T= $-16^{o}C$	6.3	4.5
T= $-20^{o}C$	5.7	2.3

Perhaps a better indicator of the agreement between the results and theory is obtained by comparing the actual change in kinetic slope that occurs when liquid water content is changed to that predicted by theory. This comparison is presented in Table 5 by the ratios of these slopes for the natural draft and maximum draft aerosols from the solution with 20 mole % NH_4ClO_4. The theoretical ratios were obtained using the kinetic slopes of Brownian collection plus wall diffusional losses. The agreement is quite good. This confirms that collisions between aerosol particles and droplets are indeed responsible for the production of ice crystals and the rate of this process.

Table 5.
LWC RATIO (0.5 gm^{-3}/1.5 gm^{-3}) OF KINETIC SLOPE AT $-12^{o}C$

	CORRECTED EXPERIMENTAL	THEORETICAL
NATURAL DRAFT	0.584	0.614
MAXIMUM DRAFT	0.443	0.548

To this point, little has been said concerning the obvious variation of rate constant with temperature, even after correction for airflow dilution. This is meaningful information in light of the governing contact nucleation mechanism. The interpretation which follows is based on a general overview of the kinetic data. It is an unfortunate consequence mainly of the lack of adequate control over aerosol size and concentration fluctuations under natural draft dilution (and to a lesser extent, cloud control) that conclusions regarding the temperature coefficient of ice crystal formation rate must be drawn from general trends. It has been stated that the kinetic plot is formed from an average rate plot. If the component rate plots for a given temperature are plotted kinetically it is found that the range of slope can be rather large. Outlier tests can also have a significant effect on the resultant slope of the average plot. For example, at $-12^{o}C$, the aerosol from combustion of the solution with 20 mole % NH_4ClO_4 forms ice crystals with an average rate plot that results in a kinetic sope of 0.1413 (at an LWC 1.5 gm^{-3}). The component slopes range from 0.1321 to 0.1705. Two outliers (out of seven total) in the lower part of the range were highly influential. At a liquid water content of 0.5 gm^{-3}, the mean kinetic slope was 0.0766 with a range of 0.0501 to 0.0991. The lack of outliers produced a more representative mean value in this case. Still, slope can vary by

as much as 0.02 from the mean over a period of time. Therefore, a large number of tests over an extended time period would be necessary to provide confidence in a mean slope value at a given temperature using the present dilution system (natural draft). Efficient operating procedures and time considerations simply did not allow this. Most often, a simple temperature was covered in a single day. Another complicating factor would be a violation of the assumed small magnitude and constancy of wall effects with temperature and LWC.

In light of the above discussion, it might seem futile to attempt to interpret this data. However, in the cases of the first four aerosols tested under natural draft (figures 34, 35, 36, 37), somewhat more numerous tests (twice as many in general) were performed over a more extended time period than for the two subsequently tested aerosols. Therefore, an overview concentrating on these data might be useful and, as will be shown, there is additional evidence to support the conclusion attained. In figures 34 and 35 (Standard and 10 mole % NH_4ClO_4 respectively) only the $-12^{o}C$ plot is out of line in a sequence which shows the rate constant value to be inversely proportional to absolute temperature.. This pattern is violated in figure 36 (20 mole % NH_4ClO_4), but even there four of the six plots show the relationship (-8C, -12C, -16C, -20C). In figure 37 (30 mole % NH_4ClO_4), only the $-6^{o}C$ plot violates the suggested inverse relationship between temperature and crystal formation rate. The less complete data sets shown in figures 38 and 41 (40 mole % NH_4ClO_4 and 6% AgI) are not conclusive in suggesting any relationship. The latter seems to show a direct relationship between temperature and crystal formation rate, but the fewest tests were run on this most variable of the generated aerosols. Thus, for four of the

aerosols tested under natural draft (representing 82% of the total tests) and under the limitations mentioned, there is a strong suggestion of an increase in rate constant as temperature decreases. Note that there is no such relationship under maximum fan generation of the 20 mole % NH_4ClO_4 aerosol (figure 40b). This is probably due to the lack of dispersity and variability of this aerosol. Acting essentially as a monodisperse aerosol, only the direct relationship between temperature and rate (from Brownian coagulation theory) would be expected to show up.

Since kinetic changes with changes in droplet concentration identify the mechanism for ice crystal formation on all of the aerosols to be solely contact at temperatures of $-16^{o}C$ and warmer, an explanation of the observed temperature-rate relationship is required. The explanation can only involve the effective particle size utilized in the formation of ice crystals at a given temperature. As the temperature is lowered, the mean particle size effective in forming ice crystals becomes smaller and consequently both rates of ice crystal formation and numbers of ice crystals produced are increased. That there is an inherent particle size effect in contact nucleation efficiency is demonstrated by figure 45 which displays the composite nucleation efficiency of three different mean sized aerosols across the temperature spectrum. Nucleation efficiency in this figure is based on 100% at $-20^{o}C$. This assumption may not be exactly valid, but the number of ice crystals per gram at this temperature are already greater than the numbers of particles per gram calculated from the particle size distributions in section 5.1.2. Also, based on the effectiveness curve shapes alone, the maximum draft aerosol is least likely to be 100% efficient at $-20^{o}C$, biasing the efficiency

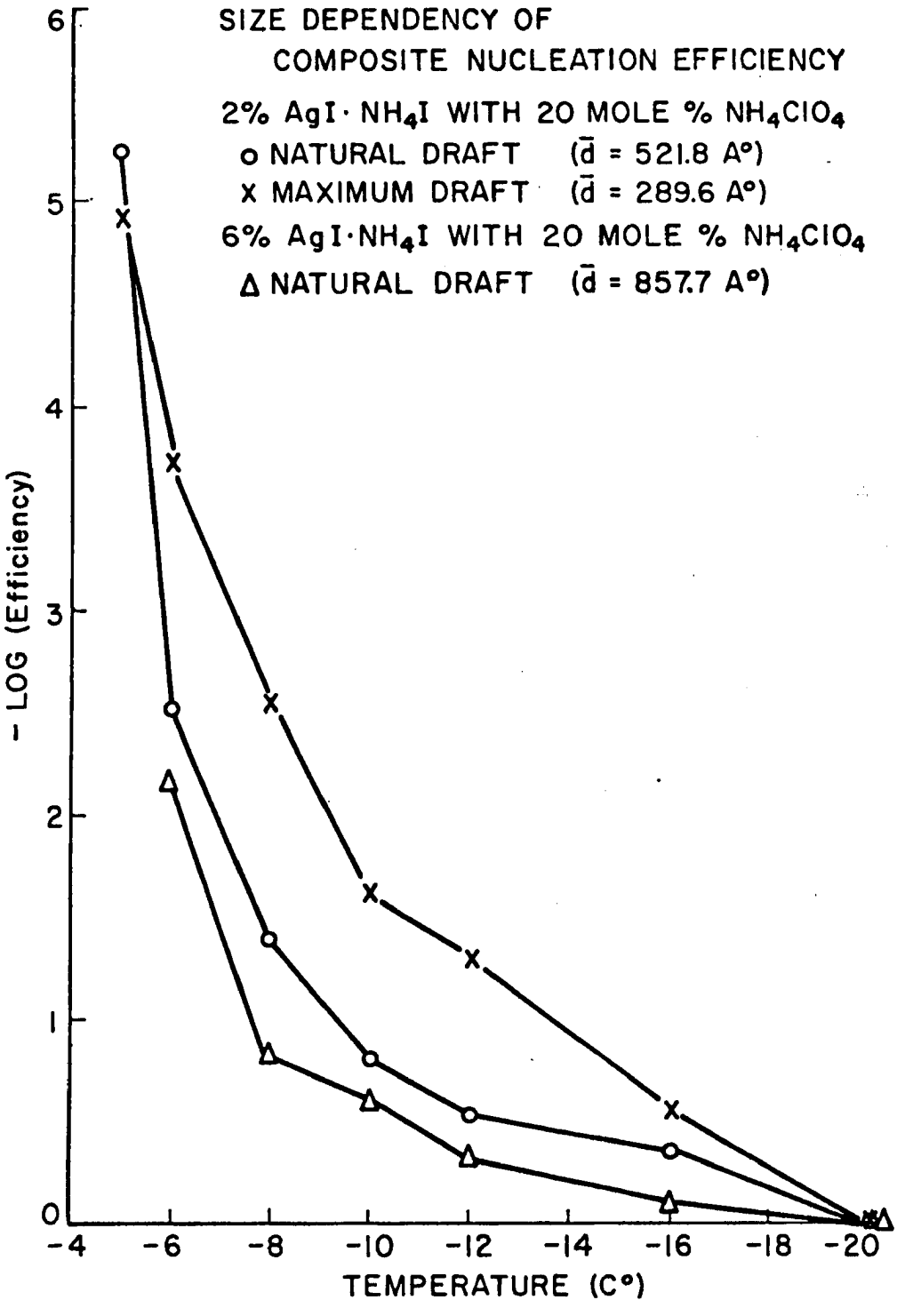

Figure 45. Size dependency of the composite nucleation efficiency.

values higher for this aerosol. Figure 45 is plotted such that the lowest curve on the vertical scale is the most efficient at a given temperature. A decrease in particle size is directly related to a decrease in efficiency. However, orders of magnitude changes in effectiveness are necessary to result in a significant change in ice crystal formation rates as temperature decreases. This suggests that there is not a strict size cut-off to nucleation by contact at a given temperature. Therefore, all sized aerosols must be participating in ice crystal formation to some degree. These results are consistent with a theory of active sites being responsible for freezing nucleation following contact.

There are two possible explanations for the enhanced warm temperature efficiency of the mixed AgI-AgCl aerosols in light of the above results. First, the presence of the chlorine atoms could simply be providing additional active sites on all particles. However, this cannot explain the the drop in effectiveness with the addition of 40 mole % NH_4ClO_4 to the standard generator solution. The trend in effectiveness results was more in agreement with a combined epitaxy and improved active sites argument for increases in ice nucleating ability. Such an improvement increases nucleation efficiency by increasing the rate of freezing of water to form ice embryos on active sites. Therefore, it is most likely that effectiveness increases are a result of an alteration of the competition between the rate of freezing and the rate of a deactivation mechanism following collisions between droplets and aerosol particles. This deactivation mechanism is probably dissolution. When an active site comes in contact with supercooled water it will be etched and ultimately destroyed if nucleation does not occur first. Solubility

rate increases with increasing temperature and decreasing particle size. For the mixed AgI-AgCl aerosols then, freezing prevails at the warmer temperatures not only due to the improved epitaxy and surface active site nature but because solubility is decreased with the removal of hygroscopic impurities. The determination of exact importance of solubility and proof that it is indeed a factor must await further testing. This question might be attacked by the observation of the dependence of nuclei effectiveness on droplet size, since solubility rate is also a function of droplet size (Matthews et al., 1972). This study was not possible with the present cloud generation technique.

VI. SUMMARY AND CONCLUSIONS

6.1 Summary and Conclusions

The concept of mixed-aerosol phase change kinetics, an examination of the rates of ice crystal formation in a macro-kinetic fashion, has been introduced to delineate mechanisms and gain information into the inter-relationships between the various characteristics of the mixed AgI-AgCl nuclei. Mixed AgI-AgCl (silver iodide-silver chloride) ice nuclei have been generated using a laboratory acetone burner similar in basic design to many used for operational weather modification. These ice nucleating aerosols have been characterized and compared to standard AgI aerosols (from the $2AgI-NH_4I$-acetone-water solution combustion system). Characterization included a documentation of chemistry and particle sizes for correlation to the effectiveness, rates, and mechanisms of ice crystal formation determined in a well characterized and controlled laboratory cloud (held isothermally and water saturated at various temperatures). The major results and conclusions which can be drawn are as follows:

Aerosol Effectiveness Versus Composition

1) The enhanced ice nucleation effectiveness of the aerosols generated has been directly related to the presence of chlorine in the aerosol. Although additional x-ray crystallographic analysis is necessary to confirm the structure of the Ag-I-Cl mixture, it seems highly likely that solid solution aerosols are produced. Assuming so, the new crystal lattice found to maximize ice nucleation efficiency contained 21.9 mole % chlorine atoms in place of the iodine atoms of the AgI lattice. This

aerosol was produced by the addition of 30 mole % NH_4ClO_4 (with respect to AgI) to the standard generator solution. This resulted in increases in aerosol effectiveness of approximately one order of magnitude (10^{15}IC/gram) at -12°C to three orders of magnitude (10^{13}IC/gram) at -6°C over the standard aerosol.

2) Mixed AgI-AgCl aerosols of the proper composition would be expected to display better epitaxy than pure AgI and the results to support such a hypothesis. The ice nucleation effectiveness displayed an increasing trend as the chlorine content of the aerosol was increased to the 21.9 mole % value. However, when the mole % was increased to 30% (aerosol from the solution with 40 mole % NH_4ClO_4), effectiveness decreased by a much larger amount than could be explained by particle size changes alone. Such a trend is expected when epitaxy is responsible for effectiveness increases because too many chlorine atoms would eventually destroy the epitaxial match of the lattice to ice. AgCl alone is a poor ice nucleant. Although epitaxy differences can explain the enhanced ice nucleation efficiencies, surface properties affecting nucleation might have also been changed with the addition of ammonium perchlorate.

3) The composition maximum effectiveness relationship found in this research is comparable to that which might be present in the highly effective aerosol from the NEI TB-1 pyrotechnic with hexachlorobenzene. If that pyrotechnic produced mixed AgI-AgCl 100% efficiently upon combustion it would contain 22.7 mole % chlorine.

Rates and Mechanisms for Ice Crystal Formation

1) Rates of ice crystal formation by the standard AgI aerosol and the mixed aerosols may be generally characterized as "slow" for the generation technique utilized and cloud conditions simulated. Typical times for 90% utilization of aerosols to produce ice crystals are from twenty to forty minutes, in a 1.5 gm^{-3} liquid water cloud. The time for utilization is highly dependent on liquid water content in an inversely proportional relationship.

2) For the conditions simulated, the mechanism for ice crystal formation on the mixed AgI-AgCl aerosols, as well as the standard AgI aerosol, is purely contact freezing nucleation at temperatures of $-16^{o}C$ and warmer. This result is derived from changes in the macro- kinetics of ice crystal production with cloud droplet (LWC) changes (while water saturation is maintained). The clean first order kinetics also assures that nucleation following contact is instantaneous when it occurs. The contact nucleation behavior is confirmed by the large increase in rate constant which occurs when the mean aerosol size is halved and by the agreement with theoretical coagulation time constants to within 20 to 40%. Also, the experimental change of ice crystal formation rate with liquid water content was shown to agree well quantitatively with that predicted by theory.

3) At a temperature of $-20^{o}C$, ice crystals are produced by both the contact nucleation mechanism and a deposition nucleation mechanism. The kinetic behavior of all aerosols to form ice crystals at this temperature is non-linear on a first order plot, but can

be readily interpreted as a combination of first order processes with differing rate constants. The slower process at a liquid water content of 1.5 gm^{-3} is identified as deposition by its kinetic insensitivity to changes in liquid water content. Chemical considerations rule out a condensation freezing mechanism. The deposition mechanism is responsible for between 20 and 60% of the ice crystal production by the aerosols tested at $-20^{o}C$ and a LWC of 1.5 gm^{-3}. It is quite certain that this is the dominant mechanism for ice crystal formation at LWC values of 0.5 gm^{-3} and below (in terms of ice crystal formation rate).

4) The rate of formation of ice crystals by deposition at $-20^{o}C$ is independent of mean particle size and composition. This was displayed by the near constancy of kinetic slope (rate constant) with changes in these parameters. However, there appeared a good correlation between the % of particles greater than 500 $A^{o}C$ and the % of ice crystals formed by deposition (as determined from the kinetic plots) at $-20^{o}C$. The existence of a particle size cut-off for deposition is in agreement with the results of previous authors. The independence of the deposition nucleation rate on particle sizes greater than this minimum size is explainable by either a particle size dependent nucleation rate or a nucleation rate which is a function of the presence of active sites only. The distinction cannot be made in this study due to the existence of many aggregate particles (and lack of knowledge of their nucleating characteristics) and inability to isolate particle sizes.

5) The efficiency versus temperature relationship of nucleation by contact can be explained by theory of nucleation at active sites on the surface of nuclei. However, the enhanced efficiency of nucleation by mixed AgI-AgCl aerosols at warmer temperatures is most likely a reflection of a change in a competition between the rate of freezing of droplets and the rate of dissolution of active sites following collision. The involvement of active sites is deduced from the fact that smaller particles are inherently less efficient in nucleating ice crystals, yet all particle sizes participate in the nucleation process to some degree. The inverse relationship between temperature and the rate constant for ice crystal formation indicated that the mean effective particle size was a decreasing function of decreasing temperature and this particle size effect was confirmed by comparing nucleation efficiency for three different mean sized aerosols. However, large changes in effectiveness were necessary to effect only small changes in rate constant, indicating that probably all particle sizes were involved in ice crystal formation at a given temperature. The data suggests that the addition of chlorine to the silver iodide lattice is indeed improving epitaxy and/or the nature of active sites. Better epitaxy only increases the rate of nucleation. Therefore this rate must be in competition with one which destroys nucleation ability. The rate of solubility is the most likely competitor, and this rate is decreased with the addition of chlorine.

Interrelationships Between Chemistry, Particle Size, Effectiveness, Rates and Mechanisms

1) Nuclei chemistry is perhaps the single most important factor determining and relating the nucleating characteristics of mixed silver iodide-silver chloride aerosols. They are efficient ice nuclei because of their chemical structure. Their mechanism for nucleating ice at most temperatures of concern is limited by their chemistry in that they are non-hygroscopic. They are more efficient nucleators of ice (for given compositions) than the AgI nuclei produced from combustion of the $2AgI.NH_4I$-acetone-water solution because their improved epitaxy favors freezing in the hypothesized competition with solubility (very little change from pure AgI) following collision with droplets.

2) Particle size is a very important factor relating the characteristics of mixed AgI-AgCl ice nuclei. Given the contact nucleation mechanism at temperatures of $-16^{o}C$ and warmer, particle size controls the rate at which ice crystals are formed. Smaller particles necessarily produce ice crystals at a faster rate, but less efficiently than larger particles. Particle size is also a controlling factor in determining the mechanism for ice crystal formation at $-20^{o}C$, and consequently rates of ice crystal formation.

6.2 Experimental Implications and Significance

Use of Kinetics to Study Ice Crystal Nucleation and Evolution

The fact that ice crystal formation data could be plotted and interpreted kinetically was itself a significant result of this study. There was no certainty that the principles of chemical reaction kinetics

could be applied to mixed aerosol systems although the similarity to heterogeneously catalyzed crystallization processes suggested it was so. The success of the procedure now provides a method to help distinguish singular or competitive mechanisms for ice crystal formation by aerosols in controlled cloud conditions which may be simulated in larger cloud chambers. This will allow better understanding of the nucleating characteristics of actual field generator effluents in atmospheric clouds, and provide a relatively simple method for studying the various nucleation mechanisms (and parameters involved) as well. Kinetics actually provides the bridge to quantitatively transfer laboratory results to the atmosphere. In this particular experiment the knowledge of the contact mechanism and the rate constant for deposition is information which would not be apparent simply from ice crystal formation rate data. This knowledge allows one to model ice crystal formation by these aerosols in water saturated clouds, with the appropriate contact nucleation model (to obtain the contact rate constant) to account for varying droplet distributions and magnitudes of non-Brownian transport mechanisms. Of course, it would have been desirable to perform tests with more realistic cloud droplet concentrations to determine whether other mechanisms were masked at warmer temperatures. However, if other mechanisms do produce ice crystals on mixed AgI - AgCl at warmer temperatures and water saturation, their rate of formation of ice crystals is obviously very much slower than the contact nucleation rate measured in this research, even at a 0.5 gm^{-3} LWC. This would be undesirable for weather modification purposes.

The fact that the interpretation of the macro-kinetics was not complicated by an aerosol size distribution has implications to the use of

these methods to study ice evolution in naturally and artificially nucleated atmospheric clouds whose ice crystal concentrations (and other parameters) can be characterized by cloud physics aircraft. Recent data published by Cooper and Vali (1981) indicate that this is indeed possible. Figure 15 from Cooper and Vali (1981) is shown as figure 46a here. It displays ice crystal concentrations as a function of time (based on horizontal wind speed) at a given level within a orographic cap cloud over Elk Mountain, Wyoming. Crystal concentrations were obtained from a Particle Measuring Systems 2-D spectrometer probe. These data can be transformed into a percent ice crystal formation versus time plot and thus into the kinetic plot of figure 46b. Although concentration estimation was made difficult by the small scale of figure 46a, the linearity of the kinetic plot is impressive. It states that a singular (and fast) mechanism for ice crystal formation begins near the edge of the water saturated cloud. Variations with temperature and droplet concentration would help identify this mechanism. However, the point made here is that the kinetic methodology outlined in this thesis is also applicable to investigating mechanisms of natural and artificial ice evolution in real clouds.

Implications to Weather Modification

The most practically applicable result of this study in terms of weather modification is the production of a new ice nucleant with superior activity at temperatures warmer than $-16^{\circ}C$. This fact needs to be confirmed for the same aerosols generated with commercial solution combustion generators. Such a confirmatory test has recently been completed using a field generator belonging to North American Weather Consultants (NAWC). With the addition of NH_4ClO_4 to their standard solu-

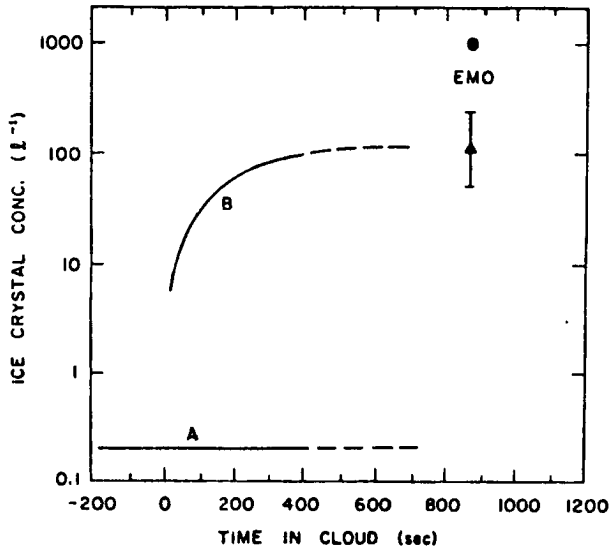

Figure 46a. Rate of formation of ice crystals in the Elk Mountain Cloud of January 10, 1975 (From Cooper and Vali, 1981).

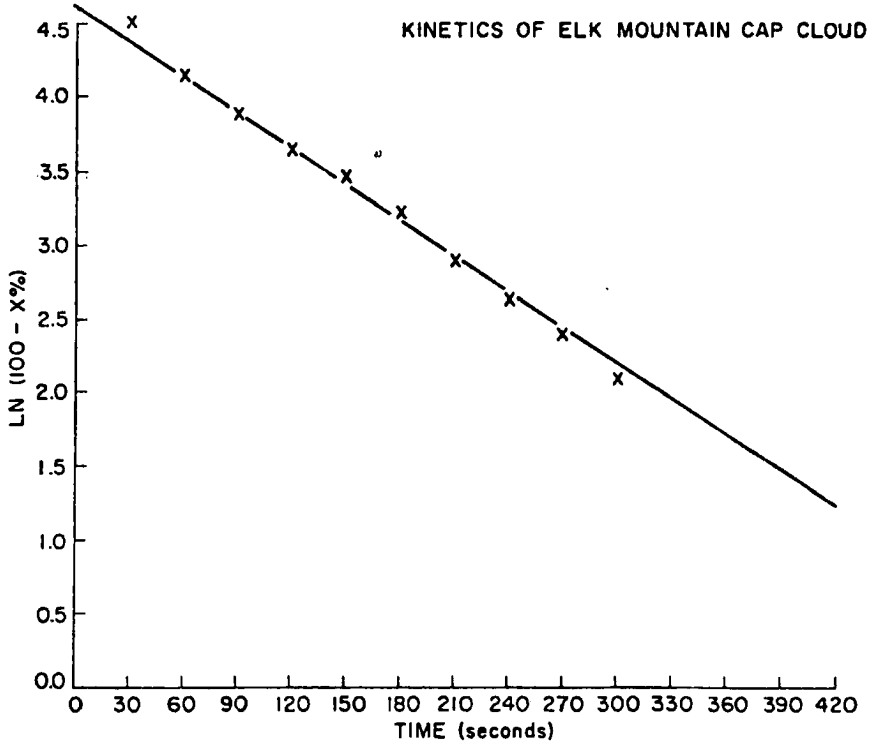

Figure 46b. Kinetic plot produced from figure 46a.

tion, one to three orders of magnitude increases in effectiveness were observed at temperatures of $-10^{o}C$ and warmer, and the threshold of detectable ice crystal formation was increased by a full $1.5^{o}C$. Preliminary kinetic studies have shown that both the standard aerosol and the mixed AgI-AgCl aerosol were forming ice crystals by contact nucleation at these temperatures. Thus, at little additional cost, the NAWC generator can produce nuclei which function the same at those presently used, but are 10 to 1000 times more efficient in nucleating ice crystals by that mechanism. The temperature regime where this enhancement is occurs is particularly important for precipitation enhancement applications.

While the behavior of the mixed AgI-AgCl aerosols has been characterized only at water saturation, the chemical nature of the aerosols would suggest that high sustained supersaturations would be necessary to force a condensation- freezing mechanism for ice crystal formation. If contact nucleation is indeed the primary mechanism for ice crystal formation by mixed AgI-AgCl aerosols in the atmosphere, the limitations of this process must be considered for some weather modification applications. In weather modification for wintertime orographic precipitation enhancement for example, cloud liquid water contents rarely exceed 0.5 gm^{-3} and more generally are in the 0.2 gm^{-3} range (depending on location), with droplet concentrations of no more than a few hundred per cm^{3}. Ice crystal formation rates by purely contact nucleation in these clouds would be a slow and continued process which might not produce the desired ice crystal concentrations over the allowed time and space frame. On the other hand, this characteristic of a contact nucleating agent might be useful over large areas if seeding rates are adjusted

appropriately. In any case, knowledge of ice crystal formation rates by such nucleating agents is absolutely vital in planning seeding strategies and in choosing nucleating agents themselves. Accurate delivery of ice nuclei into a cloud with defined weather modification potential does not assure success without due consideration to nucleation.

Laboratory Procedure Changes

More accurate and consistent determinations of ice nucleation effectiveness of weather modification nucleating agents will be possible in future testing at the Cloud Simulation Laboratory as a result of this research. Much variability in past measurements was likely due to the assumption of a constant value for aerosol dilution during ascent up the vertical dilution wind tunnel. A hot wire anemometer is now in place to determine the dilution value during every aerosol sample withdrawal. A permanent low speed fan would be most desirable in the future, so that vertical wind speed would be constant in the tunnel. This would help eliminate aerosol size distribution variability. Greater accuracy of effectiveness values is also insured with the calibration of chamber dilution airflow versus temperature and the knowledge of how to correct effectiveness values for this factor.

6.3 Suggestions for Future Research

Two tasks remain in a complete characterization of mixed AgI-AgCl ice nuclei. First is a simple study of the photodecay of the ice nucleating ability of these aerosols. This should be accomplished before these aerosols are generated operationally. It might be achieved by use of an aerosol holdng tank from which the nuclei can be withdrawn at various intervals, under both dark and irradiated conditions, and tested for effectiveness in the ICC. A more esoteric task remaining is

an x-ray chrystallographic analysis of the most effective aerosol to positively identify structure and obtain lattice constants for comparison to both AgI and ice.

A number of related studies are suggested by the concepts and results presented here. In terms of laboratory studies, a confirmatory and carefully designed quantitative kinetics experiment would be of greatest scientific merit. Such a study would properly investigate all ice nucleation mechanisms kinetically. Size classification and concentration control of aerosols and droplets would be absolutely necessary and extension of studies below and above water saturation could be achieved by use of a continuous flow ice thermal diffusion chamber and the CSU controlled expansion dynamics chamber respectively. Such a study would help quantify the interrelationships discussed in section 6.1 and this knowledge would be the basis for modelling ice crystal formation by weather modification aerosols under representative atmospheric conditions. Using the isothermal cloud chamber alone, studies similar to the one presented here should be performed on other previously or commonly used weather modification aerosols, simply to gain information on their characteristic rates and mechanisms for ice crystal formation. AgI-NaI complex aerosols, for example, likely display very different nucleating characteristics at water saturation than those studied here. This could have implications to the results obtained from operational weather modification programs using the different nucleants. Another interesting laboratory study would investigate the potentially highly efficient AgI-AgBr nuclei. In terms of field studies, the identification of ice crystal formation rates by both natural and artificial nucleants in clouds should be pursued. In addition, the kinetics

approach to their study should be applied to confirm the validity of the approach in the atmosphere and hopefully identify nucleation mechanisms. This important knowledge is noticeably lacking at the present time.

REFERENCES

Alkezweeny, A. I., 1971: A Contact Nucleation Model for Seeded Clouds. J. Appl. Meteor., 10, 732-738.

Anderson, B. J. and J. Hallett, 1976: Supersaturation and Time Dependence of Ice Nucleation from the Vapor on Single Crystal Substrates. J. Atmos. Sci., 33, 822-832.

Auer, A. H., 1970: Observations of Ice Crystal Nucleation by Droplet Freezing in Natural Clouds. J. Rech. Atmos., 4, 145-160.

Bigg, E. K., S. C. Mossop, R. J. Meade and N. C. Thorndike, 1963: The Measurement of Ice Nuclei Concentrations by Means of Millipore Filters. J. Appl. Meteor., 2, 266-269.

Blair, D. N., B. L. Davis, and A. S. Dennis, 1973: Cloud Chamber Tests of Generators Using Acetone Solutions of AgI-NaI, AgI-KI and AgI-NH_4I. J. Appl. Meteor., 12, 1012-1017.

Burkhardt, L. A. and W. G. Finnegan, 1970: Complex Ice Nuclei: The Silver Iodide-Sodium Iodide System. Preprints of the 2nd National Conference on Weather Modification, Santa Barbar, California, April 6-9, 1970, 325-328.

Cooper, W., 1974: A Possible Mechanism for Contact Nucleation. J. Atmos. Sci., 31, 1832-1837.

Cooper, W. A. and G. Vali, 1981: The Origin of Ice in Mountain Cap Clouds. J. Atmos. Sci., 38, 1244-1259.

Corrin, M. L., H. W. Edwards and J. A. Nelson, 1964: The Surface Chemistry of Condensation Nuclei: II. The Preparation of Silver Iodide Free of Hygroscopic Impurities and Its Surface Interaction with Water Vapor. J. Atmos. Sci., 21, 565-567.

Corrin, M. L., S. P. Moulik and B. Cooley, 1967: The Surface Chemistry of Condensation Nuclei: III. The Absorption of Water Vapor on 'Doped' Silver Iodide. J. Atmos. Sci., 24, 530-532.

Davis, C. I. and A. H. Auer, 1972: The Possibility of Collision Nucleation by an AgI Aerosol in Natural Orographic Cap Cloud. J. Rech. Atmos., 6, 107-115.

Davis, C. I., 1974: The Ice Nucleating Characteristics of Various AgI Aerosols. PhD. Dissertation, Dept. of Mech. Eng., Univ. of Wyoming. 267 pp.

Donnan, J., D. N. Blair and D. A. Wright, 1971: A Wind Tunnel/Cloud Chamber Facility for Cloud Modification Research. J. Wea. Mod., 3, 123-133.

Edwards, G. R. and L. F. Evans, 1960: Ice Nucleation by Silver Iodide: I. Freezing vs. Sublimation. J. Met., 17, 627-634.

Edwards, G. R. and L. F. Evans, 1961: The Effect of Surface Charge on Ice Nucleation by Silver Iodide: Faraday Soc. Trans., 58, 1649-1655.

Edwards, G. and L. Evans, 1968: Ice Nucleation by Silver Iodide: Part III. Nature of the Nucleating Site. J. Atmos. Sci., 25, 249-256.

Elliott, R. D., R. W. Shaffer, A. Court and J. F. Hannaford, 1978: Randomized Cloud Seeding in the San Juan Mountains, Colorado. J. Appl. Meteor., 17, 1298-1318.

Finnegan, W. G., L. A. Burkardt and R. L. Smitt, 1962: Chemically Produced Colored Smokes. U. S. Patent #3, 046,168.

Fletcher, N. H., 1958a: Size Effect in Heterogeneous Nucleation. J. Chem. Phy., 29, 572-576.

Fletcher, N. H., 1958b: Time Lag in Ice Crystal Nucleation in the Atmosphere: Part II Theoretical. Bull. Obs. Puy de Dome, 1, 11-18.

Fletcher, N. H., 1960: Nucleation and Growth of Ice Crystals upon Crystalline Substrates. Australian Journal of Physics, 1960, 108-119.

Fletcher, N. H., 1969: Active Sites and Ice Crystal Nucleation. J. Atmos. Sci., 26, 1266-1271.

Fletcher, N. H., 1972: On Contact Nucleation. J. Atmos. Sci., 27, 1098-1099.

Frost, A. A. and R. G. Pearson, 1953: Kinetics and Mechanism: A Study of Homogeneous Chemical Reactions. John Wiley and Sons, Inc., New York. 147-151.

Fukuta, N., 1966: Activation of Atmospheric Particles as Ice Nuclei in Cold and Dry Air. J. Atmos. Sci., 23, 741-750.

Gagin, A. and J. Newman, 1974: Modification of Subtropical Winter Cumulus Clouds- Cloud Seeding and Cloud Physics in Israel. J. Wea. Mod.,6 , 203-215.

Garvey, D. M., 1975: Testing of Cloud Seeding Materials at the Cloud Simulation and Aerosol Laboratory, 1971-1973. J. Appl. Meteor., 14, 883-890.

Garvey, D. M. and C. I. Davis, 1975: Ice Nucleation Characteristics of AgI Aerosols in an Isothermal Cloud Chamber. Proceedings of the VIII Conference on Nucleation, Leningrad, USSR. 166-173.

Gerber, H., P. A. Allee, U. Katz, C. I. Davis and L. O. Grant, 1970: Some Size Distribution Measurements of AgI Nuclei with an Aerosol Spectrometer. J. Atmos. Sci., 27, 1060-1067.

Gerber, H., 1972: Size and Nucleating Ability of AgI Particles. J. Atmos. Sci., 29, 391-392.

Gokhale, N. R., 1965: Dependence of Freezing Temperatures of Supercooled Water Drops on Rate of Cooling. J. Atmos. Sci., 22, 212-216.

Gokhale, N. R. and J. Goold, Jr., 1968: Droplet Freezing by Surface Nucleation. J. Appl. Met., 7, 870-874.

Goldsmith, P. and F. G. May, 1966: Diffusio- and Thermophoresis in Water Vapor Systems. Aerosol Science, Academic Press, New York, 163-194.

Grant, L. O. and R. Steele, 1966: The Calibration of Silver Iodide Generators. Bull. of the AMS, 47, 713-717.

Greenfield, S. M., 1957: Rain Scavenging of Radioactive Particulate Matter from the Atmosphere. J. Meteor., 14, 115-125.

Hesketh, H. E., 1977: Fine Particulates in a Gaseous Media. Ann Arbor, Michigan. 83-84.

Huffman, P. J., 1973: Supersaturation Spectra of AgI and Natural Ice Nuclei. J. Appl. Meteor., 12, 1080-1082.

Isaac, G. A., 19[illegible]: Ice Nuclei and Convective Storms. Scientific Report MW-75, Stormy Weather Group, McGill University, Montreal, Canada, 62 pp.

Isaac, G. A. and R. H. Douglas, 1972: Another 'Time Lag' in the Activation of Atmospheric Ice Nuclei. J. Appl. Met., 11, 490-493.

Katz, U. and R. J. Pilie, 1974: An Investigation of the Relative Importance of Vapor Deposition and Contact Nucleation in Cloud Seeding with AgI. J. Appl. Meteor, 13, 658-665.

Katz, U. and E. J. Mack, 1980: On the Temperature Dependence of the Relative Frequency of Ice Nucleation by Contact and Vapor Deposition. Proc. Third WMO Scientific Conference on Weather Modification, Clermont-Ferrand, France, 21-25 July, 1980. 33-36.

Knollenberg, R. G., 1976: Three New Instruments for Cloud Physics Measurements: The 2-D Spectrometer, The Forward Scattering Spectrometer Probe, and The Active Scattering Aerosol Spectrometer. Preprints, International Conference on Cloud Physics, Boulder, CO., Amer. Meteor. Soc., 554-561.

Langer, G., 1973: Evaluation of NCAR Ice Nucleus Counter. Part I: Basic Operation. J. Appl. Meteor., 12, 1000-1011.

Matthews, L. A., D. W. Reed, P. St.-Amand and R. J. Stirton, 1972: Rate of Solution of Ice Nuclei in Water Drops and Its Effect on Nucleation. J. Appl. Met., 11, 813-817.

Moore, W. J., 1972: Physical Chemistry, Prentice Hall Inc., Englewood Cliffs, N. J. 324-347.

Mossop, S. C. and L. F. Jayaweera, 1969: AgI-NaI Aerosols as Ice Nuclei. J. Appl. Meteor., 8, 241-248.

Odencrantz, F., 1969: Freezing of Water Droplets: Nucleation Efficiency at Temperatures Above -5°C. J. Appl. Meteor., 8, 322-325.

Pasarelli, R. E., Jr., H. Chessin and B. Vonnegut, 1974: Ice Nucleation in a Supercooled Cloud by CuI-3AgI and AgI Aerosols. J. Appl. Meteor., 13, 946-948.

Pruppacher, H. R. and J. D. Klett, 1978: Microphysics of Clouds and Precipitation. D. Reidel Publishing Co., Boston, Mass. p. 274.

Resnick, R. and D. Haliday, 1962: Physics: Part II. John Wily and Sons, Inc. New York, p. 747.

Sax, R. I., 1970: Drop Freezing by Brownian Contact Nucleation. Doctoral Thesis, Dept. of Physics, Imperial College of Science and Technology, University of London. 257 pp.

Sax, R. I. and P. Goldsmith, 1972: Nucleation of Water Drops by Brownian Contact with AgI and Other Aerosols. Quart. J. R. Met. Soc., 98, 60-72.

Sax, R. I., D. M. Garvey and F. P. Parungo, 1979: Characteristics of AgI Pyrotechnic Nucleant Used in NOAA's Florida Area Cumulus Experiment. J. Appl. Meteor., 18, 195-202.

Schafer, V. J., 1946: The Production of Ice Crystals in a Cloud of Supercooled Water Droplets. Science, 104(2707), 457-459.

Schaller, R. C. and N. Fukuta, 1979: Ice Nucleation by Aerosol Particles; Experimental Studies Using a Wedge-shaped Ice Thermal Diffusion Chamber. J. Atmos. Sci., 36, 1788-1801.

St.-Amand, P., L. A. Burkardt, W. G. Finnegan, L. L. Wilson, S. D. Elliott, Jr. and P. T. Jorgensen, 1970: Pyrotechnic Production of Nucleants for Cloud Modification-Part II., J. Wea. Mod., 2, 33-52.

St.-Amand, P., W. G. Finnegan and L. Burkardt, 1971a: Understanding of the Use of Simple and Complex Ice Nuclei Generated from Pyrotechnics and Acetone Burners, J. Wea. Mod., 3, 31-48.

St.-Amand, P. W. G. Finnegan and L. A. Matthews, 1971b: Effects of Contact Nucleation on Cloud Seeding Methods. J. Wea. Mod., 3, 49-92.

Steele, R. L. and F. W. Krebs, 1967: Characteristics of Silver Iodide Ice Nuclei Originating from Anhydrous Ammonia-Silver Iodide Complexes: Part I. J. Appl. Meteor, 6, 105-113.

Stevenson, C. M., 1968: An Improved Millispore Filter Technique for Measuring the Concentrations of Freezing Nuclei in the Atmosphere. Quart. J. Roy. Meteor. Soc., 94, 35-43.

Turnbull, D. and B. Vonnegut, 1952: Nucleation Catalysis. Ind. Eng. Chem., 44, 1292-1298.

Vali, G., 1968: Ice Nucleation Relevent to Formation of Hail. Scientific Report MW-58, Stormy Weather Group, McGill University, Montreal, Canada. 51 pp.

Vonnegut, B., 1949: Nucleation of Supercooled Water by Silver Iodide Smokes. Chem. Rev., 44, 277-289.

Vonnegut, B., 1950: Techniques for Generating Silver Iodide Smoke. J. Colloid. Sci., 5 37-48.

Vonnegut, B., 1957: Early Work on Silver Iodide Smokes for Cloud Seeding. Final Report of the Advisory Committee on Weather Modification, 2, 283-355.

Vonnegut, B. and H. Chessin, 1971: Ice Nucleation by Coprecipitated Silver Iodide and Silver Bromide. Science, 174, 945-946.

Warburton, J. A. and K. J. Heffernan, 1964: Time Lag in Ice Crystal Nucleation by Silver Iodide. J. Appl. Meteor, 3, 788-791.

Warner, J., 1957: An Instrument for the Measurement of Freezing Nucleus Concentration. Bull. L'Obs. Puy de Dome, 2, 33-46.

Warner, J. and T. D. Newnham, 1958: Time Lag in Ice Crystal Nucleation in the Atmosphere: Part I, Experimentall. Bull. L'Obs. Puy de Dome, 1, 1-10.

Weickmann, H. K., U. Katz and R. Steele, 1970: AgI-Sublimation or Contact Nucleus. Preprints of the 2nd National Conference on Weather Modification. Santa Barbar, California, April 6-9, 1970, 325-328.

Young, K. C., 1974: A Numerical Simulation of Orographic Precipitation, Part I: Description of the Model Microphysics and Numerical Techniques. J. Atmos. Sci., 31, 1735-1748.

Zettlemoyer, A. C., N. Tcheurekdjian and J. J. Chessick, 1961: Surface Properties of Silver Iodide. Nature, 192, 653.

APPENDIX A
Cloud Droplet Size Distributions

The following pages contain cloud droplet size distributions for the ICC across its operating temperature spectrum and at liquid water contents of 0.5 gm^{-3} and 1.5 gm^{-3} using the FSSP. Such a calibration has never been documented for the ICC and this information should prove valuable in the future. This data was also useful in the determination of the theoretical rates of ice crystal formation in a contact nucleation process, and simply in displaying that droplet concentrations do indeed change significantly when the LWC is changed. The first figure displays the droplet size distribution as determined by the soot coated slide technique in 1970 for comparison to the new results. The FSSP distributions are given as the percent of total droplets present per micron sized droplet radius bin.

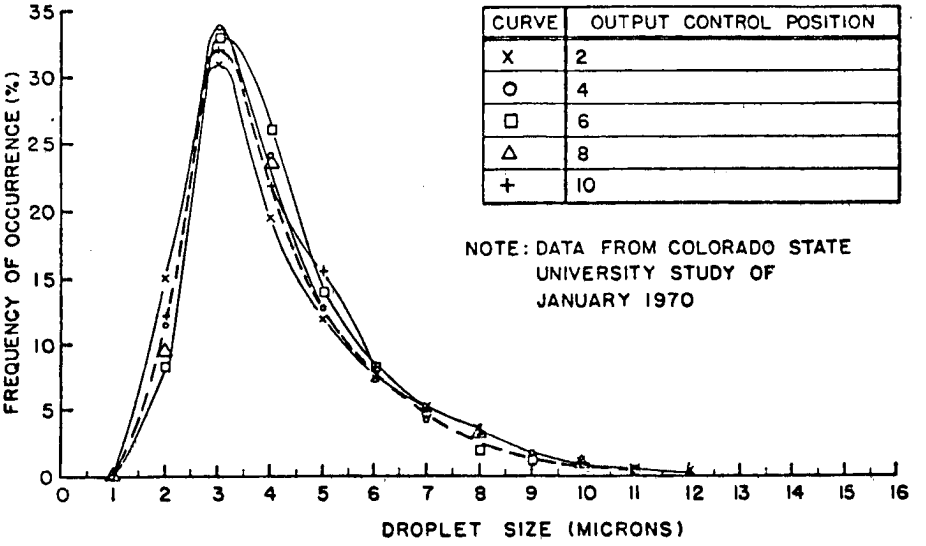

Figure 47. Cloud droplet size (radius) distribution determined from soot coated slides (from ultrasonic humidifier service manual).

Figures 48 to 57. Cloud droplet size distributions at various cloud temperatures for liquid water contents of 0.5 gm^{-3} and 1.5 gm^{-3} (determined using the FSSP).

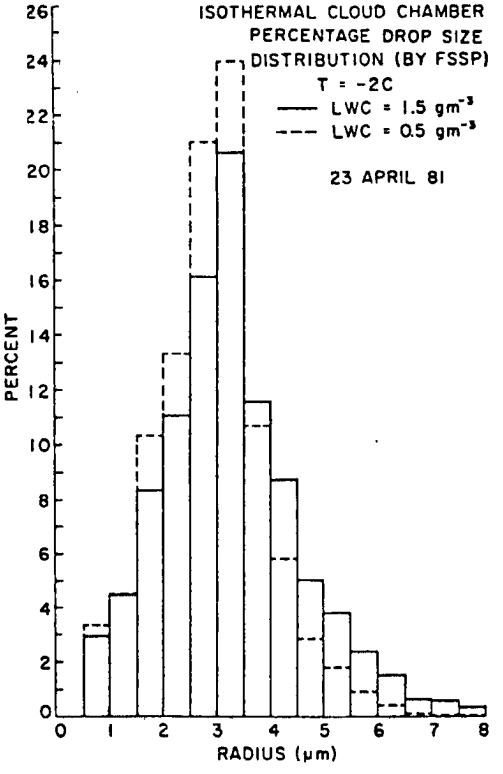

Figure 48.

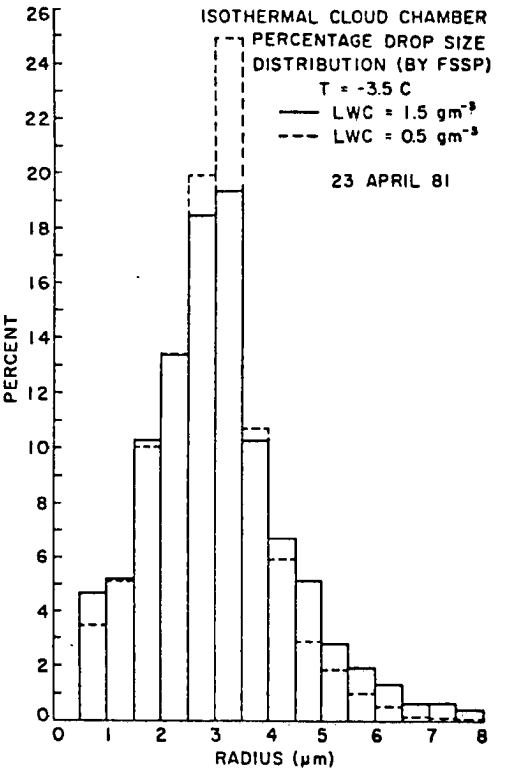

Figure 49.

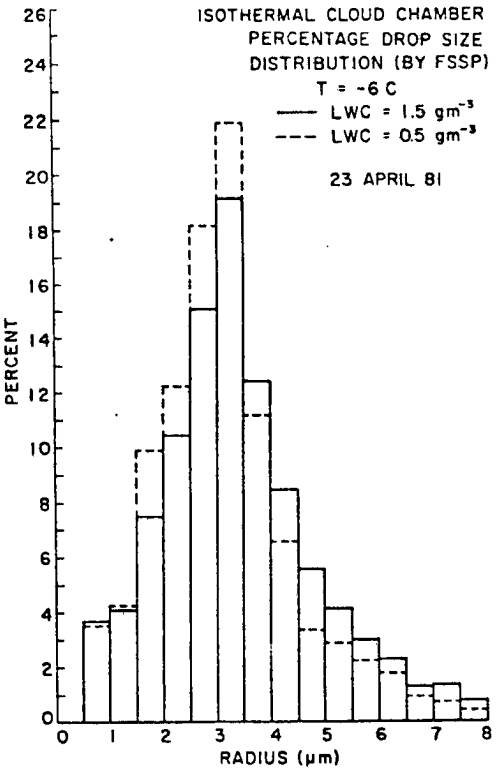

Figure 50.

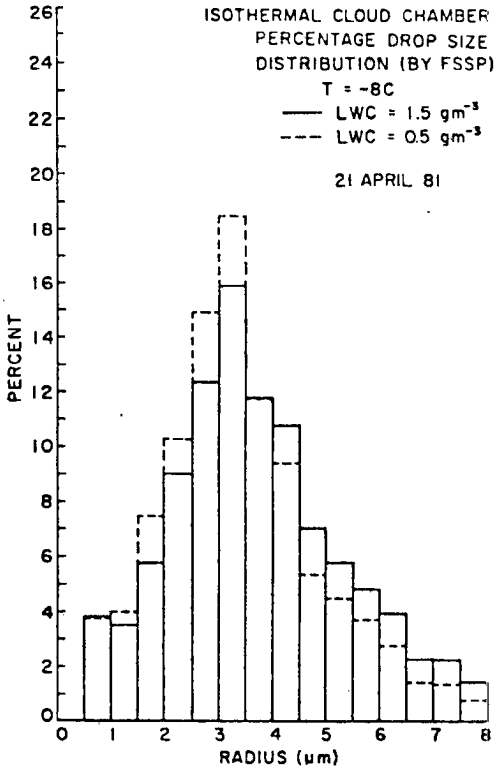

Figure 51.

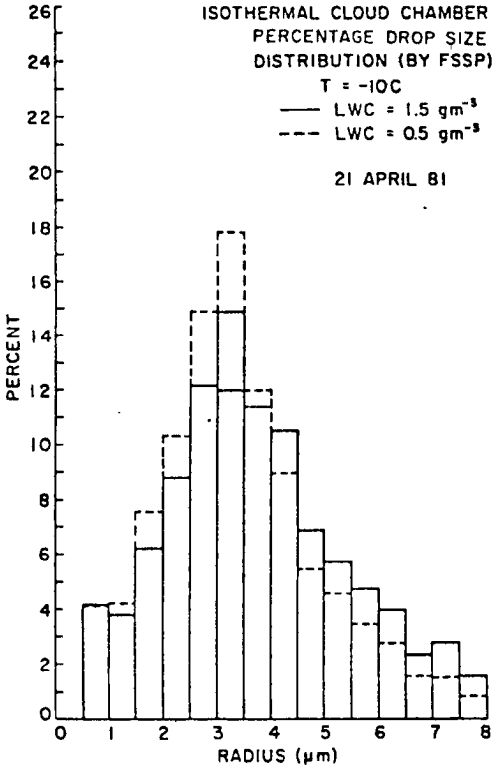

Figure 52.

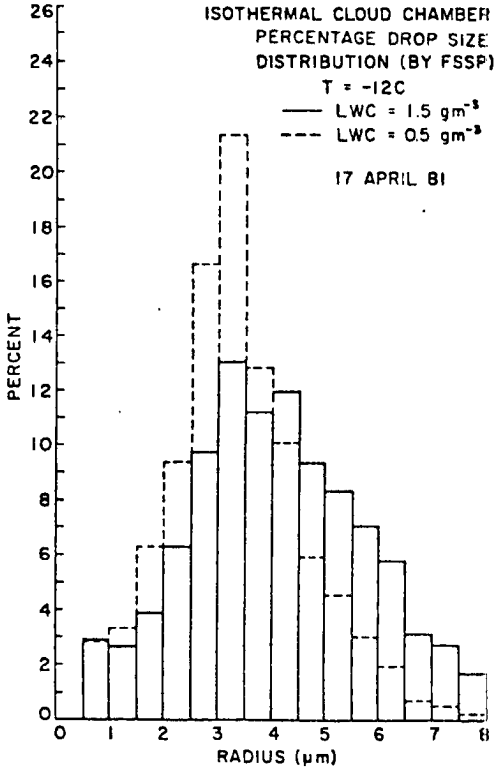

Figure 53.

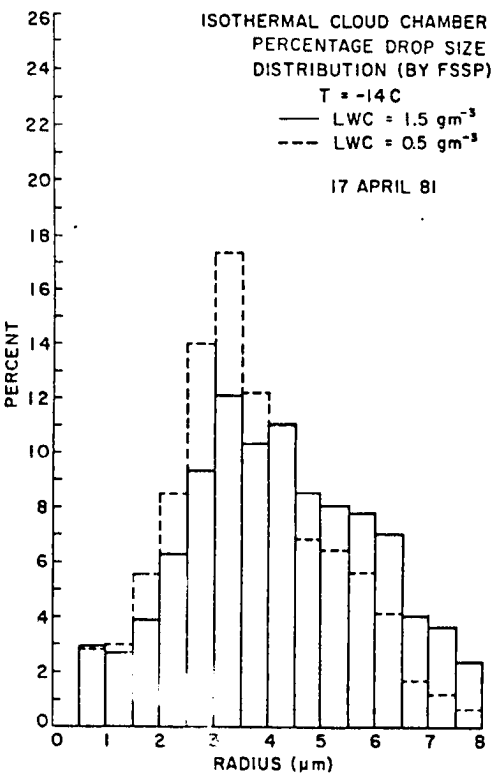

Figure 54.

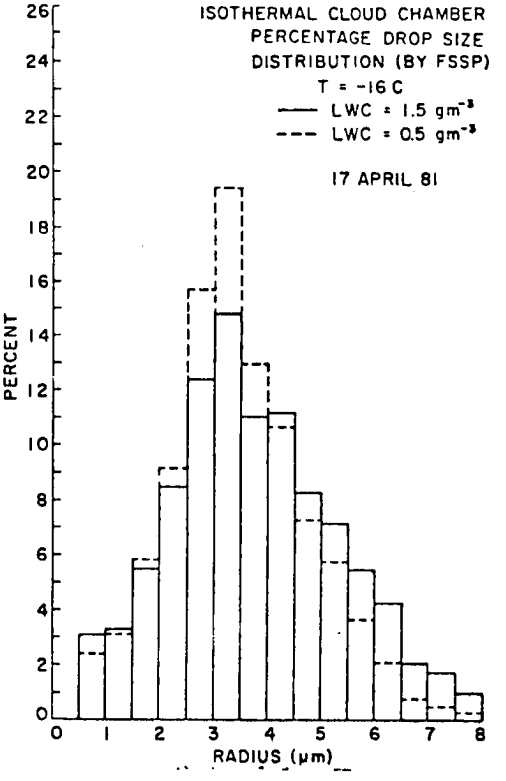

Figure 55.

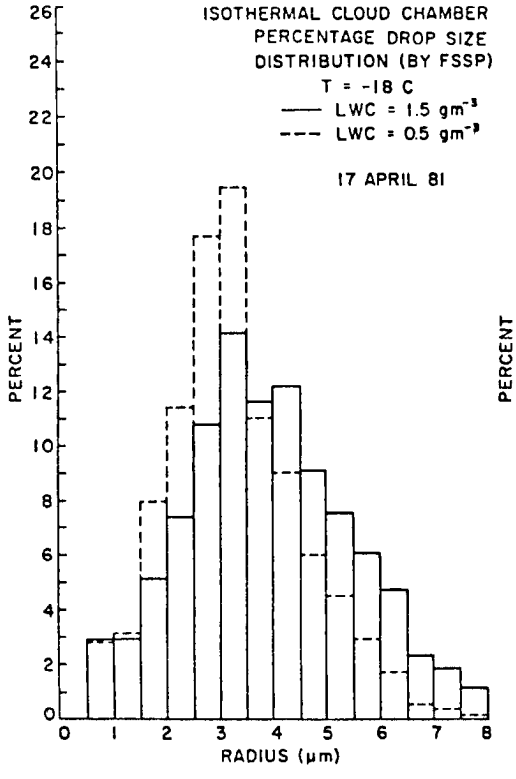

Figure 56.

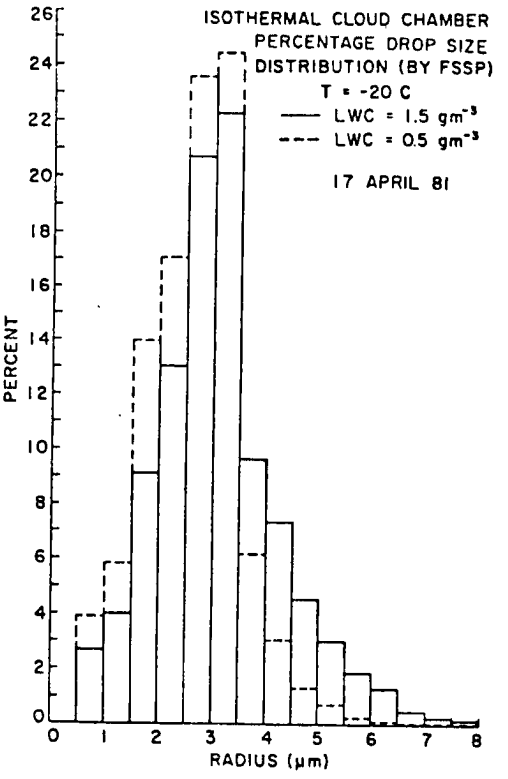

Figure 57.

APPENDIX B
The Electrostatic Precipitator

The electrostatic precipitator designed for this research uses an estimated 3000 volt potential between a cylindrical type conductor and a central rod to produce an electric field for both charging and collecting an aerosol. It is diagrammed in figure 58. From Resnick and Holiday (1962), the electric field E for a cylindrical conductor is given by,

$$E = \frac{V}{r} \ln \frac{b}{a}.$$

With r=a, an electric field strength of approximately 4000 V/cm is calculated. Following Hesheth (1977), V_e, the pullout velocity by the electric field can be calculated and a theoretical collection efficiency versus particle size can be computed for this precipitator.

$$V_e = [(1 + \frac{\lambda}{R})^2 + 2(1 + \frac{\lambda}{R})^{-1}] \frac{(4 E_o E_p R (1 + A\frac{\lambda}{R})}{6\pi\gamma \cdot 4 \times 10^5})$$

E_o = charging electric field

E_p = pullout electric field

γ = absolute viscosity of air

R = particle radius

λ = mean free path of air molecules

A = 0.864.

This expression accounts for both diffusional charging (random motion and collision of charged ions and particles) and field charging (corona discharge produces ions and electrons which are accelerated to the particles by the electric field) mechanisms. Using $\lambda = 8 \times 10^{-6}$ cm and $r = 1.85 \times 10^{-4} gcm^{-1}s^{-1}$, V_e was calculated for various particle sizes. The efficiency of collection given the geometry is then,

$$PE = 1 - \exp\left(\frac{-2LV_e}{V_f \cdot a}\right) \quad .$$

Figure 59 displays the relationship of PE versus particle radius. This is valid only for laminar flow. Assuming such, particle size distributions determined from the collecting substrate would need proper adjustment.

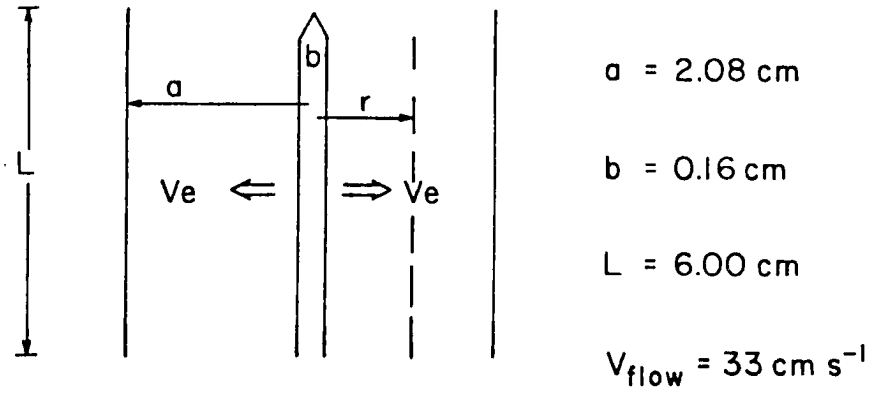

Figure 58. Schematic of the electrostatic precipitator.

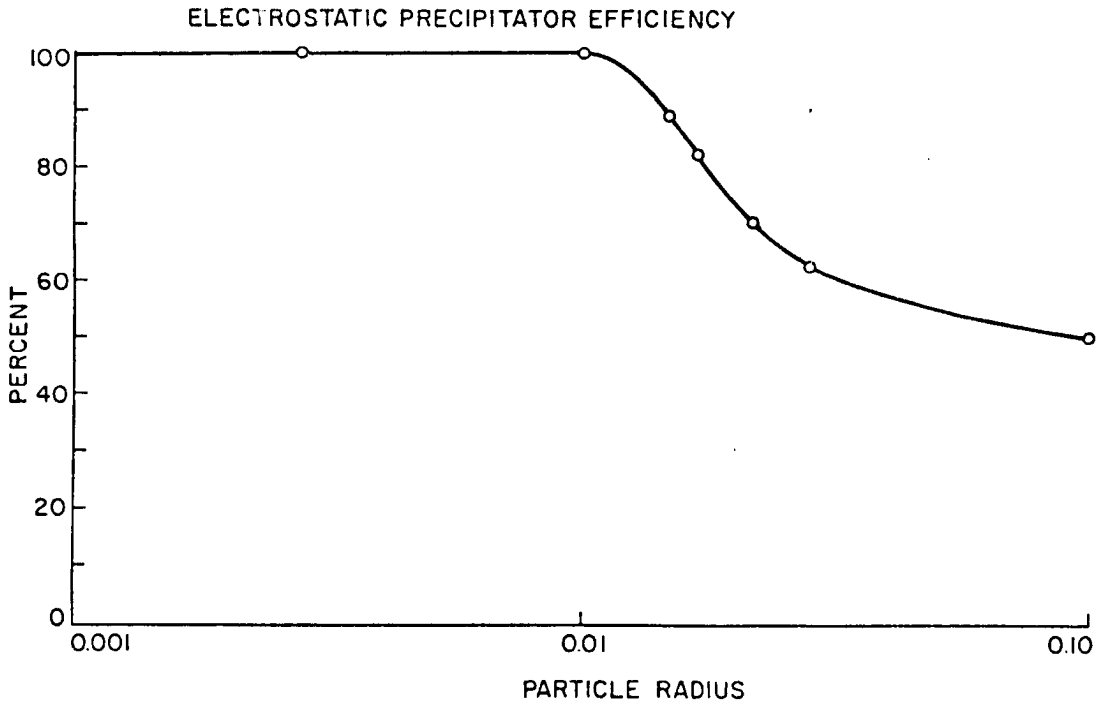

Figure 59. Precipitator collection efficiency(%) versus particle size.